

Dissertation der Fakultät für Biologie  
der Ludwig-Maximilians-Universität München

Epigenetic and pharmacological  
regulation of gene expression  
involved in senescence and tumor progression

vorgelegt von

Dmitri Lodygin

aus  
Arkhangelsk

Dissertation eingereicht am: 11.05.2005

## Erklärung

Hiermit erkläre ich, dass ich die vorliegende Dissertation selbständig und ohne unerlaubte Hilfe angefertigt habe. Sämtliche Experimente sind von mir selbst durchgeführt, außer wenn explizit auf dritte verwiesen wird. Ich habe weder anderweitig versucht, eine Dissertation oder Teile einer Dissertation einzureichen bzw. einer Prüfungskommission vorzulegen, noch eine Doktorprüfung durchzuführen.

München, den 6. Mai 2005

Dmitri Lodygin

Tag der mündlichen Prüfung: 24.10.2005

Erstgutachter: Prof. Dr. Dirk Eick

Zweitgutachter: Prof. Dr. Thomas Cremer

Betreuer: Dr. Heiko Hermeking

## CONTENTS

<b>1. Introduction</b>	<b>4</b>
1.1 Cellular senescence as a tumor suppressor mechanism	4
1.2 14-3-3 $\sigma$ in tumor suppression	9
1.3 Epigenetics and cancer	12
1.4 Prostate cancer	16
<b>2. Aim of the study</b>	<b>20</b>
<b>3. Materials</b>	<b>21</b>
3.1 Chemicals	21
3.2 Enzymes and commercial kits	21
3.3 Antibodies	22
3.3.1 Primary antibodies	22
3.3.1 Secondary antibodies	23
3.4 DNA constructs	23
3.5 Other materials	23
3.6 Equipment	24
<b>4. Methods</b>	<b>25</b>
4.1 Cell culture and treatments	25
4.2 Patient material	25
4.3 Laser-assisted tissue microdissection	26
4.4 RT-PCR analysis	26
4.5 Bisulfite treatment of genomic DNA	26
4.6 Genomic bisulfite sequencing	27
4.7 Methylation-specific PCR	27
4.8 cDNA microarray analysis of gene expression	27
4.9 Oligonucleotide microarray analysis of gene expression	28
4.10 Quantitative real-time PCR	28
4.11 Proliferation assays	29
4.12 BrdU incorporation assay	29
4.13 Measurement of DNA content and apoptosis by flow cytometry	29

<b>4.14 Senescence-associated <math>\beta</math>-galactosidase staining</b>	30
<b>4.15 cGMP assay</b>	30
<b>4.16 Northern blot hybridization</b>	30
<b>4.17 Luciferase assay</b>	30
<b>4.18 Western blot analysis</b>	31
<b>4.19 Immunofluorescent staining</b>	31
<b>4.20 Immunohistochemistry</b>	32
<b>4.21 Microscopy</b>	32
<b>4.22 Generation and analysis of knock-down and transgenic cell lines</b>	33
<b>5. Results</b>	34
<b>5.1 Expression profiling of replicative and premature senescence</b>	34
<b>5.1.1 Microarray analysis of senescence-specific gene expression</b>	34
<b>5.1.2 Induction of senescence by LY83583</b>	36
<b>5.1.3 Microarray analysis of LY83583-regulated genes</b>	38
<b>5.1.4 Rapid induction of p21<sup>WAF1/CIP1/SDI</sup> by LY83583</b>	39
<b>5.1.5 Effect of LY83583 on cancer cell proliferation</b>	42
<b>5.1.6 Requirement of p21, but not p53, for inhibition of proliferation by LY83583</b>	43
<b>5.1.7 Conversion of LY83583-induced arrest to apoptosis in pRb-negative cells</b>	45
<b>5.2 Analysis of 14-3-3<math>\sigma</math> expression in hyperproliferative skin diseases</b>	48
<b>5.2.1 Immunohistochemical analysis of hyperproliferative skin diseases</b>	48
<b>5.2.2 Analysis of 14-3-3<math>\sigma</math> CpG methylation in BCC and normal epidermis</b>	50
<b>5.3 Identification of genes epigenetically silenced in prostate cancer by pharmacological unmasking</b>	55
<b>5.3.1 Epigenetic analysis of PCa cell lines</b>	55
<b>5.3.2 The methylation pattern of candidate promoters</b>	59
<b>5.3.3 Validation of candidate genes for epigenetic silencing</b>	61
<b>5.3.4 Analysis of DNA methylation in primary PCa samples</b>	64
<b>5.3.5 Analysis of 14-3-3<math>\sigma</math> and SFRP1 protein expression in PCa</b>	69
<b>5.3.6 Functional analysis of 14-3-3<math>\sigma</math></b>	71
<b>5.3.7 Functional analysis of <i>DKK3</i> and <i>SFRP1</i></b>	73

<b>6. Discussion</b>	75
6.1 Induction of cellular senescence by LY83583	75
6.2 Epigenetic inactivation of <i>14-3-3<math>\sigma</math></i> in basal cell carcinoma	77
6.3 Functional epigenomic analysis of prostate carcinoma cell lines	79
6.4 Frequent epigenetic silencing of <i>14-3-3<math>\sigma</math></i> in prostate cancer	80
6.5 CpG methylation and down-regulation of <i>SFRP1</i> and <i>DKK3</i> in prostate cancer	82
6.6 Hypermethylation of <i>p57</i> , <i>COX2</i> , <i>GSTM1</i> and <i>GPX3</i> genes in prostate cancer	83
<b>7. Summary</b>	87
<b>8. References</b>	89
<b>9. Abbreviations</b>	109
<b>10. Supplement</b>	110
Supplemental Table 1	110
Supplemental Table 2	113
Supplemental Table 3	114
<b>Acknowledgement</b>	115
<b>Curriculum Vitae</b>	117

## 1. Introduction

### 1.1 Cellular senescence as a tumor-suppressor mechanism

Development of a multicellular organism and tissue regeneration require an enormous proliferative potential of a single cell. For example, this property is essential to form human body consisting of about  $10^{14}$  cells from one-cell embryo and to compensate for the daily physiological loss of millions of cells in adult organism. However, uncontrolled proliferation may result in a number of pathological states including the formation of malignant tumors. One of the biological mechanisms restraining proliferation is cellular senescence. This phenomenon was first described by Hayflick and Moorhead in 1961 (Hayflick and Moorhead, 1961). Primary cells in culture initially undergo a period of proliferation, during which the telomeres of their chromosomes become significantly shorter. Shortening of the telomeres arises from the inability of DNA polymerase to replicate the unprimed lagging strand at the very end of linear DNA molecule. Therefore, in the absence of a compensatory mechanism the terminal fragments of chromosomes 50-100 nucleotides in length are lost during each cycle of replication. Eventually, cellular proliferation decelerates and the cells enter a permanent cell-cycle arrest known as replicative senescence. A senescent cell shows morphological changes, such as a flattened cytoplasm and increased granularity. At the biochemical level, senescence is accompanied by changes in metabolism and the induction of senescence-associated  $\beta$ -galactosidase activity (Dimri et al., 1995). In addition, alterations to chromatin structure (Narita et al., 2003) and gene expression patterns are seen.

Initiation of the senescence program activates various cell-cycle inhibitors and requires the functions of *p53*, the *CDKN1A* gene product WAF1 (Noda et al., 1994; el Deiry et al., 1993), the *CDKN2A* gene product of the *INK4A* genomic locus (also known as p16), and the retinoblastoma protein (Alcorta et al., 1996; Dannenberg et al., 2000; Kamijo et al., 1997; Sage et al., 2003; Stein et al., 1999). The involvement of these tumor suppressors implies that one of the main functions of the senescence program is to suppress tumorigenesis — a hypothesis that has been confirmed in animal models. For example, mutant mice carrying cells that are incapable of entering senescence develop cancer at an early age (Donehower et al., 1992; Kamijo et al., 1999; Krimpenfort et al., 2001; Serrano et al., 1996; Sharpless et al., 2001). Conversely, the induction of premature senescence in murine mammary epithelial cells suppresses tumor development (Boulanger and Smith, 2001).

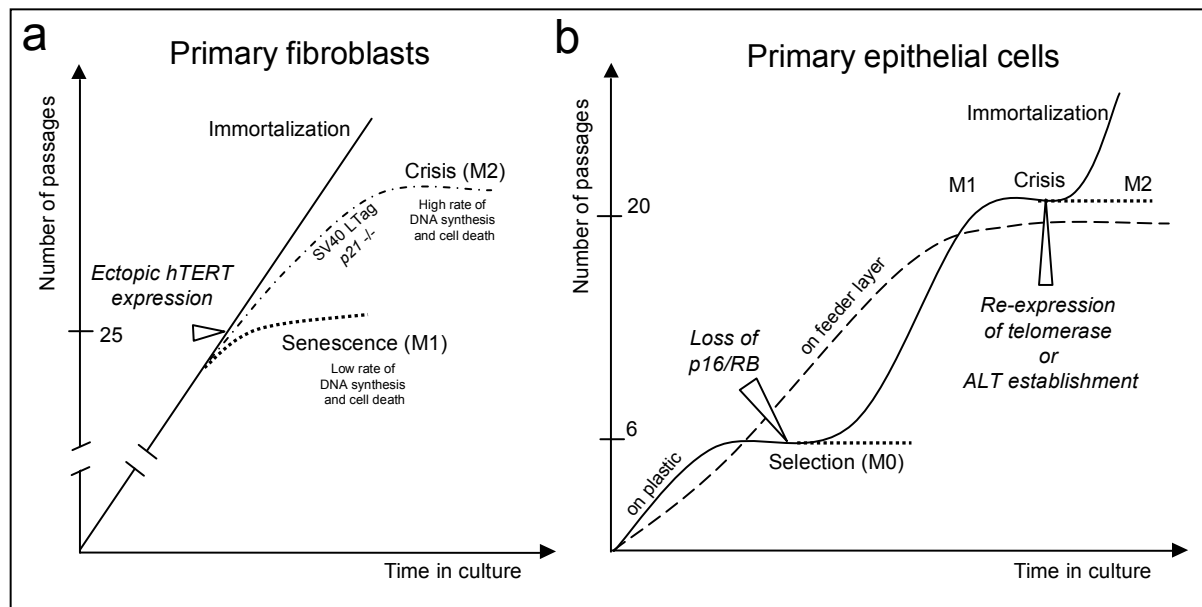


**Figure 1** Proliferation dynamics of primary human cells explanted in culture

(a) Cultured primary human fibroblasts proliferate exponentially for 70-90 population doublings (3 doublings are equivalent to 1 passage) and then enter irreversible growth arrest (M1). This state termed replicative senescence features complete insensitivity to mitogenic stimuli, retained basal level of metabolic activity and no apoptosis. Ectopic expression of the catalytic subunit of human telomerase (hTERT) in presenescent cells is sufficient to evade senescence and immortalize human fibroblasts. Fibroblasts transduced by viral oncogenic proteins (for example, SV40 large T antigen) or with a homozygous deletion of *p21* gene undergo crisis (M2). This is a state distinct from senescence in the way that the high rate of apoptosis takes over the ongoing replication. (b) Primary cells of epithelial origin (for example, mammary gland epithelium, prostate epithelium or keratinocytes) cultured under standard conditions reach the first growth plateau (M0) after a few passages (typically 6 to 8). The onset of this stage, also called selection, is associated with induction of the CDK inhibitor p16. Small fraction of cells, which has lost the p16/pRB check-point is able to surmount the M0 barrier and resume active proliferation. The second growth plateau, designated as crisis (M1) is characterized by increased genomic instability due to dysfunction of shortened telomeres. An escape from crisis requires re-expression of telomerase or activation of alternative mechanism of telomere lengthening (ALT). Culturing of primary cells on a feeder layer of irradiated fibroblasts abrogates M0 arrest and eliminates the need to inactivate p16 for immortalization of primary human epithelial cells.

Primary human skin fibroblasts represent one of the most extensively studied systems for replicative senescence. These cells undergo irreversible growth arrest (also designated as mortality stage 1, M1) after 70-90 population doublings in culture (Figure 1a). Replicative senescence in this cell type is triggered by erosion of telomeres. The ectopic expression of hTERT in presenescent primary human fibroblasts allows cells to evade replicative senescence and to become immortal without additional genomic alterations. The functional mechanism for the immortalization of skin fibroblasts is the maintenance of telomere length, not the expression of telomerase. Using a *cre*-excisable telomerase, it has been shown that the transient expression of hTERT for only seven cell divisions resulted in a 50 division extension of lifespan (Steinert et al., 2000). This increase could be entirely

explained by elongation of the shortest telomeres by 2.5 kbp and telomere shortening of 50 bp per division rate in these fibroblasts.

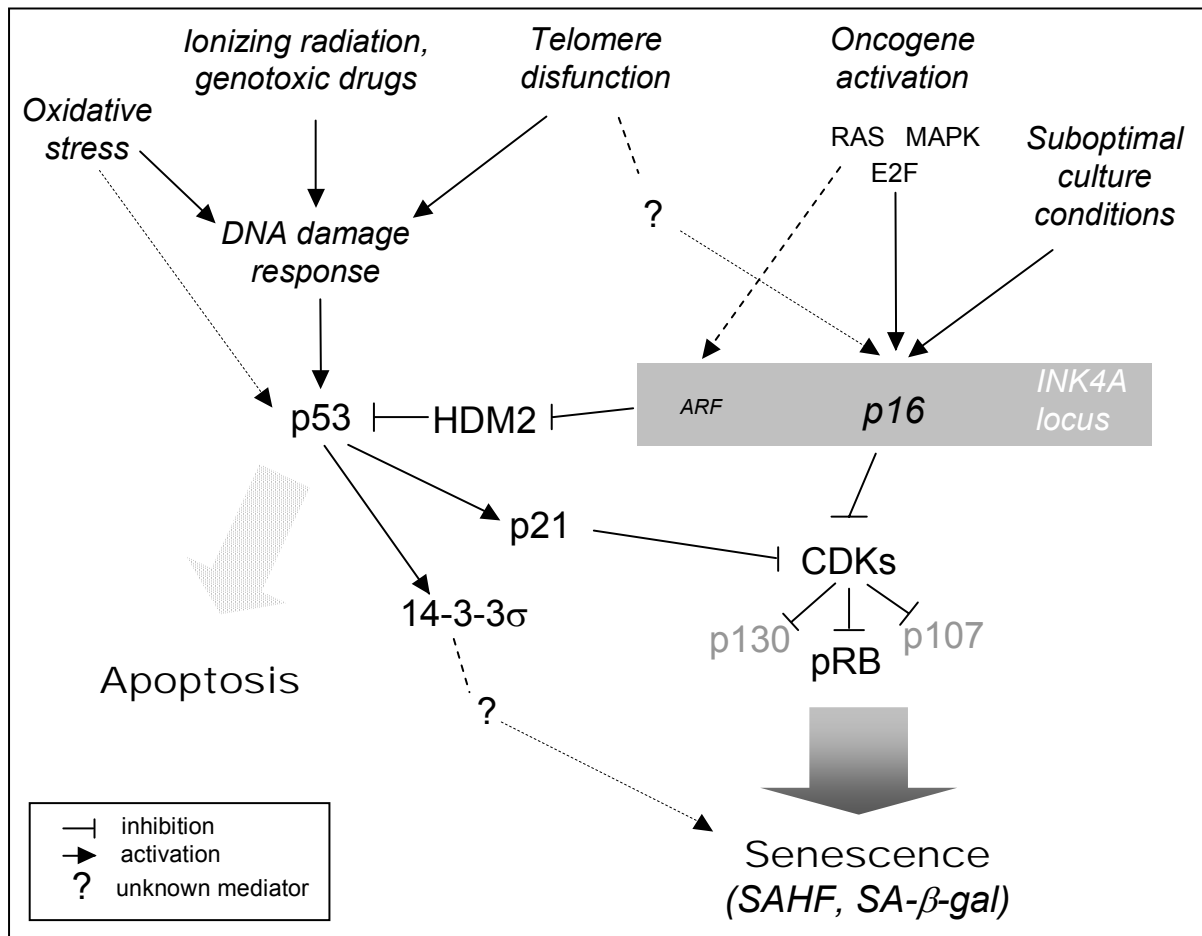


**Figure 2** Pathways involved in cellular senescence

A variety of stress conditions posing a threat of oncogenic transformation to the cell can induce terminal proliferation arrest with characteristic features of senescence - cellular enlargement and flattening, formation of heterochromatin foci (SAHF) and accumulation of acidic  $\beta$ -galactosidase (SA- $\beta$ -gal). Replication-dependent shortening of telomeres, ionizing radiation, genotoxic chemicals and oxidative stress initiate a DNA damage response resulting in the activation of the tumor suppressor protein p53 and induction of its transcriptional targets p21 and 14-3-3 $\sigma$ . p21 inhibits CDKs (particularly, CDK2-cyclin A and -cyclin E complexes) and promotes hypophosphorylation of the pocket proteins pRB, p107 and p130. Overexpression of oncogenes and inadequate culture conditions induce the CDK inhibitor p16, which inhibits CDK2 and CDK6 resulting in pRB dependent growth arrest. Inappropriate oncogene activation also induces the ARF protein, the alternative product of the INK4A locus which results in the accumulation of p53 via inhibition of its HDM2-dependent degradation.

Telomere shortening beyond a certain limit results in the activation of the DNA damage response and operates via the p53 – p21 – pRB pathway (Figure 2). The pRB protein represents a classical example of a tumor suppressor gene, inactivated in variety of familial and sporadic human cancers. The functional activity of pRB (retinoblastoma protein) is regulated by phosphorylation by cyclin-dependent kinases. Hypophosphorylated pRB binds to and inhibits the E2F family transcription factors, which mediate cell cycle progression. Inhibitors of cyclin-dependent kinases (e.g. p21,



p16, p27 and p57) prevent phosphorylation of pRB and therefore lead to inhibition of E2F resulting in cell cycle arrest.

Besides pRB, two other members of the pocket protein family, p107 and p130 are involved in the control of senescence. Germ line inactivation of *pRb* alone is not sufficient to overcome senescence in cultured mouse embryo fibroblasts (MEFs) (Dannenberg et al., 2000). However, simultaneous knock-out of the *pRb*, *p107* and *p130* genes (Dannenberg et al., 2000; Sage et al., 2000) renders MEFs completely insensitive to senescence-inducing signals, demonstrating functional redundancy between pocket proteins. Still, the relative impact of pRB on tumor prevention may be more significant than that of the other pocket proteins as mutations of *p130* and *p107* occur rarely, if ever in human cancer, whereas *pRB* mutations are common (Classon and Harlow, 2002). Consistently, acute ablation of *Rb* in senescent cells is sufficient for reversal of the cellular senescence program (Sage et al., 2003). The role of pRB in the control of senescence turned out to be more complex than simply antagonizing E2F-driven transition from G1 to S phase of cell cycle. Recently, onset of senescence has been shown to correlate with the establishment of a specific form of heterochromatin present in discrete nuclear foci, known as senescence-associated heterochromatic foci (SAHF), the formation of which is directed in part by hypophosphorylated pRB (Narita et al., 2003). These data suggest that senescence results from the stable repression of promoters associated with growth control genes.

Inactivation of cell-cycle check-points by the expression of viral oncoproteins, such as SV40 large T antigen or HPV E7, or by targeted disruption of *p21* gene in primary human fibroblasts abrogates the onset of typical replicative senescence (Figure 1a). However, cell growth eventually reaches a plateau designated as crisis (mortality stage 2, M2). In contrast to the senescent phenotype, such cells display ongoing replication (e.g. high index of BrdU incorporation), but also a high rate of apoptosis, presumably initiated due to eroded telomeres in the absence of telomerase activity. The fact, that human fibroblasts never become immortal spontaneously, underlines a very tight control of proliferation by the telomere-length check-point.

Several features of senescence in primary epithelial cells differ from those in primary fibroblasts. The time period between explanting into culture and cessation of proliferation is significantly shorter for primary epithelial cells than for fibroblasts. Typically after 6-8 passages primary human epithelial cells reach the growth plateau

(stage M0, Figure 1b) which is characterized by a very slow proliferation rate, morphological features of senescence (e.g. positive for SA- $\beta$ -Gal) and subsequent emergence of outgrowing clones capable of surmounting this first barrier (Figure 1b). After additional rounds of proliferation these “selected” at M0 stage cells undergo the next growth arrest called crisis, or M1 stage. In the absence of the p53 - and p16 - pRB-mediated checkpoints, cultured cells with dysfunctional telomeres continue to proliferate, entering a period of slow growth that is characterized by genomic instability. Clones emerging from crisis invariably reactivate telomerase or establish the alternative lengthening of telomeres (ALT) mechanism (reviewed in Sharpless and DePinho, 2004). During crisis, the unprotected telomere ends in proliferating cells can be illegitimately fused through DNA repair mechanisms, ultimately leading to the generation of complex non-reciprocal translocations, a hallmark feature of adult solid tumors.

The onset of the M0 stage is dependent on p16 induction and hypophosphorylation of pRB and precedes the shortening of telomeres beyond a critical limit required for the activation of the DNA damage pathway. Immortalization of primary epithelial cells requires both hTERT expression and p16 inactivation. However, the culturing of primary human epithelial cells on a feeder layer of mesenchymal cells prolongs the life span in culture significantly and abrogates the need to inactivate p16 for immortalization (Ramirez et al., 2001). This indicates that inadequate culture conditions may trigger the p16-dependent growth arrest *ex vivo* (Figure 2). Whereas the *in vivo* relevance of a “culture-shock”-induced and p16-mediated arrest has not explicitly been shown yet, the important role of p16 in tumor suppression is clearly demonstrated by its frequent inactivation in several human cancers, especially characteristic for malignant melanoma (Sharpless and Chin, 2003). Moreover, gradual accumulation of p16 in aging tissue was shown to be the most consistent marker of cellular senescence *in vivo* (Krishnamurthy et al., 2004).

Several stress conditions evoke a terminal proliferation arrest before telomeres become short enough to elicit the DNA damage signal (Figure 2). This state shares many features with replicative senescence and is referred to as premature senescence (reviewed in Serrano and Blasco, 2001). For example, DNA damage response induced by ionizing radiation or oxidative stress results in accumulation of p53 and growth arrest. Another trigger of premature senescence is an activation of oncogenes, such as Ras or E2F. Although this pathway is particularly relevant to the

prevention of malignant transformation, the understanding of its molecular mechanisms remains incomplete. In mouse cells senescence induced by Ras requires primarily the function of the Arf protein, which is the alternative product of the *INK4a* genomic locus. Induction of the Arf leads to the inhibition of Mdm2 and thereby accumulation of p53 (reviewed in Voorhoeve and Agami, 2004). In human cells initiation of growth arrest after overexpression of an oncogene (e.g. constitutively active RAS mutant) is characterized by a more prominent role of p16<sup>INK4a</sup> than ARF (Voorhoeve and Agami, 2003).

Expression profiling of senescent cells revealed the existence of a specific transcriptional program (Ly et al., 2000; Shelton et al., 1999; Zhang et al., 2003). An important issue is whether the senescence program can be activated in tumor cells, which already underwent malignant transformation, and therefore might be exploited for therapeutic purposes. Despite the fact that many key regulators such as p53 or p16 are often inactivated in cancer cells, under some circumstances the senescence-like growth arrest can be induced in tumor cells (reviewed in Kahlem et al., 2004). Moreover, tumor cell senescence is detectable following DNA-damaging treatment *in vivo* and significantly increases overall survival of the host (Schmitt et al., 2002; te Poele et al., 2002). Further characterization of the senescence-associated transcriptional program may help to identify novel mediators of this important biological phenomenon and potential targets for therapeutic intervention.

## 1.2 14-3-3 $\sigma$ in cancer suppression

The tumor suppressor protein p53 is a nodal point in the network of DNA damage induced signaling pathways. The p53 mediates inhibition of cell proliferation, presumably to allow time for repair or to permanently arrest damaged cells (Vogelstein et al., 2000). The net effect of p53 activation, which is typically proliferation arrest or apoptosis, is determined by the subset of transcriptional targets activated in a certain cell type and signaling context. Together with p21<sup>WAF1</sup>, 14-3-3 $\sigma$  belongs to a subset of p53 targets which mediate cell-cycle arrest, whereas other p53 target genes mediate programmed cell death (Figure 2).

14-3-3 $\sigma$ , or stratifin (SFN), belongs to the 14-3-3 family comprising six other members in mammals (designated  $\beta$ ,  $\epsilon$ ,  $\gamma$ ,  $\eta$ ,  $\tau$ ,  $\zeta$ ), characterized by high degree of homology (reviewed in Yaffe, 2002). 14-3-3 proteins form homo- and heterodimers

and bind to protein ligands that have been phosphorylated on serine/threonine residues in a consensus binding motif. The binding can regulate other proteins by cytoplasmic sequestration, masking of interaction domains and export or import sequences, prevention of degradation, modulation of enzymatic activity and transactivation, and facilitation of protein modifications (reviewed in Hermeking, 2003). Recently the crystal structure of 14-3-3 $\sigma$  bound to an optimal phosphopeptide ligand was solved, providing an explanation for specific properties of the sigma isotype with regard to other 14-3-3 proteins (Wilker et al., 2005). In contrast to other 14-3-3 isoforms, the  $\sigma$  protein preferentially forms homodimers and its ligand specificity is determined by a second binding site unique for 14-3-3 $\sigma$ , rather than by the phosphopeptide binding cleft conserved in all 14-3-3 family members (Wilker et al., 2005). Putative determinants of ligand binding and dimerization specificity were revealed by comparison of the crystal structure of 14-3-3 $\sigma$  to the structure of the  $\tau$  and  $\zeta$  isoforms (Benzinger et al., 2005).

14-3-3 $\sigma$  is the only isoform of 14-3-3 proteins, which is induced after DNA damage (Figure 3). Induction of 14-3-3 $\sigma$  mRNA by DNA damage was identified in a SAGE (serial analysis of gene expression) based screen for genes induced after  $\gamma$ -irradiation in colorectal cancer cells expressing wild type p53 (Hermeking et al., 1997). In this study p53 was found to directly activate the transcription of 14-3-3 $\sigma$  via p53-responsive element in the promoter of the gene.  $\Delta$ Np63 $\alpha$ , an isoform of the p53 homolog p63, which lacks a transactivation domain, was shown to bind to the p53-responsive element in the 14-3-3 $\sigma$  promoter, but, in contrast to p53, represses transcription of 14-3-3 $\sigma$  (Westfall et al., 2003). BRCA1 was shown to affect G<sub>2</sub>/M progression by inducing expression of 14-3-3 $\sigma$  (Aprelikova et al., 2001).

The ectopic expression of 14-3-3 $\sigma$  in colorectal cancer cells and primary prostate epithelial cells leads to the initiation of a G<sub>2</sub> arrest (Hermeking et al., 1997). A similar effect was observed in breast carcinoma cell line (Ferguson et al., 2000). The negative effect of induced 14-3-3 $\sigma$  expression on cell-cycle progression is mediated by its binding to CDC2/cyclin B1. Cytoplasmic 14-3-3 $\sigma$  prevents nuclear localization of the CDC2/cyclin B complex, which is required for progression through mitosis (Chan et al., 1999). Disruption of the 14-3-3 $\sigma$  gene by homologous recombination in colon cancer cells results in impaired G<sub>2</sub>/M checkpoint after DNA damage:  $\gamma$ -irradiated 14-3-3 $\sigma$ -knockout cells are unable to maintain a G<sub>2</sub> arrest and

eventually undergo mitotic catastrophe (Chan et al., 1999; Chan et al., 2000). Moreover, *14-3-3 $\sigma$* -deficient cells show increased genomic instability, characterized by loss of telomeric repeat sequences, chromosome end-to-end fusions and nonreciprocal translocations (Dhar et al., 2000). Altogether these facts strongly argue for an important role of *14-3-3 $\sigma$*  in the maintenance of genomic integrity.

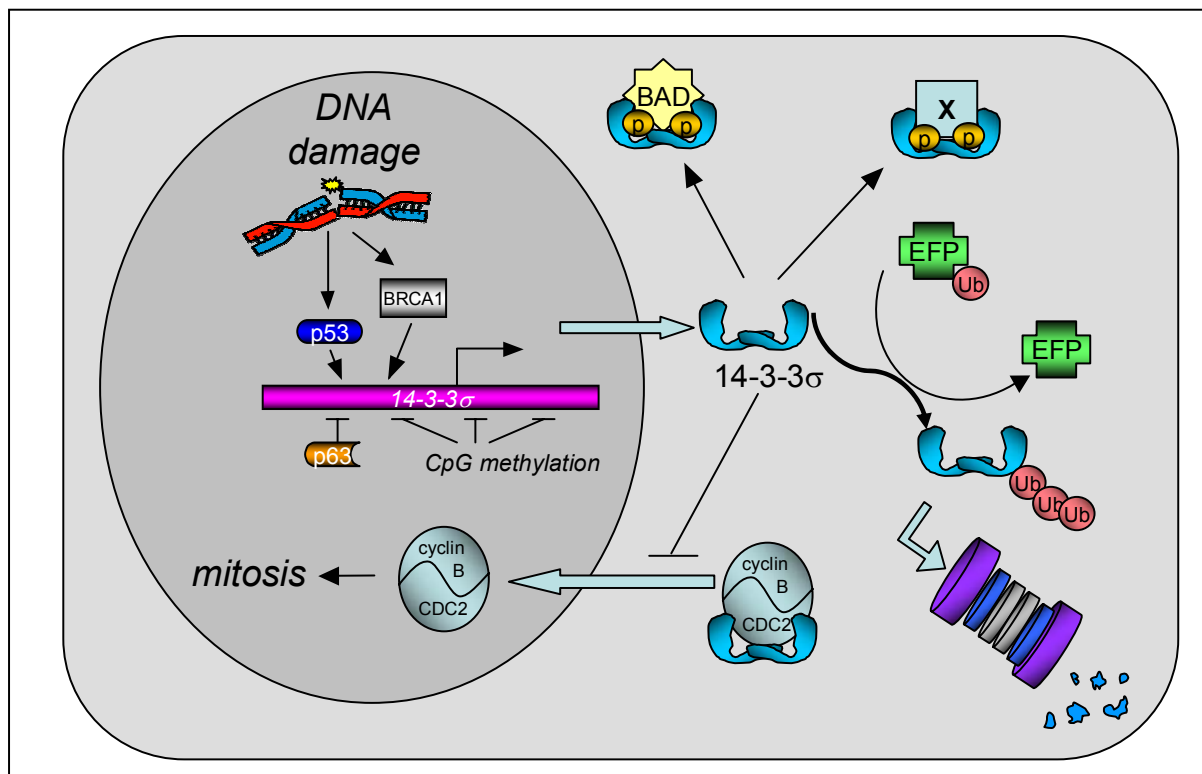


**Figure 3** Regulation and function of *14-3-3 $\sigma$*

After DNA damage p53 binds to the promoter and induces transcription of the *14-3-3 $\sigma$*  gene. BRCA1 acts as a co-activator in the induction of *14-3-3 $\sigma$*  transcription by p53. In the cytoplasm *14-3-3 $\sigma$*  forms homodimers and binds to a variety of ligands phosphorylated at the serine/threonine residues in a consensus binding motif (p). The nuclear translocation of cyclin B/CDC2 complexes required for the initiation of mitosis is inhibited by *14-3-3 $\sigma$*  binding. The BH3-domain protein BAD phosphorylated by AKT associates with *14-3-3 $\sigma$*  and loses its ability to antagonize the function of the anti-apoptotic BCL2-like proteins. A dominant negative form of p63 (e.g.  $\Delta$ Np63 $\alpha$ ) represses *14-3-3 $\sigma$*  expression. CpG methylation contributes to epigenetic silencing of *14-3-3 $\sigma$*  in neoplasia and, presumably, in normal cells of mesenchymal origin. A RING-finger-dependent E3 ubiquitin (Ub) ligase (EFP) targets *14-3-3 $\sigma$*  for proteasomal degradation. X = unknown binding partner.

A hallmark of tumor suppressive factors is their frequent inactivation in primary cancer cells. SAGE analysis revealed down-regulation of sigma in breast cancer cells (Nacht et al., 1999). A subsequent search for mutations in the *14-3-3 $\sigma$*  locus did not reveal any genetic alterations which could explain its down-regulation. Instead the epigenetic silencing by CpG methylation turned out to be responsible for the loss or reduction of *14-3-3 $\sigma$*  expression in more than 90 % of primary breast cancers (Ferguson et al., 2000). Hypermethylation of the *14-3-3 $\sigma$*  locus occurs rather early,

as it was detected in 38% of atypical hyperplasia (Umbricht et al., 2001). Moreover, hypermethylation of *14-3-3 $\sigma$*  was detected in adjacent histologically normal breast epithelium, while this was never observed in individuals without evidence of breast cancer. The treatment of breast cancer cells with an inhibitor of DNA methyltransferases, 5-aza-2'-deoxycytidine (5Aza-2'dC), results in induction of the *14-3-3 $\sigma$*  mRNA indicating a causative role of hypermethylation in the loss of *14-3-3 $\sigma$*  expression (Ferguson et al., 2000). Consistent with a function of *14-3-3 $\sigma$*  in preventing the acquisition of chromosomal abnormalities as revealed by somatic knock-out in colon cancer cell line, breast cancer cells with hypermethylation of *14-3-3 $\sigma$*  display increased genomic instability (Ferguson et al., 2000).

Among epithelial tissues, the epidermis is characterized by the highest level of *14-3-3 $\sigma$*  expression. Differentiation and exit from the stem cell compartment in keratinocytes is accompanied by an increase of *14-3-3 $\sigma$*  expression (Pellegrini et al., 2001). Experimental inactivation of *14-3-3 $\sigma$*  in primary human keratinocytes by an anti-sense approach was shown to be sufficient for their immortalization, suggesting that *14-3-3 $\sigma$*  is involved in control of the cellular senescence (Dellambra et al., 2000). Taken together these data indicate that *14-3-3 $\sigma$*  may function to restrain aberrant proliferation in the epidermis. However, *14-3-3 $\sigma$*  expression in skin tumors and non-neoplastic skin diseases has not yet been analyzed systematically.

### **1.3 Epigenetics and cancer**

In the process of neoplastic transformation changes in the function of critical genes which allow cells to overgrow their neighboring cells are selected for. The altered genes which are causally involved in carcinogenesis can be broadly divided in two major classes: oncogenes and tumor-suppressor genes. Whereas oncogenes gain an increased function via activating point mutations or gene amplification, tumor suppressor genes lose their function in cancer cells. Tumor suppressor genes may be subdivided into caretakers and gatekeepers (Kinzler and Vogelstein, 1997). Caretaker genes encode proteins which function in the preservation of genomic integrity, whereas gatekeepers keep cells in a defined state of differentiation.

The inactivation of tumor suppressor genes is mediated by two mechanisms: genetic inactivation by DNA mutations and epigenetic silencing. In some cases

genetic and epigenetic events complement each other. In general bi-allelic gene inactivation resulting in complete loss of function is characteristic for tumor suppressor genes.

The term *epigenetic* refers to information which is transmitted from the parental genome to the next generation of cells and is not encoded by the primary DNA sequence. Epigenetic mechanisms are essential for the regulation of gene expression and genome integrity in normal cells (Bird, 2002; Jaenisch and Bird, 2003; Li, 2002). The maintenance of epigenetic information is mediated by polycomb group proteins and cytosine methylation within CpG-dinucleotides, also referred to as DNA methylation.

Patterns of DNA methylation and chromatin structure are profoundly altered in neoplasia and include genome-wide losses of and regional gains in DNA methylation. Global hypomethylation compromises stability of the genome and in turn may promote secondary genetic alterations (Eden et al., 2003; Gaudet et al., 2003), whereas the local hypermethylation of promoter regions is associated with transcriptional silencing and possible loss of tumor suppressor gene expression.

Epigenetic inactivation of tumor suppressor genes contributes significantly to tumor development (Feinberg and Tycko, 2004; Jones and Baylin, 2002). The genes aberrantly methylated in human cancer fall into several functional categories intimately involved in cellular processes relevant to carcinogenesis such as DNA repair (*MGMT*, *MLH1*, *BRCA1*), cell cycle control (CDK inhibitors - *p15*, *p16*, *p27*), apoptosis (*APAF1*, *CASP8*), invasion (*CDH1*, *TIMP3*), angiogenesis (*THBS1*, *VHL*) and others. Nearly 50% of the genes that cause familial forms of cancer when mutated in the germ line are known to undergo methylation-associated silencing in various sporadic forms of cancer (Jones and Baylin, 2002). Although some methylation changes seem to be common to many kinds of cancer, tissue-specific differences exist. For example, the *p15<sup>INK4B</sup>* promoter is frequently methylated in lymphoid, but not in solid cancers (Herman et al., 1997), and *glutathione S-transferase π 1* (*GSTP1*) is methylated in prostate, breast and hepatic cancers, but rarely in others (Lin et al., 2001).

The molecular mechanisms of epigenetic silencing during tumor formation are only partially understood. In normal cells the pattern of CpG methylation is established by two types of methyltransferases catalyzing the addition of a methyl-group at the C-5 position of cytosine: DNMT1 serves as a maintenance

methyltransferase, whereas DNMT3A and DNMT3B mediate *de novo* DNA methylation. All three DNMTs are modestly over-expressed at the mRNA and/or protein level in many types of tumor cells (De Marzo et al., 1999b; Robertson et al., 2000). Ectopic expression of DNMT1 cooperates with oncogenes in the transformation of primary cells supporting the idea that aberrant expression of DNA methyl-transferases may contribute to abnormal promoter methylation in cancer cells (Bakin and Curran, 1999).

Factors directing the activity of DNMTs to specific genomic sites under normal and pathological conditions remain largely unknown. Covalent modifications of core histones may serve as plausible marks for the establishment of DNA methylation. The methylation of histone H3 lysine 9 was shown to be a prerequisite for DNA methylation in *Neurospora crassa* and *Arabidopsis thaliana* (Jackson et al., 2002; Tamaru and Selker, 2001). Although this requirement does not seem to be conserved in mammalian cells, the concept that histone methylation provides a signal which somehow can be interpreted by DNA methylation machinery is supported by experimental data. For example, the histone methyltransferase Suv39H1 directs DNA methylation to satellite repeats at pericentric heterochromatin (Lehnertz et al., 2003). The *p16<sup>INK4A</sup>* gene has been shown to undergo re-activation after reversal of DNA methylation after experimental removal of *DNMT* activity in colorectal cancer cells (Bachman et al., 2003). Subsequent re-silencing of *p16<sup>INK4A</sup>* occurred after prolonged passage of these cells. Methylation of histone H3-K9 was detected in association with re-silencing of this tumor suppressor gene in the absence of DNA methylation (Bachman et al., 2003). Therefore, the methylation of histones may precede methylation of DNA during epigenetic silencing of tumor suppressor genes. In plants and some animals double stranded RNAs were implicated in the guidance of *de novo* methylation (Bender, 2001; Matzke et al., 2001). Also, RNAi-mediated transcriptional silencing has been associated with promoter methylation in human cells (Kawasaki and Taira, 2004; Morris et al., 2004). In addition, transcription factors which interact with DNA in a sequence-specific manner may direct CpG methylation to specific promoters. In line with this hypothesis, it was recently shown that Myc protein recruits DNMT3A methyltransferase to the *p21<sup>WAF1</sup>* promoter and represses its expression through CpG methylation (Brenner et al., 2005). However, so far it is unclear whether any of these mechanisms plays a role in establishing the aberrant methylation patterns seen in human malignancies.



Methylated CpG-dinucleotides are bound by the methyl-CpG-binding domain (MBD) containing proteins MBD1, MBD2, MBD3, MBD4 and MeCP2. The protein Kaiso binds to methylated CpG groups via its zinc-finger motif. With the exception of MBD4, which operates in mismatch repair, these proteins were shown to recruit chromatin remodeling factors (e.g. Mi2/NuRD complex) and histone deacetylases (HDAC) to the respective promoters and thereby establish transcriptionally inactive chromatin (Figure 4). How and at which stage the CpG methylation of tumor suppressor genes is established during tumor progression is still unclear. Stochastic, age-associated accumulation of aberrantly methylated CpG-sites may be involved in this process.

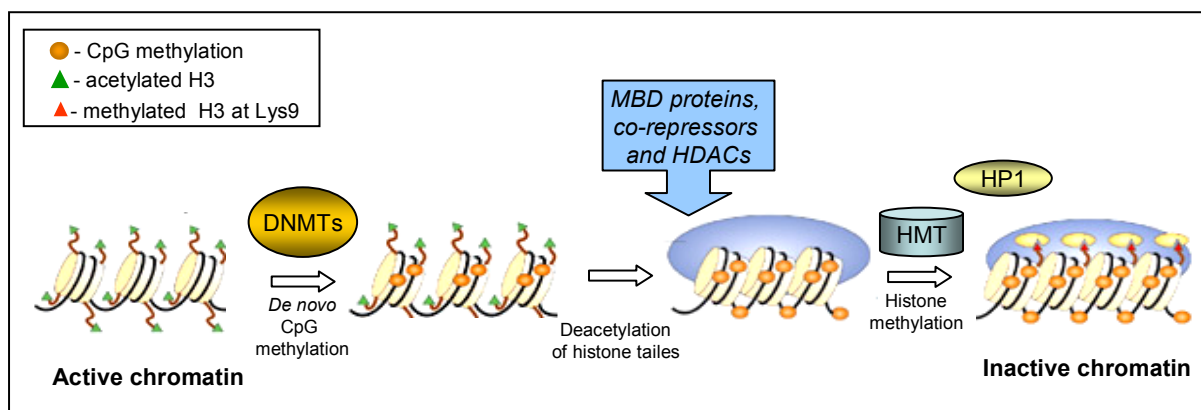


**Figure 4** The relationship between DNA methylation and chromatin structure

The carbon atom at the 5' position of cytosines within a CpG-dinucleotide context can be methylated by DNA methyltransferases (DNMTs). Clusters of methylated CpGs are recognized and bound by specific proteins sharing a methyl-CpG binding domain (MBD). In turn, MBD proteins recruit transcriptional co-repressors, chromatin remodeling complexes and histone deacetylases (HDACs). Deacetylation of histone tails (N-terminal parts of histone H3 and H4) results in alteration of nucleosomal structure and decrease in transcriptional activity of the chromatin. Subsequent methylation of histone tails by histone methyltransferases (HMTs) (particularly, lysine 9 of H3 and lysine 20 of H4) and recruitment of auxiliary proteins, such as heterochromatin binding protein 1 (HP1), enhance the formation of transcriptionally incompetent heterochromatin.

Experimental reversion of DNA methylation leads to re-expression of silenced genes in tumor cells, which may have consequences at the cellular level: e.g. restored sensitivity to apoptotic stimuli after reactivation of *caspase 8* (Hopkins-Donaldson et al., 2003) and *APAF1* (Soengas et al., 2001) or inhibition of cell-proliferation after re-expression of the CDK-inhibitor *p16* (Rhee et al., 2002). Consistent with a role of hypermethylation-mediated gene repression in tumor formation, inactivation of *DNMT1* or *MBD2* suppresses intestinal tumorigenesis in *Apc<sup>min</sup>* mice (Eads et al., 2002; Sansom et al., 2003).

Although CpG methylation patterns can be erased during DNA replication in the absence of DNMT activity, aberrant epigenetic marks persist through multiple

generations of cells and are as stable as genetic alterations. For example most cancer cell lines maintain the pattern of aberrant DNA methylation characteristic for primary tumors of the same tissue origin (Paz et al., 2003). Moreover, aberrant methylation of CpG-islands, also called epimutation, can be transmitted through the germ line, as recently shown for the *MLH1* gene (Suter et al., 2004).

The estimated number of CpG-islands abnormally methylated in a particular type of cancer is about 600 (Costello et al., 2000), which is significantly greater than the number of genes experimentally shown to undergo epigenetic inactivation in any one cancer type. Therefore, genome-wide rather than candidate gene approach is desirable for the efficient identification of novel targets for epigenetic inactivation in human cancer. As one kind of approach the comprehensive analysis of the genes expression after treatment of tumor cell lines with inhibitors of DNA methyltransferases (5Aza-2'dC) and HDACs (TSA) was recently used to identify genes specifically silenced in tumors of the colon and oesophagus (Suzuki et al., 2002; Yamashita et al., 2002). The key component of this strategy is a microarray technique exploited for the analysis of genome-wide transcriptional changes. The major advantage of this approach is the functional link between demethylation and re-expression of a particular gene, which other approaches, such as restriction landmark genomic scanning, differential methylation hybridization or methylation-specific RDA do not provide (Jones and Baylin, 2002).

#### **1.4 Prostate Cancer**

Prostate cancer (PCa) is the most commonly diagnosed malignancy in the male population of the western world. Small prostatic carcinomas are detected in 29% of men between 30 and 40 years of age and in 64% of men from 60 to 70 years of age (Nelson et al., 2003). In 25% of the affected men this usually indolent disease behaves aggressively and progresses to metastasis. In the year 2005 Pca will presumably be responsible for 30,350 of deaths in the US, accounting for 10% of all male cancer deaths, second only to lung cancer (American cancer society. Cancer facts and figures, 2005.). The molecular basis of PCa is still poorly understood, particularly due to the extreme heterogeneity of primary tumors and the limited number of available stable cell lines.

The identification of PCa-specific tumor suppressor genes has been hindered by several factors. First, no known syndrome predisposing to PCa has been identified, which could serve to identify genetic loci harboring tumor suppressor genes. Second, the high prevalence of PCa makes it difficult to identify familial clustering and cases of early onset, although a role for genetic predisposition has been proposed for ~40% of all PCa cases (Nelson et al., 2003). At least seven chromosomal regions have been associated with a predisposition to PCa (reviewed in Schulz et al., 2003). However, the candidate genes identified in these regions are altered at low frequencies, which suggests that genetic predisposition to PCa involves alterations in additional genes. Polymorphisms in detoxifying or repair genes, such as *GSTT*, *GSTP1* and *MTHFR* may also contribute to predisposition for PCa (Kimura et al., 2000; Kote-Jarai et al., 2001; Steinhoff et al., 2000).

The timing and progression of PCa is not understood. Benign prostatic hyperplasia (BPH), a very common hyperproliferative lesion in the aged prostate, does not develop into a malignant tumor. The putative precursor of carcinoma is thought to be a lesion called prostate intraepithelial neoplasia or PIN (Figure 5), which resembles the *carcinoma in situ* stage of a breast or cervical cancer. PIN displays focal proliferation areas with nuclear heterogeneity and atypia confined within epithelial layer. It was proposed, that the stage designated as proliferative inflammatory atrophy (PIA) can precede the development of PIN (De Marzo et al., 1999a) thus representing the earliest pre-cancer lesion in the prostate (Figure 5).

At the time of diagnosis, prostate-cancer cells contain many somatic mutations, gene deletions, gene amplifications, chromosomal rearrangements, and changes in DNA methylation (Figure 5). These alterations probably accumulate over a period of several decades. The most commonly reported chromosomal abnormalities in PCa appear to be gains at 7p, 7q, 8q, and Xq, and losses at 8p, 10q, 13q, and 16q (reviewed in Karan et al., 2003). A striking heterogeneity in chromosomal abnormalities has been seen in different cases, in different lesions in the same case, and in different areas within the same lesion. Additional somatic genomic alterations appear to arise in association with the progression of prostate cancer.

Genetic inactivation of tumor suppressor genes, which are known from other types of cancer, is detected at a relatively low frequency in early stage PCa, e.g. mutations of p53 are rare (reviewed in Abate-Shen and Shen, 2000; Karan et al., 2003; Nelson et al., 2003). *PTEN* may be one of the most consistently affected tumor

suppressor genes in PCa. 30% of primary PCa and 63% of metastatic PCa display mutation or deletion of *PTEN* (reviewed in Dahia, 2000; Suzuki et al., 1998). The *NKX3.1* gene, located at 8p21, encodes a prostate-specific homeobox protein that is likely to be essential for normal prostate development and is therefore a candidate gatekeeper gene. Although genetic studies in mouse models provided support for this hypothesis (Abdulkadir et al., 2002; Bhatia-Gaur et al., 1999), molecular analyses have not yet established *NKX3.1* as a somatic target for inactivation during prostatic carcinogenesis, as somatic mutations of a remaining allele are not detected in tumors with heterozygous deletion of the *NKX3.1*.

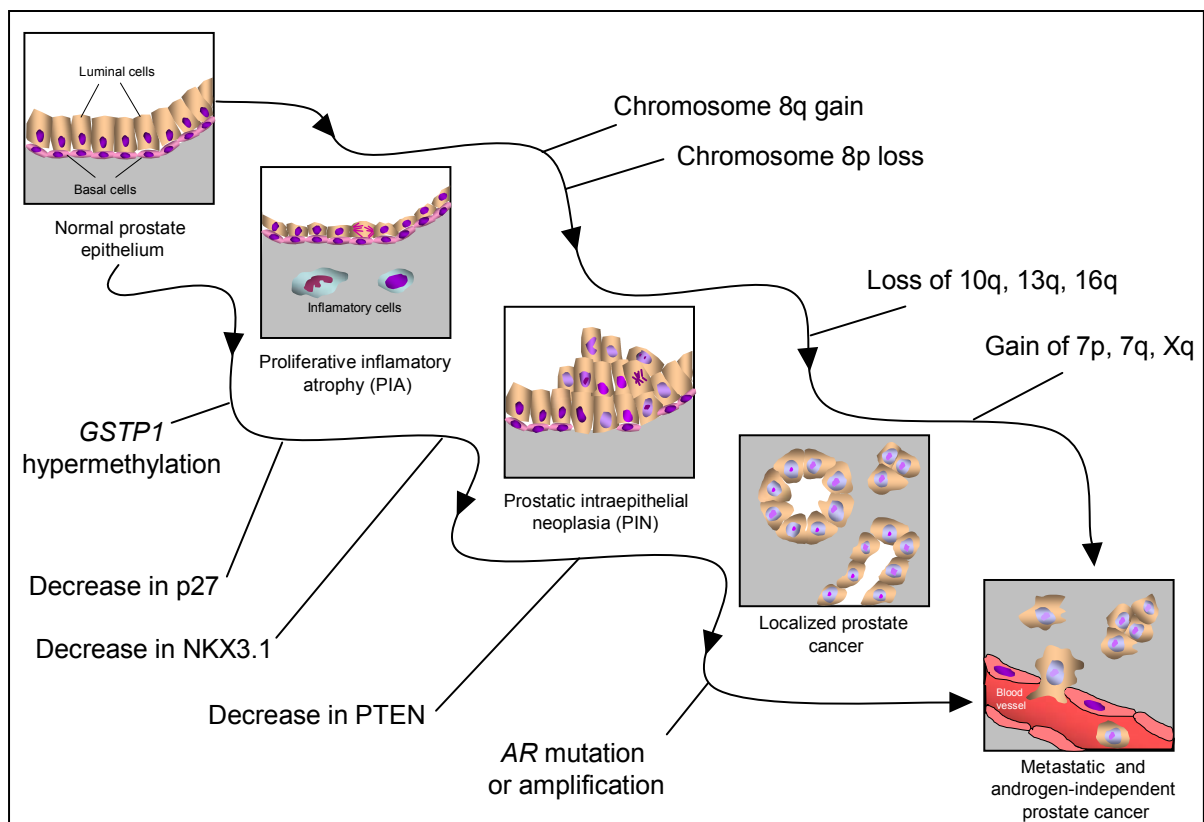


**Figure 5** The molecular pathogenesis of prostate cancer (adapted from Nelson et al., 2003)

AR = androgen receptor gene. For details see text.

Abnormal DNA methylation is commonly found in PCa (reviewed in Li et al., 2005). For example, aberrant CpG methylation was found for *GSTP1* in ~90%, for *RASSF1A* in ~63% and for *RAR $\beta$ 2* in ~79% of the analyzed PCa (Kuzmin et al., 2002; Nakayama et al., 2001; Singal et al., 2001). Other examples of genes frequently silenced in PCa are *APC*, *MGMT* and *MDR1* (Flori et al., 2004; Kang et al., 2004; Yegnasubramanian et al., 2004). Detection and quantification of specific CpG methylation patterns has advantages over protein- and RNA-based diagnostic methods (Laird, 2003) and can be performed in different clinical samples including

plasma, prostate secretions, voided urine or ejaculates (Li et al., 2005), providing an additional tool for noninvasive diagnostics of PCa. The use of a panel of CpG methylation markers in combination with standard histologic review of needle biopsies was shown to increase the sensitivity of PCa diagnosis (Tokumaru et al., 2004).

In spite of the advance in PCa diagnosis attributed to the introduction of serum prostate specific antigen (PSA) determination in clinical practice, early detection of PCa remains a problem. In general, prostate cancer is diagnosed by needle biopsies taken from the patients, in which raised level of serum PSA or lower urinary tract symptoms have been revealed. However, serum PSA levels can be increased in benign conditions, and biopsies may miss microscopic foci of cancer (Ercole et al., 1987; Smith and Catalona, 1995). Therefore, the development of a more sensitive and specific set of markers that could facilitate the diagnosis of prostate cancer at the earliest stages should improve the current standard of care. Moreover, it would be useful to identify molecular markers that cannot only sensitively and specifically diagnose early-stage prostate cancer but also help identify men that would later progress to having symptomatic or metastatic disease.

The identification of new genes aberrantly methylated in PCa promises a better understanding of the etiology and progression mechanisms of this disease. Furthermore, this information will aid to establish tumor markers of increasing specificity and sensitivity potentially useful for diagnosis and prognosis of PCa.

## **2. Aim of the study**

The present study had the following aims:

- I. Analysis of the transcriptional program associated with replicative senescence in primary human cells in order to identify genes and signaling pathways which may be amenable to pharmacologic interference in order to induce cellular senescence in cancer cells
  
- II. Analysis of possible mechanisms of down-regulation of 14-3-3 $\sigma$  expression in human skin diseases.
  
- III. Identification and functional analysis of genes commonly inactivated by aberrant DNA methylation in prostate cancer.

### 3. Materials

#### 3.1 Chemicals

Magnesium chloride, sodium dodecyl sulfate (SDS), sodium citrate, sodium bisulfite, sodium nitroprusside (SNP), ethylene glycol-bis( $\beta$ -aminoethyl ether)-N,N,N',N'-tetraacetic acid (EGTA), ethylenediaminetetraacetic acid (EDTA), sodium orthovanadate, sodium fluoride, sodium chloride, phenylmethylsulfonyl fluoride, potassium ferricyanide ( $K_3Fe(CN)_6$ ), potassium ferrocyanide ( $K_4Fe(CN)_6$ ), ampicillin, puromycin, geneticin (G418), doxorubicin (adriamycin), trichostatin A, 5-aza-2'-deoxycytidine, crystal violet, propidium iodide, ethidium bromide, hydroquinone, paraformaldehyde, polyoxyethylensorbitanmonolaureate (Tween 20), Trizma® base, eosin Y solution were from Sigma (Munich, Germany).

Hydrochloric acid, dimethylsulfoxide, xylene, Mayer's hematoxylin solution were from Merck (Darmstadt, Germany).

6-anilino-5,8-quinolinedione (LY 83583) (Calbiochem, Bad Soden, Germany)

5-brom-4-chloro-3-indolyl-beta-D-galactopyranoside (X-gal) (Promega, Mannheim, Germany)

Etoposide (Alexis, Lausen, Switzerland)

Phenol/chloroform/isoamylalcohol mixture (Carl Roth, Karlsruhe, Germany)

Triton X-100 (Carl Roth)

Biotin-CTP and biotin-UTP ribonucleotides (Loxo, Dossenheim, Germany)

$\alpha$ -<sup>32</sup>P-dCTP (Amersham, Freiburg, Germany)

Oligonucleotides (Metabion, Martinsried, Germany)

Glutaraldehyde (Serva, Heidelberg, Germany)

Agarose for gel electrophoresis (Peqlab, Erlangen, Germany)

#### 3.2 Enzymes and commercial kits

*Platinum Taq* DNA polymerase (Invitrogen, Karlsruhe, Germany)

Proteinase K (Sigma)

RNAse (Roche, Mannheim, Germany)

RNAse A (Sigma)

T4 DNA ligase (NEB)

T4 DNA polymerase (NEB, Frankfurt, Germany)

Annexin V-FITC apoptosis detection kit (BD Pharmingen, San Diego, CA, USA).

APAAP immunostaining system kit (DAKO, Copenhagen, Denmark)  
BigDye terminator 3.1 sequencing kit (Applied Biosystems, Darmstadt, Germany)  
Bradford assay (Bio-Rad Laboratories, Hercules, CA, USA)  
BrdU Labelling and Detection Kit I (Roche)  
cGMP immunodetection kit (Sigma)  
ECL kit (PerkinElmer, Cologne, Germany)  
FastStart-DNA Master SYBR Green 1 kit (Roche)  
GalactoLight  $\beta$ -galactosidase detection kit (Tropix, Bedford, MA, USA)  
Gel extraction kit (Qiagen, Hilden, Germany)  
Lipofectamine™ 2000 transfection reagent (Invitrogen)  
Luciferase Assay System kit (Promega)  
Miniprep kit (Qiagen)  
Nucleotide removal kit (Qiagen)  
PCR purification kit (Qiagen)  
QuickHyb hybridization solution (Stratagene, Amsterdam, The Netherlands)  
Readiprime II random prime labeling system (Amersham)  
RevertAid First Strand cDNA synthesis kit (MBI Fermentas, St. Leon-Rot, Germany)  
Ribomax T7 in vitro transcription kit (Promega)  
RNAgent RNA isolation kit (Promega)  
RNeasy RNA purification kit (Qiagen)  
SuperScript™ III first strand cDNA synthesis kit (Invitrogen)  
SuperScript™ double stranded cDNA synthesis kit (Invitrogen)  
TOPO-TA cloning kit for sequencing (Invitrogen)  
Vectastain Elite ABC kit (Vector Laboratories, Burlingame, CA, USA)

### **3.3 Antibodies**

#### **3.3.1 Primary antibodies**

Mouse monoclonal anti- $\beta$ -catenin (clone 19) (Transduction Laboratories, Lexington, KY, USA)  
Mouse monoclonal anti-p63 (4A4) (DAKO, Copenhagen, Denmark)  
Mouse monoclonal anti-p53 (Pab 1801) (Santa Cruz Biotechnology, CA, USA)  
Mouse polyclonal anti-p21 (Ab-11) (NeoMarkers, Fremont, CA, USA)  
Rabbit polyclonal anti-p16 (C-20) (Santa Cruz Biotechnology)  
Mouse monoclonal anti- $\alpha$ -tubulin (TU-02) (Santa Cruz Biotechnology)



Rabbit anti-14-3-3 $\sigma$  affinity purified serum described in (Chan et al., 1999)  
 Mouse monoclonal anti-pRB (BD Pharmingen)  
 Rabbit polyclonal anti-phosphor-ERK1/2 (Thr202, Tyr204) (Cell Signaling Technology, Frankfurt, Germany)  
 Rabbit polyclonal anti- ERK1/2 (Cell Signaling Technology)  
 Goat polyclonal anti-SFRP1 (C-19) (Santa Cruz Biotechnology)  
 Mouse monoclonal anti-VSV (p5d4) (Sigma)

### 3.3.2 Secondary antibodies

Goat anti-rabbit IgG HRP-conjugate (Promega)  
 Goat anti-mouse IgG HRP-conjugate (Promega)  
 Donkey anti-goat IgG HRP-conjugate (Jackson ImmunoResearch Laboratories, West Grove, PA, US)  
 Rabbit anti-mouse IgG Cy3-conjugate (Jackson ImmunoResearch Laboratories)  
 Horse anti-mouse IgG biotinylated (Vector Laboratories)  
 Mouse anti-rabbit IgG (DAKO)

### 3.4 DNA constructs

pCMV- $\beta$ -gal (BD Clontech), pLXSN (BD Clontech) , TOPO-TA vector (pCR<sup>®</sup>4-TOPO) (Invitrogen), pIRES-EGFP2 (BD Clontech), pEGFP-C1 (BD Clontech), pcDNA3.1-His-A (Invitrogen)

Other constructs were described:

pWWW-Luc *p21* promoter luciferase reporter (el-Deiry et al., 1993)  
 pcDNA3-His-WNT1 WNT1 expression plasmid (Suzuki et al., 2004)  
 pCMV-HA-SFRP1 SFRP1 expression plasmid (Suzuki et al., 2004)  
 pGL3-OT and pGL3-OF TCF/LEF reporters (He et al., 1998)  
 pSuper vector for short hairpin RNA expression (Brummelkamp et al., 2002b) and  
 pRetroSuper self-inactivating retroviral vector for short hairpin RNA expression (Brummelkamp et al., 2002a)

### 3.5 Other materials

“Human Unigene 1” cDNA microarray (IncyteGenomics, Palo Alto, CA, USA)  
 GeneChip<sup>®</sup> Human Genome U133 A oligonucleotide microarray (Affymetrix, Santa Clara, CA)

Novex 4-20% pre-cast gradient SDS-polyacrylamide gels (Invitrogen)  
Immobilon-P PVDF membrane (Millipore, Schwalbach Germany)  
Protran nitrocellulose membrane (Schleicher & Schuell BioScience, Dassel, Germany)  
Hyperfilm™ X-ray film (Amersham)  
Microcon YM-50 filter columns (Millipore)  
CELLocate glass grids (Eppendorf, Hamburg, Germany)  
ProTaqS IV buffer for IHC (Biocyc, Luckenwalde, Germany)

### **3.6 Equipment**

Fluorescent microscope Axiovert 200M (Carl Zeiss, Oberkochen, Germany) equipped with a CoolSNAP-HQ CCD camera (Photometrics, Tucson, Arizona, USA) and Metamorph software (Universal Imaging, Downingtown, PA, USA).  
Axiovert 25 microscope (Carl Zeiss) equipped with a HyperHAD CCD camera (Sony) and ImageBase software (Kappa Optoelectronics, Gleichen, Germany)  
MicroBeam laser pressure catapulting system (PALM, Bernried, Germany) coupled to an Axiovert 200M microscope (Carl Zeiss) equipped with a DXC-390P CCD camera (Sony, Tokyo, Japan) and a PALMRobo V2.1.1 software (PALM)  
Phosphoimager BAS-2500 (Fuji, Tokyo, Japan).  
MicroLumatPlus LB96V luminometer (EG&G Berthold, Bad Wildbad, Germany).  
ELISA reader LAMBDA E (MWG-Biotech, Ebersberg, Germany)  
Coulter counter Z1 (Coulter Electronics, Beds, United Kingdom)  
FACScan unit (BD Biosciences, Mountain View, CA, USA)  
PCR thermocycler Perkin Elmer 9700 (ABI)  
LightCycler™ real-time PCR system (Roche)  
Capillary sequencer 3700 (Applied)  
GeneChip® Scanner 3000 (Affymetrix)  
Microarray Suite 4.0 software (Affymetrix)

## 4. Methods

### 4.1 Cell culture and treatments

Neonatal skin HDFs were obtained from Clonetics (San Diego, California, USA) and cultivated in DMEM (Invitrogen) supplemented with 10% FBS (Sigma). To obtain senescent HDF, the cells were diluted every three days in a ratio of 1:10 (equal to 1 passage) until they ceased to proliferate. HCT116 cells were cultured in McCoy's medium (Invitrogen) supplemented with 10% FBS. A-375, HeLa, HEK293, *p16*<sup>-/-</sup> mouse embryo fibroblasts (MEF) and NIH3T3-L1 derivatives were kept in DMEM containing 10% FBS. 6-Anilino-5,8-quinolinedione (LY83583, referred to as LY hereafter) was dissolved in DMSO at a concentration of 300  $\mu$ M (< 300 $\times$  solution). As a control, cells were treated with equal volumes of DMSO (<1%). The LY concentration was restored at intervals of 24 hours by media exchange.

The PCa cell lines Du-145, LNCaP, PC3, PPC1 and TSU-Prl were cultured in RPMI-1640 supplemented with 10% FBS and antibiotics (Invitrogen). The PCa cell line LAPC-4 was kept in RPMI-1640 in the presence of 20% FBS. Human benign prostate hyperplasia cells immortalized with SV40 large T-antigene (BPH1) were obtained from the German Collection of Microorganisms and Cell Cultures and passaged in RPMI-1640 medium supplemented with 20% FBS, 20 ng/ml testosterone, 50  $\mu$ g/ml transferrin, 50 ng/ml sodium selenite, 50  $\mu$ g/ml insulin and a mixture of trace elements (Invitrogen). Human primary prostate epithelial cells (PrECs) from an 18-year old donor (Cambrex Bio Science, Walkersville, MD, USA) were cultured in PrEGM according to the supplier's instructions on Collagen Type I coated dishes (BioCoat, BD Falcon). LNCaP, Du-145 and PC3 cells were seeded at low density 24 hours before de-methylation. Cells were exposed to 1 $\mu$ M of 5Aza-2'dC for 72 hours and 300 nM TSA for the last 24 hours or, as a control, to 300 nM TSA for 24 hours.

### 4.2 Patient material

Specimens of basal cell carcinoma, squamous cell carcinoma of the skin, psoriasis, actinic keratoses and genital warts (condylomata acuminata) were obtained from the Department of Dermatology, Ludwig-Maximilians University, Munich.

Archival formalin fixed paraffin-embedded samples of primary prostate carcinoma (Gleason Sum 5-10) and cancer free samples of prostate were obtained from the

Institute of Pathology, Ludwig-Maximilians University Munich. The specimens were taken from consecutive cases of a single year (2001). All patients had undergone surgery at the same institution. In all cases, two board-certified pathologists agreed on the carcinoma diagnosis.

### **4.3 Laser-assisted tissue microdissection**

Archival specimens of primary PCa and tumor free prostate tissue were deparaffinized in xylene and briefly stained with hematoxylin and eosin. One section was covered and used as a reference slide. Microdissection and laser-pressure catapulting was performed using a MicroBeam system. Material obtained from 2-3 parallel sections ( $\sim 10^3$  cells) was pooled and genomic DNA was isolated by the proteinase K/SDS method (see **Bisulfite treatment of genomic DNA**). Before bisulfite-treatment, 1  $\mu\text{g}$  of herring sperm carrier DNA (Promega) was added to each sample of microdissected DNA.

### **4.4 RT-PCR analysis**

Five  $\mu\text{g}$  of total RNA was reverse transcribed using an oligo-(dT)<sub>18</sub> primer and SuperScript™ III cDNA synthesis kit at 50°C for 60 min in a total volume of 20  $\mu\text{l}$ . cDNA was diluted two-fold, first tested by qPCR on the LightCycler with *EF1 $\alpha$* -specific primers using FastStart-DNA Master SYBR Green 1 kit, then diluted to equal concentrations and used for PCR. Two units Platinum Taq polymerase were used per 20  $\mu\text{l}$  reaction with 2  $\mu\text{l}$  cDNA. The total reaction volume was analyzed by agarose gel electrophoresis. The primer sequences and PCR cycle numbers for each of the analysed genes are provided in Table 3.

### **4.5 Bisulfite treatment of genomic DNA**

Genomic DNA was isolated by overnight incubation in a solution containing 100  $\mu\text{g}/\text{ml}$  proteinase K and 0.1% SDS at 55°C with subsequent phenol/chloroform extraction and isopropanol precipitation. 2  $\mu\text{g}$  DNA were denatured in 0.2 M NaOH for 10 min at 37°C in 50  $\mu\text{l}$  of volume. After addition of 30  $\mu\text{l}$  of 10 mM hydroquinone and 520  $\mu\text{l}$  of 3.5 M sodium bisulfite pH 5.0, the mixture was incubated for 16 hours

at 50°C. After column-purification using the PCR purification kit, the DNA was incubated in 0.3 M NaOH for 5 min at RT. Converted DNA was ethanol precipitated and dissolved in 40 µl TE. 2 µl and 5 µl were used for a single MSP or bisulfite-PCR reaction, respectively.

#### **4.6 Genomic bisulfite sequencing**

Converted genomic DNA was used as a template to amplify regions of interest (400-1000 bp fragments with a high CpG-content around the transcription start site) by PCR using gene specific primers (listed in supplemental Table 1). After 5 min incubation at 95°C, 39-41 cycles were performed: 20 s at 95°C, 30 s at annealing temperature, 60-90 s at 72°C using 5 units of Platinum Taq polymerase per 100 µl reaction. PCR-products were isolated by gel purification and subcloned into a TOPO-TA vector. At least 6 individual clones for each gene were sequenced in both directions using M13 primers and BigDye terminator, and analysed on a 3700 capillary sequencer.

#### **4.7 Methylation-specific PCR**

MSP was performed in a total volume of 20 µl using 3 units Platinum Taq per reaction and gene specific primer sets listed in Supplemental Table 2, discriminating between methylated and unmethylated DNA (Herman et al., 1996). After 5 min denaturation at 95°C, 40 PCR-cycles were performed for genomic DNA obtained from cell lines and 45 for micro-dissected genomic DNA. Amplified fragments were separated by 8% polyacrylamide gel electrophoresis and visualized by ethidium bromide staining.

#### **4.8 cDNA microarray analysis of gene expression**

Total RNA was isolated using RNeasy. The poly-A fraction was isolated using oligotex beads. The integrity and enrichment was ensured using Northern blot analysis. Six hundred nanograms of poly-A mRNA were converted to cDNA with incorporation of Cy3- or Cy5-labeled deoxynucleotide-triphosphates (dNTPs). Hybridization to arrays coated on glass, quality control, and normalization were performed by IncyteGenomics. The "Human Unigene 1" array contained cDNA

probes representing 8,392 annotated genes/expressed sequence tag (EST) clusters and 74 non-annotated genes/ESTs.

#### 4.9 Oligonucleotide microarray analysis of gene expression

Total RNA was isolated from cell lines using the RNeasy kit and assessed photometrically and by agarose gel electrophoresis. Oligonucleotide microarray analyses were performed on the GeneChip Human Genome U133A (the list of genes is available at [www.affymetrix.com](http://www.affymetrix.com)) according to the manufacturer's protocol. In brief, 25 µg of total RNA were reverse transcribed using an anchored oligo-dT-T7 primer (5'-GGCCAGTGAATTGTAATACGACTCACTATAGGGAGGCGG-T<sub>24</sub>-VN-3') and the double-stranded cDNA synthesis kit. After treatment with RNase for 30 min at 37°C and proteinase K for 30 min at 37°C cDNA was extracted three times with a phenol/chloroform/isoamylalcohol mixture and purified by ultrafiltration on Microcon-YM50 column. Using the *in vitro* transcription RiboMax T7 kit, biotin-labelled cRNA was produced from a double-stranded cDNA template, cleaned up with the RNeasy kit, fragmented by incubation in 40mM Tris-acetate pH 8.1, 100mM potassium acetate and 30mM magnesium acetate solution for 35 min at 95°C. The probes were hybridized to the U133A oligonucleotide arrays (15 µg of the cRNA per chip) and analysed with a GeneChip® Scanner 3000. Genes up-regulated by combined 5Aza-2'dC plus TSA treatment versus TSA alone were identified by an algorithm provided by Affymetrix using the Microarray Suite 4.0 software.

#### 4.10 Quantitative real-time PCR

Quantitative real-time PCR (qPCR) was performed using the LightCycler and the FastStart DNA Master SYBR Green 1 kit as previously described. For qPCR of cDNA, primer pairs were designed to generate intron-spanning products of 100–200 bp. Primer sequences were as follows: *GUCY1A3*, sense 5'-TTCAGAGGAGGCAGCAGG-3' and antisense 5'-GCAACATTCAGCCGTTCAA-3' (annealing temperature, 62°C); and *GUCY1B3*, sense 5'-AGGAATCACGCATCAGCC-3' and antisense 5'-TATGAGGACGAACCAGCGA-3' (annealing temperature, 62°C). cDNA was generated using the RevertAid First Strand cDNA synthesis kit. The generation of specific PCR products was confirmed by melting-curve analysis and gel electrophoresis. Each primer pair was tested with a logarithmic dilution of a cDNA mix to generate a linear standard curve (crossing point

[CP] plotted vs. log of template concentration), which was used to calculate the primer-pair efficiency ( $E = 10^{(-1/\text{slope})}$ ). *EF1 $\alpha$*  mRNA was used as an external standard, since its expression was not altered significantly in senescent versus early passage confluent HDF (data not shown). For data analysis, the second-derivative maximum method was applied, and induction of a cDNA species (geneX) was calculated according to Pfaffl (Pfaffl, 2001) as follows:

$$\frac{E_{\text{geneX}}^{\Delta\text{CP}}(\text{confluent cDNA} - \text{senescent cDNA})^{\text{geneX}}}{E_{\text{ELF1}\alpha}^{\Delta\text{CP}}(\text{confluent cDNA} - \text{senescent cDNA})^{\text{ELF1}\alpha}} = \text{fold induction}$$

#### 4.11 Proliferation assays

Cells were seeded in equal numbers in six-well plates 24 hours before the addition of LY. Cells were treated in triplicates (3 replicas of the same experiment) with daily exchange of medium containing drug or drug-free vehicle. For each time point, cells were trypsinized and cell proliferation was assessed using Z1 Coulter Counter. For the assessment of the net proliferation capacity cells were seeded in 6-well plates at low density (~2.000/well), cultured for 10 days and stained with crystal violet.

#### 4.12 BrdU incorporation assay

Cells were plated on CELLocate glass grids and labelled for 6 hours using the 5'-bromo-2'-deoxyuridine Labelling and Detection Kit I. After staining with a FITC-labelled anti-bromodeoxyuridine (anti-BrdU) antibody, positive cells were detected by fluorescence microscopy.

#### 4.13 Measurement of DNA content and apoptosis by flow cytometry

Cells were trypsinized. Both adherent and floating cells were washed once with PBS and fixed on ice in 70% ethanol for more than 2 hours, washed once with PBS, and incubated for 30 minutes at room temperature in staining solution containing 50  $\mu\text{g/ml}$  propidium iodide (PI), 0.2 mg/ml RNase A, and 0.1 % (v/v) Triton X-100 in PBS. Quantification of apoptotic cells was performed using the Annexin V-FITC apoptosis detection kit. Samples were analyzed with a FACScan unit.  $1 \times 10^4$  cells were analyzed for each assay.

#### 4.14 Senescence-associated $\beta$ -galactosidase staining

Cells were fixed by incubation in 0.5% glutaraldehyde in PBS for 5 minutes at room temperature and stained for senescence-associated  $\beta$ -galactosidase (SA- $\beta$ -gal) at pH 6.0 as described (Dimri et al., 1995).

#### 4.15 cGMP assay

Cells of early and late passages were seeded in equal numbers in six-well plates. Twenty-four hours later, sodium nitroprusside (SNP) dissolved in complete medium was added at a final concentration of 100  $\mu$ M. Controls received the same volume of drug-free medium. After 2 hours of incubation, the medium was removed and cells were lysed by addition of 400  $\mu$ l of 0.1 M HCl per well for 10 minutes. The cGMP concentration in lysates was determined using a competitive immunoassay according to the manufacturer's instructions. The LAMBDA E plate reader was used to detect the signal at 405 nm. Experiments were performed in triplicates, with all samples measured twice.

#### 4.16 Northern hybridization

Total RNA was isolated using the RNAgent kit. 15 $\mu$ g of total RNA were separated on denaturing 1.5 % formaldehyde agarose gel, transferred to a Protran nitrocellulose membrane and cross-linked by exposure to UV. Probe for the 3' untranslated region of the *EF1a* mRNA was generated by PCR using EST as a template. *p21* probe was generated by excision of the respective open reading frame from the p21-EYFP construct. Probes against *14-3-3 $\sigma$*  and *GSTP1* were amplified by PCR from cDNA and subcloned in a TOPO-TA vector. Labelling with <sup>32</sup>p-dCTP was done using the random labelling kit and the product was purified using the nucleotide removal kit. Hybridization was performed in QuickHyb solution according to the manufacturer's protocol. The signal was detected on a phosphoimager.

#### 4.17 Luciferase assay

HCT116 cells with a knock-out of the *p53* gene were co-transfected with the *p21* promoter reporter construct pWWW-Luc and pCMV- $\beta$ -gal in triplicates using



Lipofectamine™ 2000 reagent. After 24 hours, cells were exposed to 1.5  $\mu$ M LY or an equal volume of DMSO for 12 hours.

The use of pGL3-OT, a TCF-LEF responsive reporter, pGL3-OF, a negative control with a mutated TCF-LEF binding site, and pcDNA3.1 His-WNT1 constructs was described previously. LNCaP, PC3, Du-145 and HCT116 cells were plated at medium density the day before transfection in 12-well plates in triplicate for each cell line. The transfection was performed using Lipofectamin™ 2000 reagent. Three constructs were co-transfected in each experiment: (i) 0.5  $\mu$ g of pGL3-OT or pGL3-OF; (ii) 0.5  $\mu$ g of pcDNA3.1-His-WNT1 or pcDNA3.1-His-A; (iii) 50 ng of pCMV- $\beta$ -gal. After 36 hours, cells were lysed and assayed for luciferase activity.

Luciferase activity was measured according to the manufacturer's instructions for the Luciferase Assay System kit.  $\beta$ -galactosidase activity was measured in the same lysates using Galacto-Light reagents. Luciferase and  $\beta$ -galactosidase determination were performed on a MicroLumatPlus LB96V luminometer.

#### **4.18 Western blot analysis**

Exponentially growing cells were lysed in 50 mM HEPES (pH 7.5), 150 mM NaCl, 1 mM EGTA, 10% glycerol, 1% Triton X-100, 100 mM NaF, 10 mM  $\text{Na}_4\text{P}_2\text{O}_7$ , 1  $\mu$ M phenylmethylsulfonylfluoride, and 1  $\mu$ M  $\text{Na}_3\text{VO}_4$ . Protein concentration was determined using a Bradford assay. Eighty micrograms of protein were mixed with 2x Laemmli buffer, separated on Novex 4-20% gradient SDS-polyacrylamide gels, and transferred to Immobilon-P membranes or nitrocellulose membranes. Antibodies against  $\alpha$ -tubulin (TU-02) diluted 1:1000 and affinity purified rabbit 14-3-3 $\sigma$  anti-serum diluted 1:500 were used in combination with HRP-conjugated secondary antibodies diluted 1:10,000. Primary antibodies specific for p21, p53, p16, pRB, SFRP1 and VSV tag were used at dilutions 1:500, 1:1000, 1:300, 1:500, 1:200 and 1:2,000 respectively. Target proteins were visualized after enhanced chemiluminescence treatment of membranes and subsequent exposure to Hyperfilm™ X-ray film.

#### **4.19 Immunofluorescent staining**

For immunofluorescent staining a mouse anti- $\beta$ -catenin antibody was used. The cells growing on CELLocate slides were fixed in 3.7 % paraformaldehyde solution for 20 min, permeabilized in 0.2 % Triton X in PBS for 15 min and blocked in

FBS for 30 min. Primary antibodies diluted 1:50 in 10% FBS, 0.05% Tween 20 PBS were added for 1 hour. After three times washing in Tween20/PBS cells were incubated with Cy3-conjugated donkey anti-mouse antibodies diluted 1:200 for 30 min, then washed again three times and mounted. All steps were performed at room temperature.

#### **4.20 Immunohistochemistry**

Skin sections of 4  $\mu\text{m}$  thickness from formalin-fixed, paraffin-embedded tissue were deparaffinized in xylene and re-hydrated in a decreasing ethanol series. Antigen retrieval was carried out in citrate buffer (0.01 M, pH 6.0) at 98°C for 15 min in a pressure cooker. Then, sections were incubated with the 14-3-3 $\sigma$  antibodies diluted 1:200 for 25 min at room temperature, rinsed twice in Tris-HCl buffer and incubated with linking mouse anti-rabbit antibodies diluted 1:100 for 25 min. For p63 staining the antigen retrieval was carried out in EDTA buffer (pH 8.0) at 98°C for 20 min. Anti-p63 antibodies were used at a dilution 1:200 for 25 min at room temperature. The APAAP system was used for the visualisation of the signal according to the manufacturer's instructions.

For the 14-3-3 $\sigma$  staining the same procedure was used in prostate tissue as for skin samples. For the detection of SFRP1, deparaffinized and re-hydrated 4  $\mu\text{m}$  sections of prostate tissue were subjected to the antigen retrieval procedure by boiling in a microwave oven for 30 min in ProTaq $\sigma$  IV buffer. Anti-SFRP1 antibodies diluted 1:25 were used in combination with the Vectastain Elite kit. After counterstaining with hematoxylin, the images were acquired on an Axiovert 200M microscope coupled to a DXC-390P CCD camera using a PALMRobo V2.1.1 software.

#### **4.21 Microscopy**

For phase contrast and  $\beta$ -galactosidase staining an Axiovert 25 microscope equipped with a HyperHAD CCD camera and ImageBase software was used. In vivo expression of histone-H2B-EGFP,  $\beta$ -catenin immunostaining and BrdU staining were documented on an inverted Axiovert 200M microscope equipped with a CCD camera CoolSNAP-HQ and Metamorph software.

#### 4.21 Generation and analysis of knock-down and transgenic cell lines

For stable expression of siRNAs, pSUPER-based constructs were used. Targeting of three different 19 bp sequences was tested in transient transfection experiments by assessing the ability to down-regulate expression of a 14-3-3 $\sigma$ -EYFP fusion protein (data not shown). All target sequences did not show any homology to other cDNAs in public databases. The most efficient construct targeted the sequence GGAGCCGGGGACGCCGAG of the 14-3-3 $\sigma$  transcript and was used here. For vector construction, two oligonucleotides (5'-CGGGATCCCCGGAGGCCGGGGACGCCGAGTTCAAGAGTCTCG-3'; 5'-CGCTCGAGCCAAAAGGAGGCCGGGGACGCCGAGACTCTTGA-3') with a 12 bp overlap were annealed at 37°C and subjected to five PCR cycles resulting in a double-stranded fragment, which was digested with *Bam*HI and *Xho*I and ligated into the *Bgl*III and *Xho*I sites of pSUPER. Then the entire H1-promoter-sh14-3-3 $\sigma$  cassette was released from pSUPER by restriction with *Eco*RI and *Xho*I and inserted into the same restriction sites of the self-inactivating retroviral vector pRetroSUPER. The resulting construct was transfected into a Phoenix A packaging cell line. pRetroSuper was used as a control. PC3 cells were infected by incubation with virus-containing supernatant and subjected to puromycin selection for 7 days. Single cell clones were established by limiting dilution.

For the analysis of nuclear aberrations cells growing in 60 mm dishes were fixed in methanol and stained with DAPI. Phase contrast and fluorescent images were acquired using the Axiovert 200M fluorescent microscope and Metamorph software. For the quantification of the total cell number and number of multinuclear cells, at least 10 randomly chosen areas were counted per clone.

For stable expression of *DKK3* or *SFRP1* the retroviral vector pLXSN, which had been modified by insertion of an IRES-EGFP fragment derived from the plasmid pIRES-EGFP2, was used. PC3 cells were retrovirally infected using pLXSN-IRES-EGFP2, pL-DKK3vsv-IRES-EGFP2 or pL-SFRP1-IRES-EGFP2. 72 hours after infection GFP positive cells were sorted by FACS and expanded. For the assessment of colony formation, cells were seeded at low density in 6-well plates (2000 cells per well) and grown for 10 days. Cells were fixed in 1 % formaldehyde and stained with crystal violet. Apoptosis was assessed by propidium iodide staining and flow cytometry.

## 5. Results

### 5.1 Expression profiling of replicative and premature senescence

#### 5.1.1 Microarray analysis of senescence-specific gene expression

Microarray analysis of gene expression was used to identify genes and pathways involved in the induction and maintenance of replicative senescence. Primary HDF were cultivated until all cells were terminally arrested ( $n = 75$  population doublings) and showed characteristic signs of senescence: cellular enlargement, SA- $\beta$ -gal staining at pH 6, and stable arrest in the presence of high serum concentration. Presenescent HDF, which had been arrested in the G<sub>1</sub> phase by confluence at population doubling 12, were used as a reference. This state was selected to avoid a comparison of non-proliferating senescent HDF with proliferating early-passage HDF, which would presumably result in the detection of a large number of differences in gene expression secondary to growth arrest. mRNA was isolated from senescent and control HDF and subjected to analysis using a microarray representing 8,392 annotated cDNAs. The culturing, analysis and isolation of RNA from early and late passage fibroblasts were performed by Dr. Heiko Hermeking. Generation of cDNAs and quality control was performed by Dr. Antje Menssen. The Microarray analysis was performed by the company Incyte Genomics (USA).

**Table 1** Detection of senescence-specific gene regulation using microarray analysis

Symbol	Description	Differential expression
<i>PAI1</i>	plasminogen activator inhibitor I	+5.9
<i>PAI2</i>	plasminogen activator inhibitor II	+4.7
<i>MMP10</i>	matrix metalloproteinase 10	+3.1
<i>p21</i>	cyclin-dependent kinase inhibitor 1A	+2.0
<i>CTGF</i>	connective tissue growth factor	+3.7
<i>CCND1</i>	cyclin D1	+5.0
<i>PK3</i>	pyruvate kinase	+5.0
<i>ID2</i>	inhibitor of DNA binding 2	-2.0

Gene expression patterns of early-passage confluent HDF were compared to those of senescent HDF using microarrays as described in **Methods**.

Several genes previously identified as consistently up- or down-regulated during senescence of HDF (Ly et al., 2000; Shelton et al., 1999; West et al., 1996) were detected as regulated in a similar fashion in the system used here (Table 1): for example, *PAI-1* was previously detected as up-regulated in senescent HDF and was induced 5.9-fold in senescent HDF in this study (Table 1). Among the genes

repressed during senescence were four genes encoding enzymatic components of the cGMP pathway (Table 2): *soluble guanylate cyclase  $\alpha 3$*  (*sGC- $\alpha 3$* ), *sGC- $\beta 3$* , and *cGMP-dependent protein kinase I and II*. Differential regulation of *sGC- $\alpha 3$*  and *sGC- $\beta 3$*  during senescence was confirmed by qPCR (Table 2). Down-regulation of *sGC- $\beta 3$*  during senescence was also detected using Northern blot analysis (Figure 6a). *sGC- $\alpha 3$*  and *sGC- $\beta 3$*  represent the large and small subunit of soluble guanylate cyclase, which converts GTP to 3',5'-cyclic GMP and pyrophosphate (Giuli et al., 1992). Interestingly, both genes are located in close proximity on chromosome 4q31.3-q33 (Giuli et al., 1993), which could provide the basis for the co-regulation observed here.

**Table 2** Repression of genes encoding components of the cGMP signaling pathway

Symbol	Description	Differential expression	qPCR (SD)
<i>GUCY1B3</i>	soluble guanylate cyclase- $\beta 3$	-7.8	-9.4 (0.7)
<i>GUCY1A3</i>	soluble guanylate cyclase- $\alpha 3$	-2.5	-2.2 (0.4)
<i>PRKG2</i>	cGMP-dependent protein kinase II	-9.7	
<i>PRKG1</i>	cGMP-dependent protein kinase I	-2.5	

Gene expression patterns of early-passage confluent HDF were compared with those of senescent HDF using microarrays as described in **Methods**. Confirmation of expression data by quantitative real-time PCR is indicated in the column labeled "qPCR" including standard deviation in brackets.

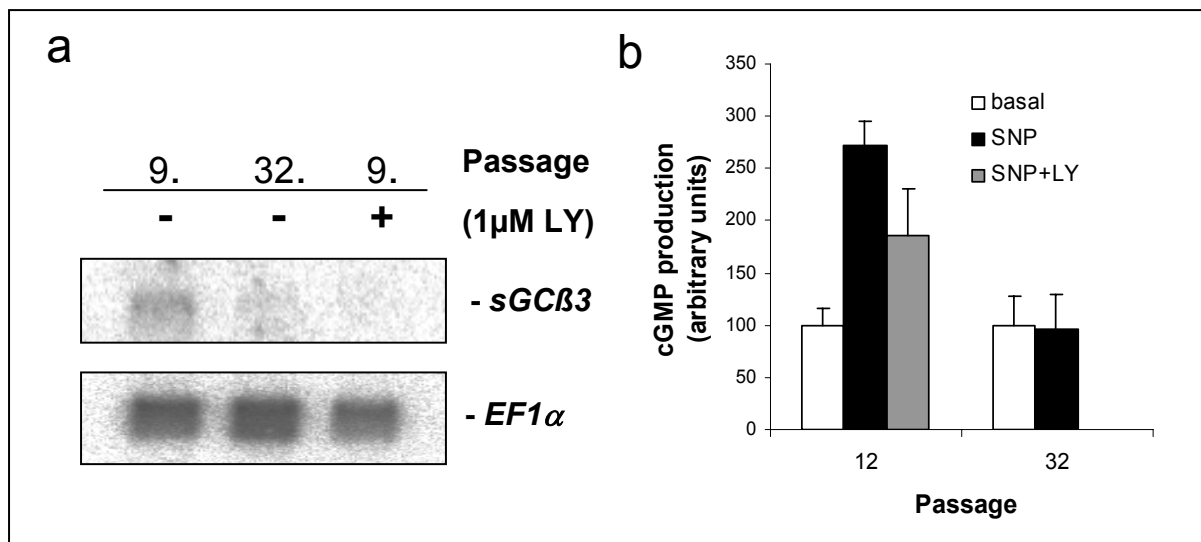


**Figure 6** Modulation of the cGMP pathway in HDF

(a) Northern blot analysis of *GUCY1B3* expression in HDF. Total RNA was isolated from early- ("9.") and late-passage ("32.") HDF and HDF ("9. passage") treated with 1  $\mu$ M LY for 4 days; 2.5  $\mu$ g of total RNA was loaded per lane. *GUCY1B3* and, as a control, *EF1 $\alpha$*  mRNA were detected with  $^{32}$ P-labeled probes. (b) Response of early-passage and senescent HDF to activation of cGMP synthesis. Cells were treated with 100  $\mu$ M SNP for 2 hours in the absence or presence of LY. Treatments were performed in triplicates and measured twice.

The coordinated repression of two genes encoding the subunits of soluble guanylate cyclase, which generates cGMP in response to signals — for example, extracellular nitric oxide (NO) (reviewed in Hofmann et al., 2000) — suggested that senescent cells may have an attenuated response to NO donors such as SNP. Indeed, exposure to SNP did not result in elevated cGMP levels in senescent HDF, whereas early-passage HDF showed a 2.7-fold increase in cGMP levels after the addition of SNP (Figure 6b).

### **5.1.2 Induction of senescence by LY83583**

To specifically inhibit the cGMP signaling pathway, a competitive inhibitor of soluble guanylate cyclase, LY, with an  $IC_{50}$  of 2  $\mu$ M was used (Fleisch et al., 1984). Addition of 1  $\mu$ M LY to HDF significantly inhibited the SNP-induced synthesis of cGMP by 50% (Figure 6b), showing that LY had the expected inhibitory effect on guanylate cyclase. The effect of LY on the proliferation of early-passage HDF was tested at concentrations ranging from 0.25–1.5  $\mu$ M (Figure 7a). Indeed, treatment of early-passage fibroblasts with a concentration of 1  $\mu$ M of LY was sufficient to completely inhibit proliferation, and the presence of 250 nM LY led to a 50% reduction in proliferation of HDF after 3 days (Figure 7a). Strikingly, the inhibition of proliferation of early-passage HDF by LY was accompanied by morphological changes characteristic of senescence and by SA- $\beta$ -gal staining at pH 6 (Figure 7c). Consistent with the induction of cellular senescence, inhibition of proliferation by LY was irreversible after a treatment period of more than 2 days (Figure 7b). Extended treatment of HDF with LY for 8 days did not cause significant reduction of cell number due to cell death but resulted in stable inhibition of proliferation (Figure 7b). In order to characterize the cell-cycle arrest induced by LY, HDF were synchronized in the  $G_1$  phase by confluence (91.2%  $G_1$  phase and 2% S phase) and then released by splitting (Figure 7d). Untreated cells entered the S phase at a high percentage, whereas addition of LY almost completely blocked the entry of HDF into the S phase, suggesting that LY acts during the  $G_1$  phase of the cell cycle. Furthermore, addition of 1  $\mu$ M LY to synchronized HDF caused complete inhibition of DNA synthesis as determined by BrdU incorporation (Figure 7e).

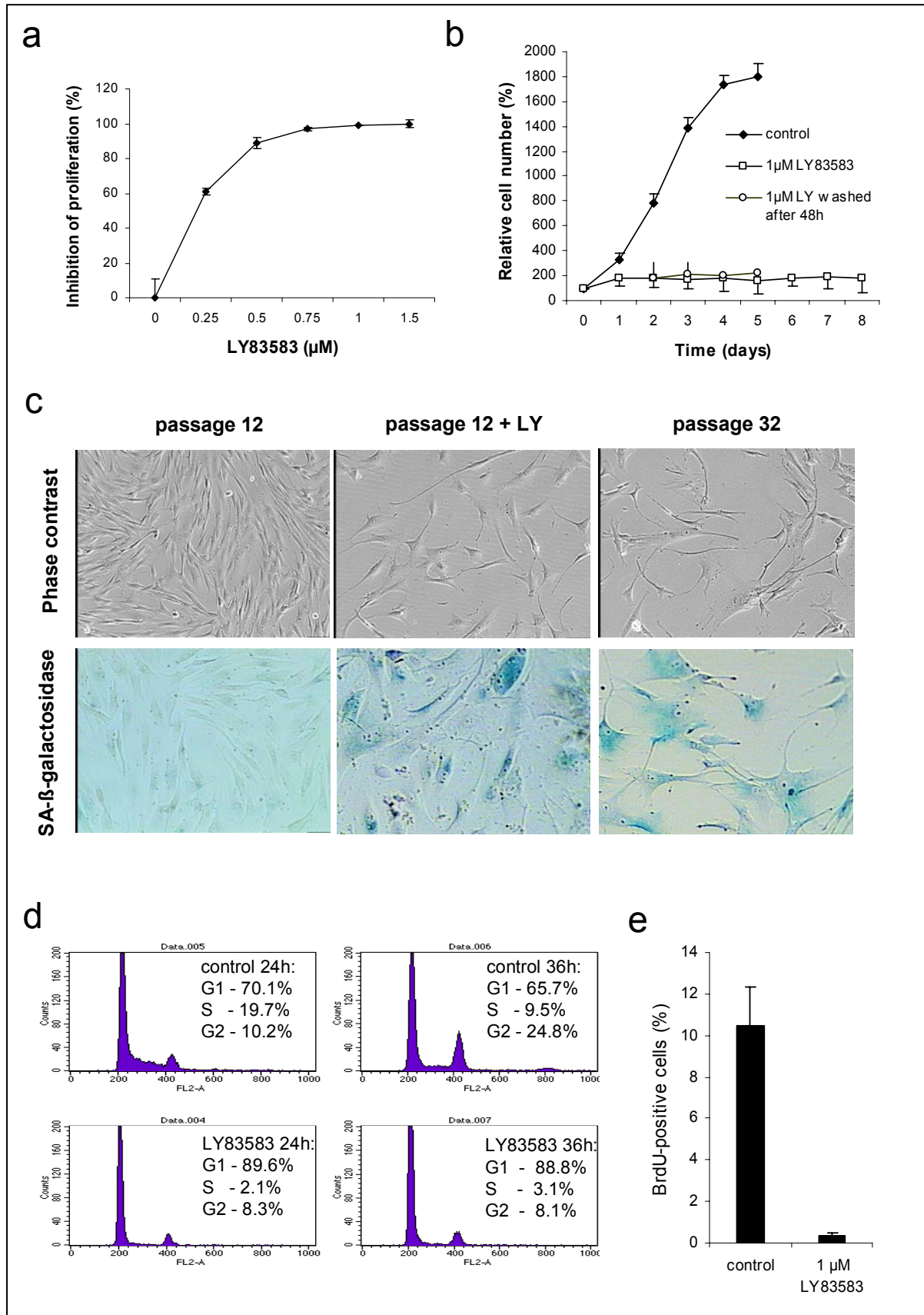


### Figure 7 Effect of LY on HDF proliferation

(a) Inhibition of proliferation by LY. Subconfluent HDF were treated with the indicated concentrations of LY for 3 days. Cell numbers were determined in triplicates. (b) Irreversible effect of LY on proliferation of HDF. Cells were treated with 1  $\mu$ M LY for the indicated periods. After trypsinization, cell numbers were determined in triplicates. (c) Shown is a comparison of HDF after reaching replicative senescence with HDF after LY treatment. The upper panels show morphology (magnification, x100) and the lower panels show detection of SA- $\beta$ -gal at pH 6 (magnification, x200), using phase-contrast microscopy. (d) FACS analysis of HDF treated with LY. HDF were synchronized by confluence and released by trypsinization. After 24 and 36 hours of incubation in media containing 1  $\mu$ M LY or vehicle, cells were collected for FACS analysis. (e) Rate of DNA synthesis after LY treatment. BrdU incorporation was determined after incubation of HDF in 10  $\mu$ M BrdU for 6 hours. For details, see **Methods**.

#### 5.1.3 Microarray analysis of LY-regulated genes

In order to identify the downstream mediators of the LY-induced cell-cycle arrest and senescence, a microarray analysis of LY-treated HDF was performed with the same arrays used for the analysis of replicative senescence in HDF described above (for details, see **Methods**). RNA was isolated 36 hours after exposure of early-passage HDF to LY. The control RNA was isolated from confluent early-passage HDF. In HDF that had reached replicative senescence, 216 transcripts were induced significantly, whereas 272 mRNAs were induced after LY treatment. Repression was observed for 266 mRNAs in HDF undergoing replicative senescence, whereas 294 mRNAs were repressed after LY treatment. There was a substantial overlap in the differentially expressed genes observed during replicative senescence and during LY-induced senescence, with 114 transcripts differentially regulated in a similar manner (Table 3). Among these were genes that had been previously identified as differentially regulated during replicative senescence: *PAI-1*, *matrix metalloproteinase 10*, *fibrillin*, *cdc25b*, *cyclin D1*, *fibromodulin*, and *osteoblast specific factor 2* (Cristofalo et al., 1998; Ly et al., 2000; Shelton et al., 1999). However, most of the genes identified here represent new additions to the growing number of genes identified as components of the senescence program. Supporting this notion, many of the co-regulated genes have functions that may contribute to the phenotype of terminally arrested cells. For example, down-regulation of the *PDGF receptor  $\alpha$*  and  *$\beta$  chains* may contribute to the refractory state of senescent cells, which do not respond to mitogenic stimulation with growth factors. The changes in expression observed in genes encoding components of the cytoskeleton (e.g.,  *$\alpha$ 1-tubulin*,  *$\beta$ 2-tropomyosin*,  *$\gamma$ -filamin C*,  *$\alpha$ -actinin*) may contribute to the flattened and enlarged shape characteristic of senescent HDF (Figure 7c). Interestingly, the *sGC $\beta$ 3* mRNA was down-regulated in LY-treated HDF (Table 3 and Figure 6a).



**Table 3** Detection of 114 mRNAs coregulated in replicative senescence and LY-treated cells by microarray analysis

Gene name (functional class)	repl.sen. fold	LY fold	Gene name (functional class)	repl.sen. fold	LY fold
<b>Cell cycle</b>			<b>Extracellular Matrix</b>		
wee1+ homolog	-4.2	-3.2	fibulin 2	-3.4	-3.4
cell division cycle 25B	-2.3	-3.8	fibrillin 2	-2.2	-4.8
cyclin G2	-1.7	-1.9	fibromodulin	-2.2	-3.8
checkpoint suppressor 1	-1.8	-2.2	lumican	-2.2	-4.8
cdc-like kinase 1	-2.2	-2.6	matrix metalloproteinase 1	-3.3	-2.6
cyclin D1	+5.0	+2.0	matrix metalloproteinase 2	-3.9	-2.4
cyclin-dependent kinase inhibitor 1A (p21, Cip1)	+2.0	+3.0	matrix metalloproteinase 10 (stromelysin 2)	+2.3	+2.9
cyclin-dependent kinase 7	+1.7	+1.6	matrix metalloproteinase 15	-8.9	-3.6
<b>Transcription</b>			matrix Gla protein	-4.8	-3.1
transcription factor 8	-1.8	-2.2	adducin 3, gamma	-4.1	-2.6
Cbp/p300-interacting transactivator (CITED2)	+3.0	+2.3	dermatopontin	-2.0	-2.9
TBP-associated factor, RNA pol II, G, 32kD	+1.4	+1.8	procollagen C-endopeptidase enhancer	-2.5	-3.3
zinc finger protein 238	-5.5	-5.6	cathepsin O	-2.0	-3.2
SWI/SNF rel., matrix assoc., reg. of chromatin 2	-3.5	-2.8	cathepsin F	-2.0	-2.7
ribonuclease, RNase A family, 4	-4.8	-7.6	protein geranylgeranyltransferase type I, b	-2.0	+3.2
RNA helicase-related protein	+3.2	+5.5	complement component 1, r subcomponent	-15.7	-5.2
c-maf	-4.8	-2.8	complement component 1, s subcomponent	-9.8	-5.4
microphthalmia-associated transcription factor	-2.1	-2.5	limbic system-associated membrane protein	-1.8	-3.9
<b>Signaling</b>			protein S, alpha	-5.7	-2.7
PDGF receptor-like (PDGFRL)	-2.9	-3.0	thrombospondin 2	-2.0	-2.6
PDGF receptor, alpha	-2.0	-2.5	carboxypeptidase Z	-2.4	-2.7
PDGF receptor, beta	-2.4	-2.7	glypican 3	-32.1	-3.1
guanylate cyclase 1, soluble, beta 3	-7.8	-3.9	PAI-1	+5.9	+12.6
mitogen-activated protein kinase 7	-1.9	-2.2	coagulation factor III	+4.3	+2.3
B-factor, properdin	-2.5	-5.0	metallothionein 1L	+2.9	+5.0
glutamate receptor, ionotropic, AMPA 1	-2.8	-4.3	<b>Cell shape and motility</b>		
TGFβ receptor III (betaglycan, 300kD)	-3.8	-5.1	laminin, alpha 2	-1.9	-2.2
purinergic receptor P2X, lig.-gated ion channel, 4	-1.3	-1.8	microfibrillar-associated protein 4	-4.0	-5.6
prostaglandin F receptor (FP)	-2.1	-2.2	microfibrillar-associated glycoprotein-2	-3.6	-2.0
IGFBP 5	-16.7	-10.1	tropomyosin 2, beta	+3.7	+2.1
interleukin 1 receptor, type I	-4.9	-2.2	filamin C, gamma	+1.9	+3.3
mitogen-activated protein kinase kinase 5	-1.8	-2.0	tubulin, alpha 1	+1.8	+4.3
interleukin 11 receptor, alpha	-2.9	-2.1	actin, gamma 1	+2.2	+3.7
connective tissue growth factor	+3.7	+5.0	actinin, alpha 1	+3.8	+1.9
fibroblast growth factor 2 (basic)	+3.0	+3.0	actin, beta	+2.5	+2.8
annexin A2	+4.1	+2.3	moesin	+2.6	+2.4
adenylyl cyclase-associated protein	+2.0	+2.0	ARP3 (actin-related protein 3, yeast)	+3.1	+2.5
regulator of G-protein signaling 4	+1.6	+5.7	<b>Other functions</b>		
neurotrophic tyrosine kinase, receptor, type 1	+2.5	+2.8	cysteine-rich, angiogenic inducer, 61	+4.1	+5.5
SHC 1	+1.9	+1.8	BRCA1 associated protein	+3.8	+4.7
regulator of G-protein signaling 4	+1.6	+5.7	heat shock 70kD protein 4	+1.9	+1.9
osteoblast specific factor 2 (fasciclin I-like)	-59.9	-3.3	heat shock 70kD protein 8	+1.9	+3.7
stromal cell-derived factor 1	-19	-2.2	glioma pathogenesis-related protein	+2.7	+2.3
<b>Metabolism</b>			butyrophilin, subfamily 3, member A2	-2.2	-2.8
mannosidase, alpha, class 1A, member 1	-4.2	-4.0	glycoprotein A repetitions predominant	-2.1	-3.0
alcohol dehydrogenase 1A (class I), a	-3.6	-3.6	thioredoxin reductase 1	+2.2	+7.8
glucosidase, alpha; acid	-2.6	-2.8	clusterin	-2.3	-3.1
superoxide dismutase 2, mitochondrial	-2.0	-2.8	upregulated by 1,25-dihydroxyvitamin D-3	-3.6	-3.3
phosphatidic acid phosphatase type 2B	-7.1	-6.5	selenium binding protein 1	-2.3	-2.9
short-chain dehydrogenase/reductase 1	-2.1	-3.5	arginyl-tRNA synthetase	+2.0	+1.8
prostaglandin I2 (prostacyclin) synthase	-2.1	-2.3	ubiquitin carboxyl-terminal esterase L1	+2.1	+2.0
acid ceramidase	-1.9	-2.5	Fc fragment of IgG, receptor transporter, alpha	-2.6	-2.8
selenophosphate synthetase	-2.4	-2.2	retinoic acid receptor responder 2	+2.0	-2.3
fucosyltransferase 8	-1.9	-2.6	PEG1	-2.1	-2.5
phospholipid scramblase 1	-2.3	-2.1	latent TGFβ binding protein 4	-11.2	-2.1
pyruvate kinase	+5.0	+2.1	matrilin 2	-3.9	-1.9
UDP-N-acetylglucosamine pyrophosphorylase 1	+2.2	+4.1	carboxypeptidase E	-2.4	-2.0
prostaglandin-endoperoxide synthase 2 (COX2)	+2.1	+1.8	TGFβ inducible early growth response 2	-1.8	-1.9
sialic acid synthase	+2.0	+1.9	gamma-interferon inducible protein 16	-1.8	-1.8
			poliovirus receptor	+2.0	+2.5
			glypican 1	+2.1	+2.6

Genes, which showed a similar differential regulation (>1.7 fold induction or repression) in the two microarray analyses, are shown after classification according to their function. For each gene, fold differential expression during replicative senescence (repl. sen.) or after LY83583 treatment (LY) is shown. For details of the microarray analyses see **Methods**.

#### 5.1.4 Rapid induction of $p21^{WAF1/CIP1/SDI}$ by LY83583

Among the genes induced by both replicative senescence and LY was  $p21^{WAF1/CIP1/SDI}$  (Table 3), which encodes an inhibitor of cyclin-dependent kinases (CDKs). CDK/cyclin complexes drive cell-cycle progression and proliferation by phosphorylation of key substrates. Since induction of  $p21$  could potentially explain the antiproliferative effect of LY, the connection between LY and  $p21$  was analyzed in more detail. Six hours after treatment with LY, the levels of  $p21$  mRNA in HDF were similar to the levels observed 6 hours after addition of a DNA damaging agent adriamycin, as shown by Northern blot analysis (Figure 8a). However, after treatment with LY, the level of p53 protein, which consistently increases after generation of DNA damage and mediates transactivation of  $p21$ , did not increase (Figure 8b), indicating that LY does not induce DNA damage. The induction of  $p21$  mRNA by adriamycin demonstrates, that the signaling pathways necessary for p53 activation were still intact in the HDF used (Figure 8a). Induction of  $p21$  protein was detectable between 3 and 6 hours after addition of LY, whereas the CDK inhibitor  $p16^{INK4A}$  was not induced even after 48 hours of treatment with LY (Figure 8b). This result was unexpected, since  $p16^{INK4A}$  is commonly induced in scenarios that lead to premature senescence — for example, ectopic expression of an activated *RAS* gene (Serrano et al., 1997) or suboptimal cell-culture conditions (Ramirez et al., 2001).

The main cell-cycle-relevant targets of the CDK inhibitor  $p21$  are cyclin-dependent kinases 2, 4, and 6 (Harper et al., 1993; Harper et al., 1995), which keep the pocket-proteins pRB, p107, and p130 in an inactive hyperphosphorylated state during cell-cycle progression (reviewed in Grana et al., 1998).

Therefore,  $p21$ -mediated inhibition of  $G_1/S$  phase-associated CDK/cyclin complexes leads to hypophosphorylation of pocket proteins, which allows their subsequent binding and inhibition of E2F transcription factors. The association between pocket proteins and E2Fs results in inhibition of  $G_1/S$  progression and proliferation (reviewed in Weinberg, 1995). Consistent with the induction of  $p21$  by LY, the phosphorylation status of pRB changed rapidly after addition of LY. After only 6 hours the ratio of phosphorylated to hypophosphorylated, active pRB was clearly shifted toward the hypophosphorylated form, and by 19 hours pRB was almost completely hypophosphorylated (Figure 8c). Even after extension of the LY treatment to 12 days the pRB hypophosphorylation was not reversed (Figure 8c). These results

show that LY inhibits proliferation by inducing *p21* to levels that are sufficient to inhibit CDK activity and to activate the cell-cycle inhibitory function of pRB.

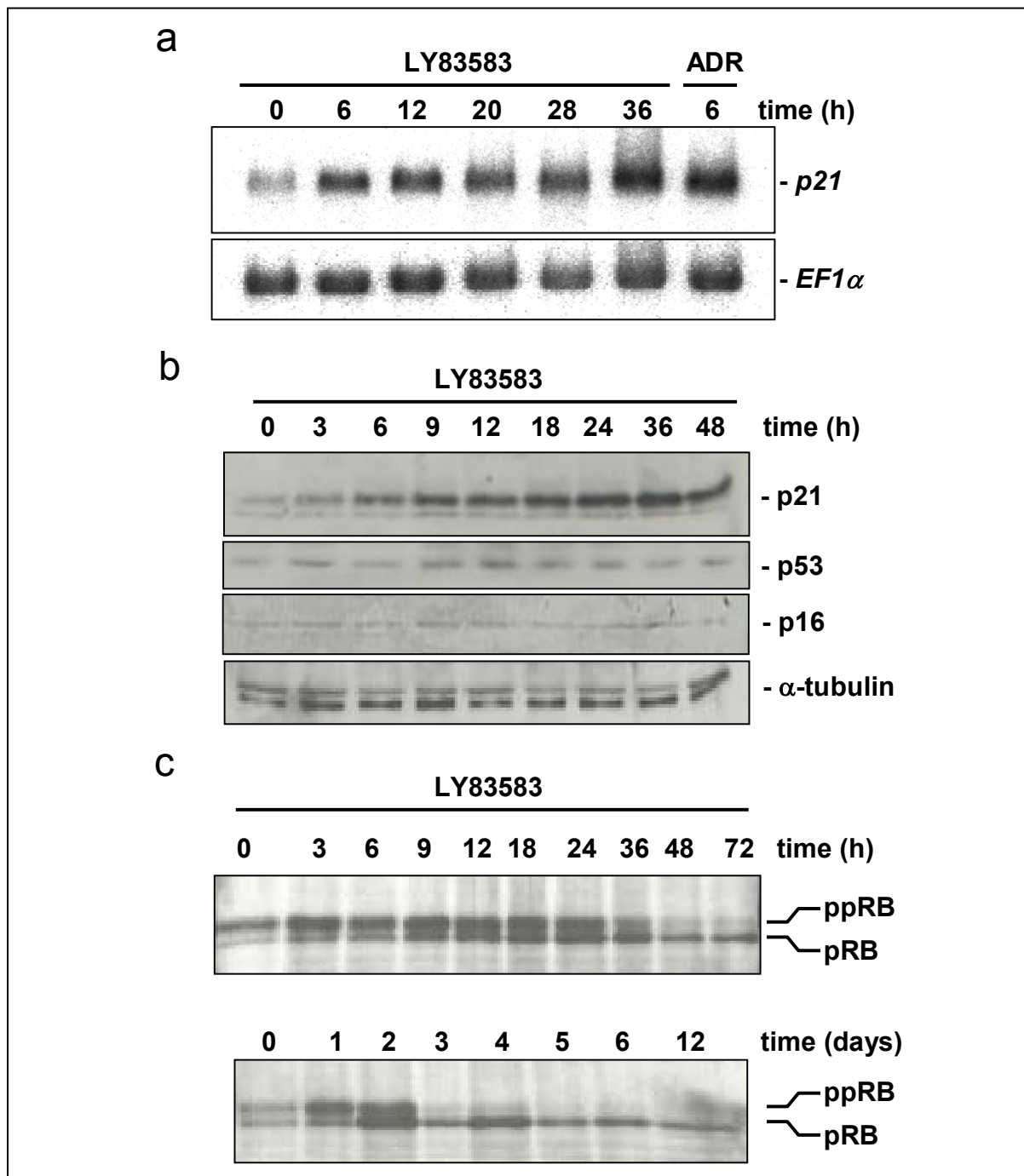


**Figure 8** Effects of LY on the expression and phosphorylation status of cell cycle regulatory proteins

(a) Northern blot analysis of LY-treated HDF. Total RNA was isolated from HDF treated with 2  $\mu$ M LY or 0.2  $\mu$ g/ml adriamycin for the indicated periods; 7.5  $\mu$ g of total RNA was loaded per lane. *p21<sup>WAF1/CIP1/SD1</sup>* and, as a control, *EF1 $\alpha$*  mRNA were detected with  $^{32}$ P-labeled probes. (b) Western blot analysis of HDF treated with LY. Lysates were obtained from HDF treated with LY for the indicated periods; 20  $\mu$ g of protein was loaded per lane. After separation on 4–20% gradient gels and transfer to PVDF membranes, proteins were detected with antibodies against human p21, p53, p16, and — as a loading control —  $\alpha$ -tubulin. (c) pRB phosphorylation status after treatment with LY. After addition of LY for the indicated periods, cell lysates were prepared and proteins were separated by a 7–12% gradient SDS-PAGE; ppRB, hyperphosphorylated pRB; pRB, hypophosphorylated pRB.

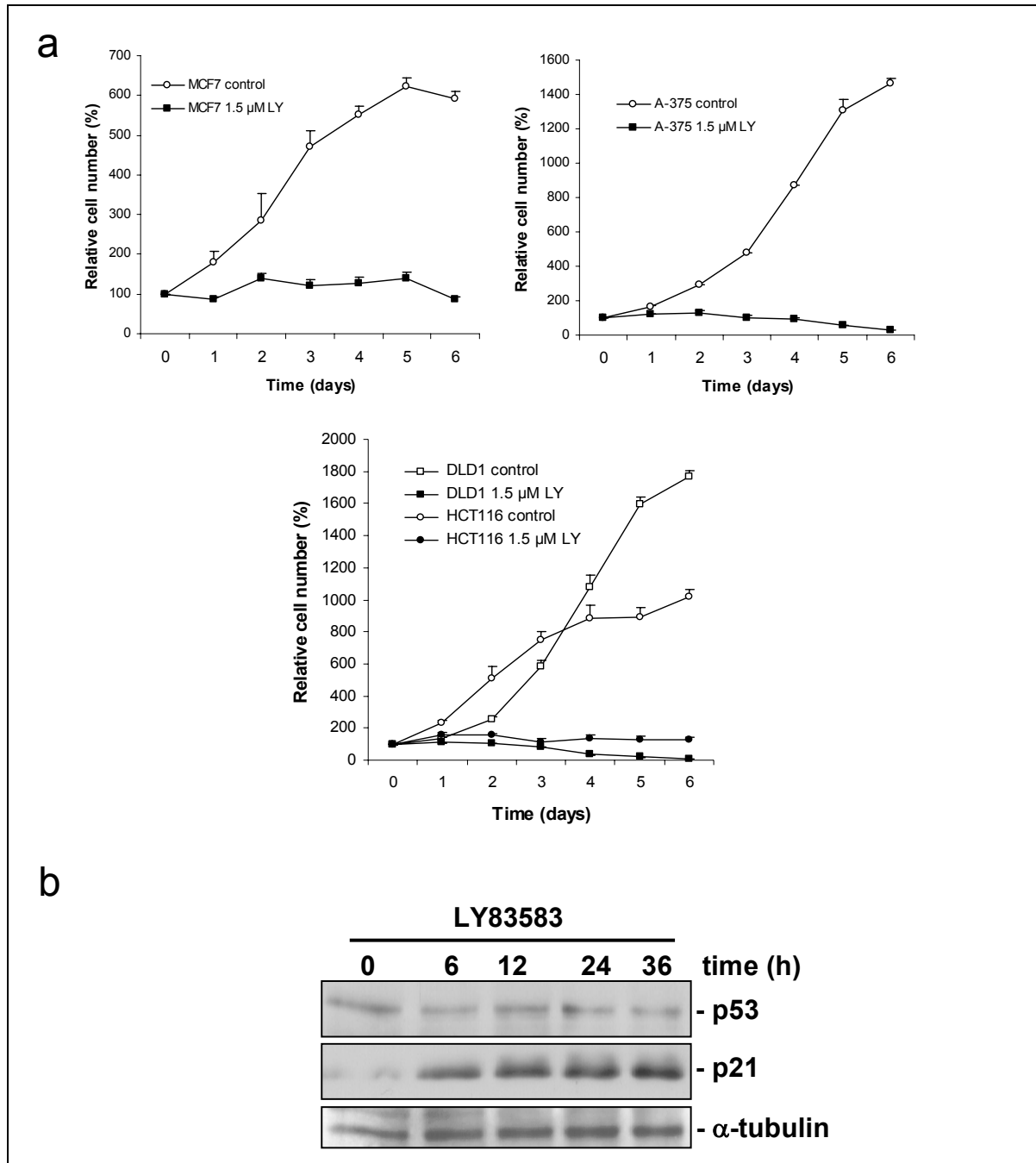


**Figure 9** Effects of LY on epithelial cancer cells

(a) Growth curves of MCF7, A-375, HCT116, and DLD1 cells. Cells were trypsinized at the indicated time points and cell numbers were determined. (b) Induction of p21 protein after treatment with LY. HCT116 colorectal cancer cells were treated with 1.5  $\mu$ M LY for the indicated periods. Cell lysates were prepared and subjected to Western blot analysis.

### 5.1.5 Effect of LY83583 on cancer cell proliferation

In order to determine whether LY may be useful to terminate cancer cell proliferation, colorectal cancer cell lines (HCT116, DLD1), a breast cancer-derived cell line (MCF7), and a melanoma cell line (A-375) were analyzed after addition of

LY. All cell lines showed complete cessation of cell proliferation (Figure 9a). Consistent with the findings in HDF, HCT116 cells showed induction of p21 at the protein level after addition of LY (Figure 9b). Furthermore, *p21* mRNA was induced by LY in MCF7 cells (data not shown).

#### 5.1.6 Requirement of p21, but not p53, for inhibition of proliferation by LY83583

To determine whether induction of *p21* is essential for the inhibition of proliferation by LY, *p21*-deficient HCT116 cells, generated through homologous recombination (Waldman et al., 1996), were analyzed (Figure 10a). *p21*-deficient HCT116 cells were largely resistant to LY, whereas wild-type HCT116 cells showed complete cessation of proliferation (Figure 9a). These results show that *p21* is required for the inhibitory effects of LY on cellular proliferation. Consistent with the absence of p53 accumulation in LY-treated HDF, *p53*-deficient HCT116 cells (Bunz et al., 1998) showed a complete block of proliferation after addition of LY (Figure 10b). The properties of the three different HCT116 cell lines used in this study were confirmed by treatment with adriamycin, which induces DNA double-strand breaks (Figure 10c). As expected, only wild-type HCT116 cells showed induction of p21 protein after exposure to adriamycin (Figure 10c). HCT116 cells deficient in *p53* and transiently transfected with a reporter construct of human *p21* promoter fused to the luciferase gene showed a more than 10-fold increase in luciferase activity after 12 hours of LY treatment (Figure 10d). The levels of *p21* mRNA and protein of *p53*<sup>-/-</sup> HCT116 cells after treatment with LY were induced with kinetics similar to those observed in HDFs (Figure 10, e and f). These results exclude p53 and thereby induction of DNA damage as mediator of the cell-cycle arrest by LY and induction of *p21* expression. Furthermore, LY treatment did not lead to induction of the CDK inhibitors p27 and p15 (data not shown). In addition, proliferation of *p16*<sup>INK4A</sup>-deficient MEFs (described in Serrano et al., 1996) was inhibited by LY, showing that *p16*<sup>INK4A</sup> is not required for the effects of LY on the cell cycle (data not shown). Supporting this conclusion, the HCT116 colorectal cancer cell lines used in this study do not express functional *p16*<sup>INK4A</sup>; one *p16*<sup>INK4A</sup> allele carries an inactivating point mutation, and the other *p16*<sup>INK4A</sup> allele is completely silenced by CpG methylation (Myohanen et al., 1998). Taken together, these results show that the inhibitory effects of LY on proliferation are mediated through induction of *p21*.

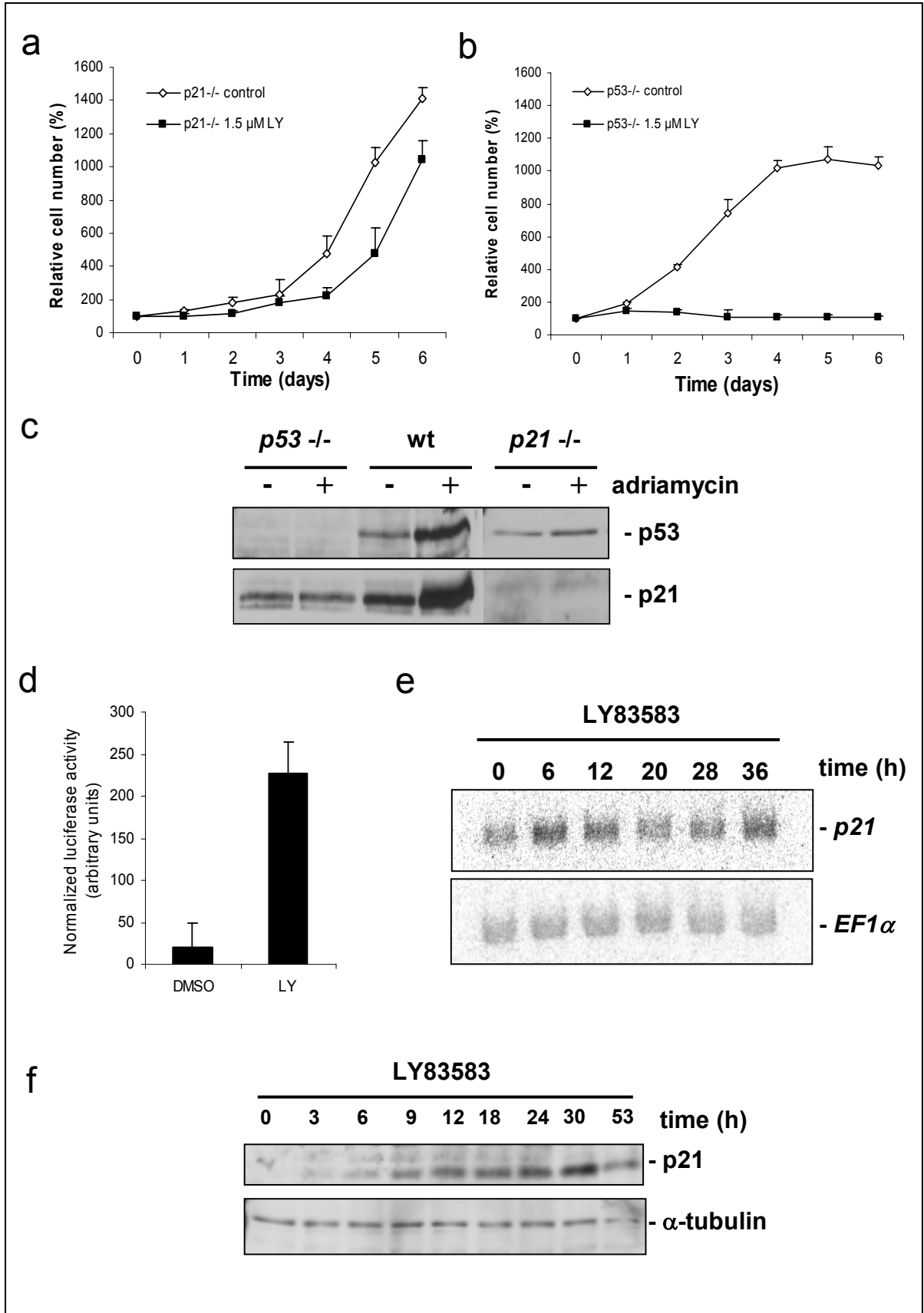


**Figure 10** Requirement of *p21*, but not *p53*, for inhibition of proliferation by LY

(a) Response of HCT116 colorectal cancer cells deficient for *p21* to LY. Cells were treated with LY or, as a control, with vehicle (DMSO), and cell numbers were assessed. Measurements were performed in triplicates. (b) Response of *p53*<sup>+/+</sup> and *p53*<sup>-/-</sup> HCT116 cells to LY. Cells were treated with LY or, as a control, with vehicle (DMSO), and cell numbers were assessed. Measurements were performed in triplicates. (c) Analysis of HCT116-derived knock-out cell lines. Shown are the results of a Western blot analysis of p53 and p21 protein levels after addition of adriamycin at 0.2 µg/ml for 8 hours. (d) *p21* promoter reporter activity in *p53*-deficient HCT116 cells after treatment with 1.5 µM LY for 12 hours. The experiment was performed in triplicates. For details, see **Methods**. (e) p53-independent induction of *p21* mRNA by LY. Shown are the results of a Northern blot analysis with RNA isolated at the indicated time points after addition of 1.5 µM LY to p53-deficient HCT116 cells. (f) p53-independent induction of p21 protein levels by LY. Shown are the results of a Western blot analysis with lysates from *p53*<sup>-/-</sup> HCT116 cells treated with 1.5 µM LY. Membranes were probed with antibodies specific for p21 and, as a loading control,  $\alpha$ -tubulin.

### 5.1.7 Conversion of LY83583-induced arrest to apoptosis in pRB-negative cells

Since the antiproliferative effect of p21 is mediated through pocket proteins (pRB, p107, p130) (reviewed in Grana et al., 1998), the response of cells with nonfunctional pocket proteins to treatment with LY was analyzed. Isogenic NIH3T3-L1 cell lines (described in Hermeking et al., 1994) stably expressing either SV40 large T-antigen or an SV40 large T-antigen point mutant (K1) (DeCaprio et al., 1988) deficient in binding and inactivating pocket proteins were treated with LY. NIH3T3-L1 cells expressing the K1-mutant showed inhibition of proliferation, whereas NIH3T3-L1 cells expressing wild-type SV40 large T antigen underwent apoptosis (Figure 11, a and b). Induction of apoptosis by LY was further quantified using annexin V staining (Figure 11c).

In order to extend these observations to human cancer cells, the cell lines HeLa and HEK293 were analyzed. The cervical cancer cell line HeLa expresses the human papilloma virus (HPV) 18 which codes for the E7 protein. E7 binds to and inactivates pocket proteins. In HEK293 cells, the adenoviral E1A protein performs analogous functions. HeLa and HEK293 cells did not arrest after treatment with LY but instead underwent cell death (Figure 12a, data not shown), which was accompanied by cell shrinkage suggesting apoptosis (data not shown). HeLa cells expressing a histone H2B-EGFP fusion protein were used to confirm the induction of apoptosis by LY (Figure 12b). Treatment with LY led to chromatin condensation, which is characteristic of apoptosis. Furthermore, flow cytometry analysis revealed a substantial increase of cells with a sub-G<sub>1</sub> DNA content after addition of LY (Figure 12c).

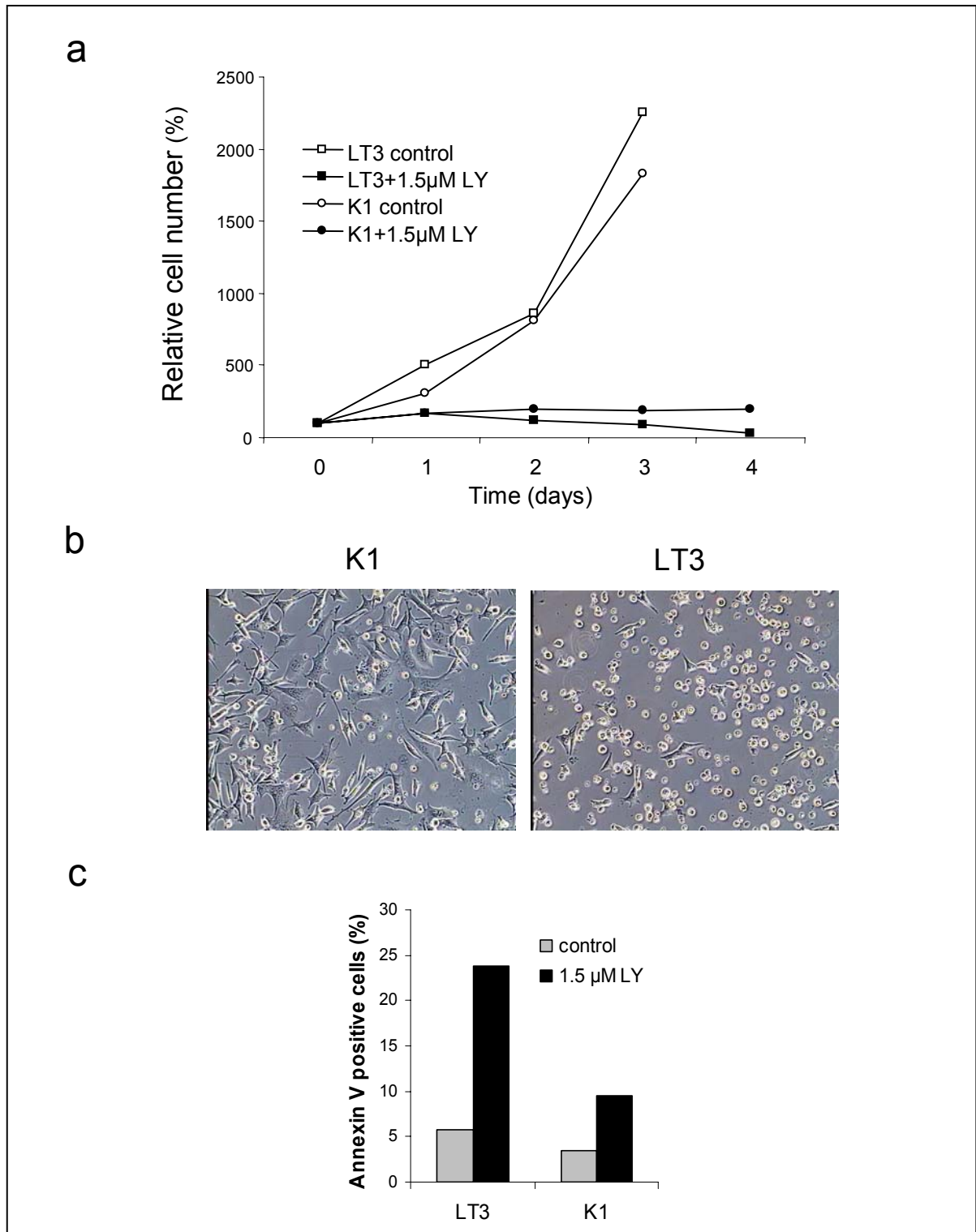


**Figure 11** Modulation of the effect of LY through the functional status of pRB  
**(a)** Response of cell lines with lesions in the pRB pathway to LY. NIH3T3-L1 cells expressing SV40 large T antigen (LT3) and NIH3T3-L1 cells expressing a point mutant of SV40 large T antigen unable to bind to pRB-like proteins (K1) were treated with 1.5 µM LY. Cell numbers were determined at the indicated time points in triplicates. **(b)** Morphology of NIH3T3-L1 cells after LY treatment. Phase-contrast microscopy was performed after incubation of NIH3T3-L1-K1 (K1) and NIH3T3-L1-LT3 (LT3) cells in 1.5 µM LY for 3 days (magnification x100). **(c)** Quantification of early stages of apoptosis. K1 and LT3 cells (control cells and cells treated with LY for 48 hours) were subjected to double staining with anti-annexin V and PI to discriminate living, early apoptotic, and late apoptotic/necrotic populations and were analyzed by flow cytometry. The percentage of PI-negative, annexin V-positive cells is shown.



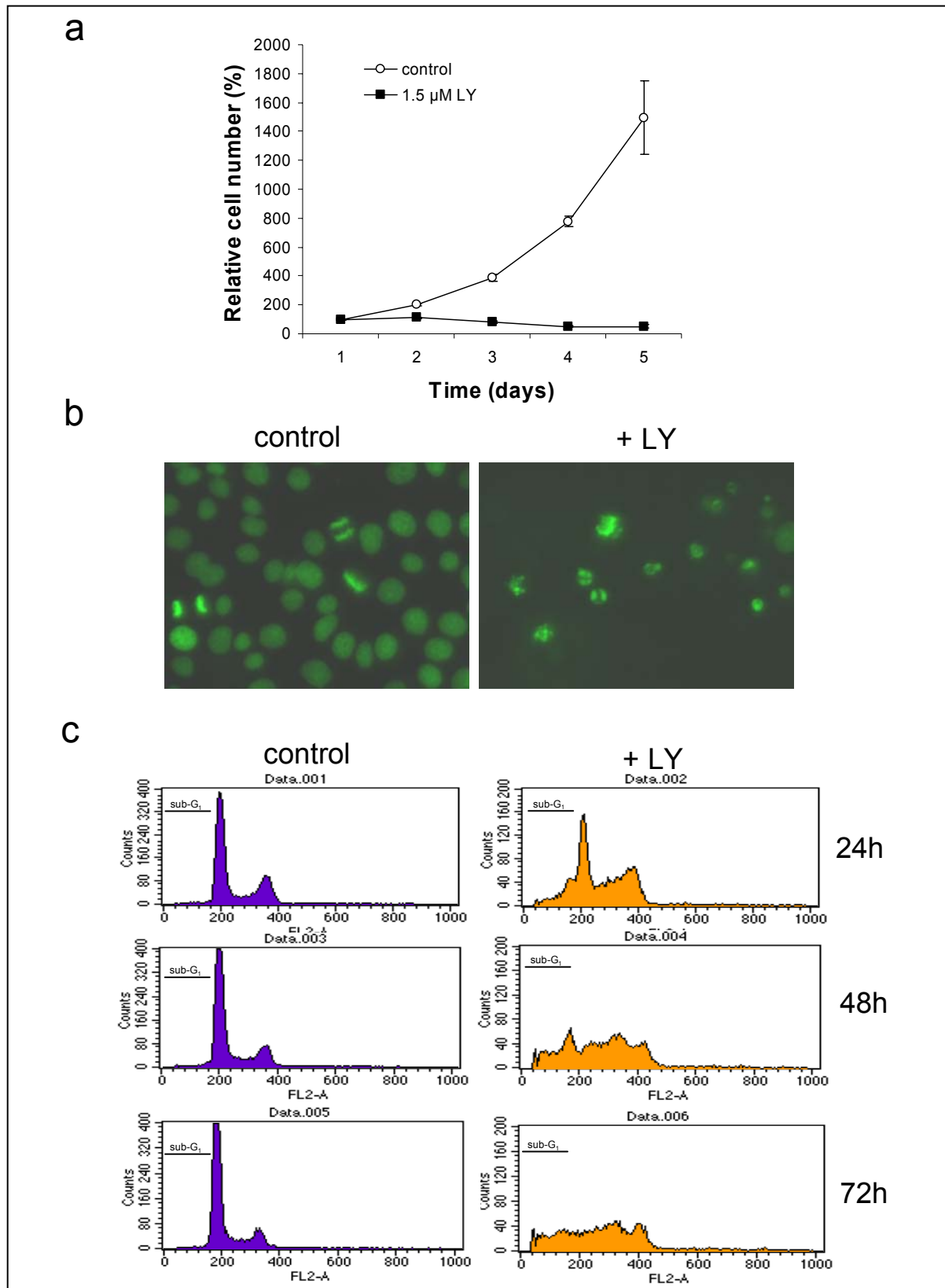


**Figure 12** Effect of LY on HeLa cells

(a) Growth curves of HeLa cells. Cells were trypsinized at the indicated time points and cell numbers were determined. (b) Induction of apoptosis by LY. HeLa cells expressing a histone H2B-EGFP fusion protein (kindly provided by G. Wahl) were treated with 2  $\mu$ M LY for 48 hours, and the chromatin morphology in living cells was analyzed at a wavelength of 495 nm. (c) The quantification of apoptosis by detection of cells with a sub-G<sub>1</sub> DNA content. HeLa cells were treated with LY for the indicated period of time. DNA content was determined after PI staining as described in **Methods**.

## 5.2 Analysis of 14-3-3 $\sigma$ expression in hyperproliferative skin diseases

### 5.2.1 Immunohistochemical analysis of hyperproliferative skin diseases

14-3-3 $\sigma$  antisense expression immortalizes primary keratinocytes. Therefore, Dr. Heiko Hermeking established a collaboration with Dr. Thomas Herzinger (Dermatologisches Klinikum, LMU, München) to examine the expression of 14-3-3 $\sigma$  protein in several benign and neoplastic skin diseases. The specificity of the employed antibody was verified using sections of paraffin embedded 14-3-3 $\sigma$  wt (+/+) and knock-out (-/-) colon cancer cells (Chan et al., 1999). Unexpectedly, in actinic keratoses (Figure 13a), genital warts (condylomata acuminata; Figure 13b), psoriasis (Figure 13c) and cutaneous squamous cell carcinoma (SCC; Figure 13d) the level of 14-3-3 $\sigma$  expression was equal to that of normal epidermis (Figure 13e, arrow) in all cases analysed (Table 4). Keratinocytes within the hair follicles and the germinative portion of sebaceous glands stained strongly positive for 14-3-3 $\sigma$  (Figure 13g and 13i). However, 14-3-3 $\sigma$  protein levels were markedly down-regulated in basal cell carcinoma (BCC derived from five different patients; Figure 13e-k). As shown in Figure 13j and k (higher magnification of the BCC section shown in Figure 11i) the basal cells of the epidermis express 14-3-3 $\sigma$  protein. Towards the outer layers of the epidermis the level of 14-3-3 $\sigma$  expression increases. Only a few keratinocytes within the tumor nests stained positive for 14-3-3 $\sigma$ , particularly in portions of the tumor with a more morphoeic (Figure 13h) or squamous differentiation pattern, where expression of 14-3-3 $\sigma$  was found around cysts (Figure 13f). In total, 41 BCC were analysed for expression of 14-3-3 $\sigma$ : 29 (70.7%) showed no or strongly reduced expression of the 14-3-3 $\sigma$  protein (Table 5).

Different molecular alterations could be responsible for the loss of 14-3-3 $\sigma$  expression in BCC. Recently, the p53 homolog p63 was found to be a specific marker for keratinocyte stem cells (Pellegrini et al., 2001). The loss of 14-3-3 $\sigma$  expression detected in BCC could therefore be due to expression of a dominant-negative splice variant of p63 ( $\Delta$ Np63/CUSP), which is expressed in the epidermal stem cell compartment, from which BCC is presumably derived, and may affect 14-3-3 $\sigma$  expression via the p53-binding sites in the 14-3-3 $\sigma$  promoter (Westfall et al., 2003).

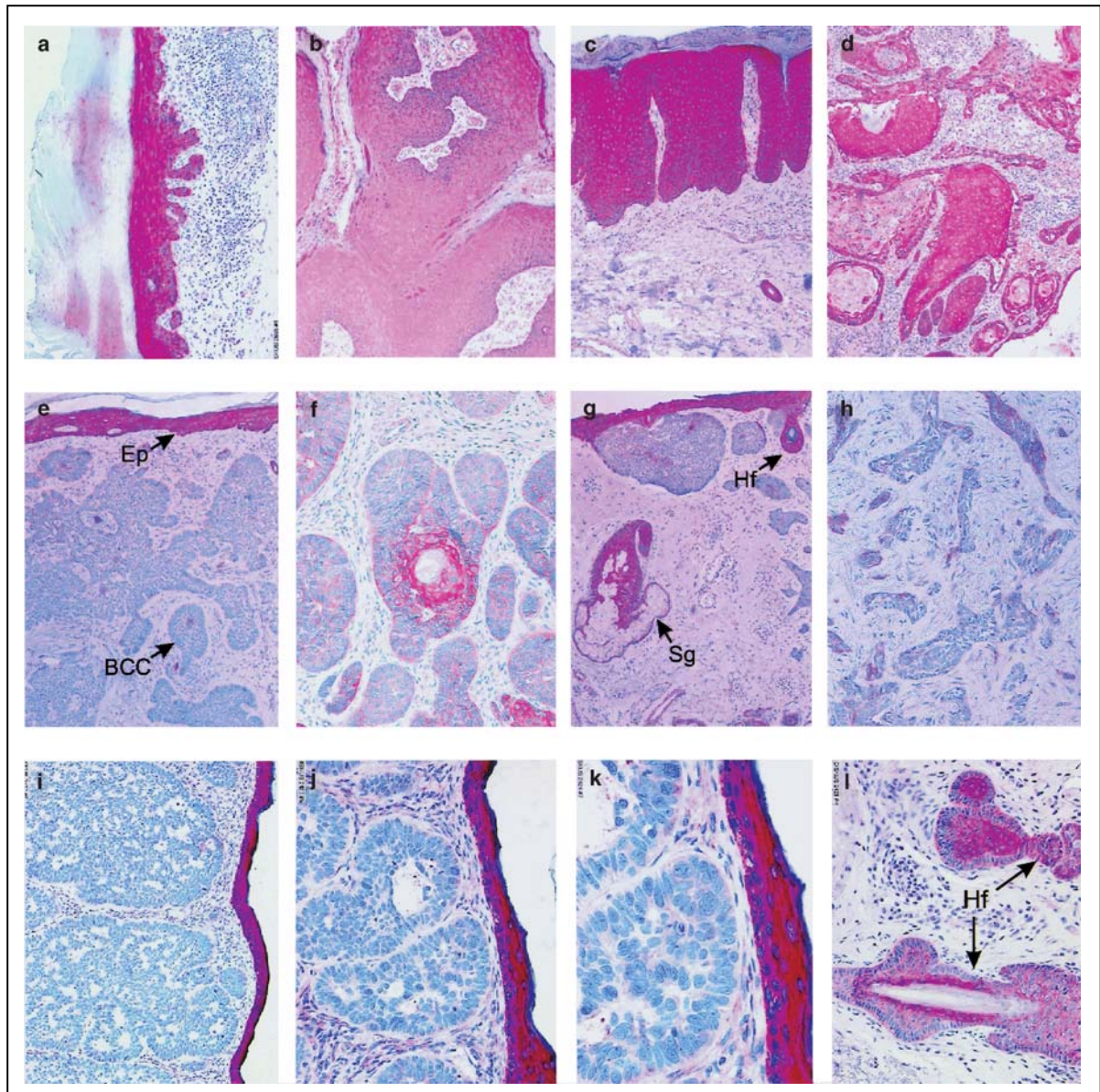


**Figure 13** 14-3-3 $\sigma$  protein expression in hyperproliferative diseases of human skin. Paraffin-embedded samples of actinic keratosis (a), genital condyloma (b), psoriasis (c), SCC (d) and five different BCCs (e-i) were stained with an affinity-purified, polyclonal antibody specific for 14-3-3 $\sigma$  (red). Higher magnifications of the tissue section shown in (i) are provided in (j) and (k). Nuclei (blue) were counterstained with haematoxylin (Ep: epidermis; Hf: hair follicle; SCC: squamous cell carcinoma; Sg: sebaceous gland). These analyses were performed by Dr. Amir Yazdi and Dr. Thomas Herzinger (Department of Dermatology, LMU, Munich)

Therefore, the expression of p63 protein was analyzed. Indeed, all 20 BCC analysed were positive for nuclear p63 protein (Figure 14a; Tables 4 and 5). However, seven of the 20 BCC tested showed expression of both 14-3-3 $\sigma$  and p63 protein (Table 5). Furthermore, cells representing actinic keratoses (7/7) and SCC (6/6), which expressed high levels of 14-3-3 $\sigma$ , were also positive for p63 (Figure 14b, e, c, f Table 4). Therefore, no direct correlation exists between the absence of 14-3-3 $\sigma$  expression and presence of p63 in BCC



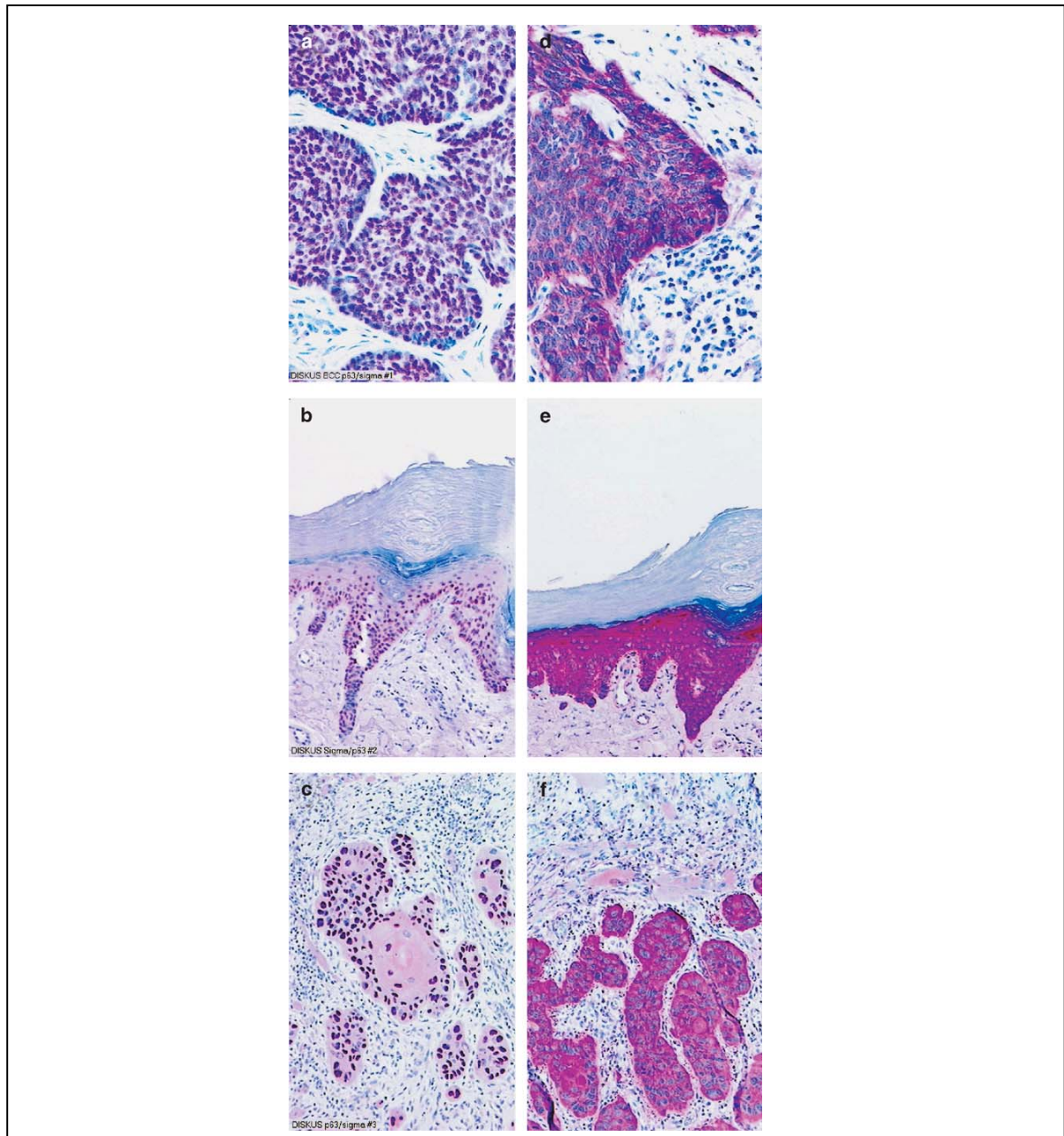


**Figure 14** Analysis of p63 protein expression in 14-3-3 $\sigma$ -positive cases of BCC, actinic keratosis and SCC

Sections of BCC (**a, d**), actinic keratosis (**b, e**) and SCC (**c, f**) were analysed for expression of p63 (**a, b, c**; red nuclear signals). High levels of 14-3-3 $\sigma$  were confirmed in parallel sections of the tissue (**d, e, f**; red cytoplasmic signals). In case of BCC (**a**), a sample from patient 14 (Table 5) is shown. These analyses were performed by Dr. Amir Yazdi and Dr. Thomas Herzinger (Department of Dermatology, LMU, Munich)

### 5.2.2 Analysis of 14-3-3 $\sigma$ CpG methylation in BCC and normal epidermis

Since it has recently been reported that 14-3-3 $\sigma$  is silenced by CpG-island methylation (Ferguson et al., 2000), this epigenetic mechanism appeared to be one possible explanation for down-regulation of 14-3-3 $\sigma$  in BCC. Therefore, I analysed

the methylation status of *14-3-3 $\sigma$*  in BCC by methylation specific PCR (MSP). The specificity of the employed PCR-primers (Figure 15, a and b) and the conditions for MSP were confirmed by analysis of the *14-3-3 $\sigma$*  methylation status in the breast cancer cell line MDA-MB-435S, in which *14-3-3 $\sigma$*  undergoes complete methylation (Ferguson et al., 2000). As shown in Figure 15b only a 105 bp (base-pair) PCR product specific for methylated DNA but no product representing an unmethylated *14-3-3 $\sigma$*  allele was detected in MDA-MB-435S cells with MSP. Furthermore, the colorectal cancer cell line HCT116, which expresses *14-3-3 $\sigma$* , did not show methylation by MSP, but was positive for the 107 bp MSP product representing an unmethylated *14-3-3 $\sigma$*  allele (Figure 15b). Laser microdissection was employed to isolate BCC tissue samples from paraffin sections obtained from 41 patients. This approach allowed the precise separation of BCC from stroma, in which *14-3-3 $\sigma$*  is silenced by CpG methylation (Umbricht et al., 2001). Consistent with CpG methylation of *14-3-3 $\sigma$*  in stroma the signal corresponding to methylated *14-3-3 $\sigma$*  allele was detected in normal human diploid fibroblasts (HDF) passaged *in vitro* (Figure 15b). MSP with genomic DNA extracted from BCC revealed, that *14-3-3 $\sigma$*  promoter methylation was present in 28 of 41 (68%) of the analyzed BCC samples (Figure 15c, Table 5). All samples also demonstrated a signal specific for the unmethylated allele of *14-3-3 $\sigma$*  (Figure 15c, Table 5). The concomitant presence of unmethylated and methylated promoter sequences has also been observed in micro-dissected tumor-samples obtained from breast cancer lesions (Umbricht et al., 2001). Immunohistochemical analysis of adjacent sections from all 38 BCC analyzed by MSP shown in Table 1 with the *14-3-3 $\sigma$* -specific antiserum confirmed strong suppression, and in most cases absence, of *14-3-3 $\sigma$*  protein expression in BCC (data not shown).

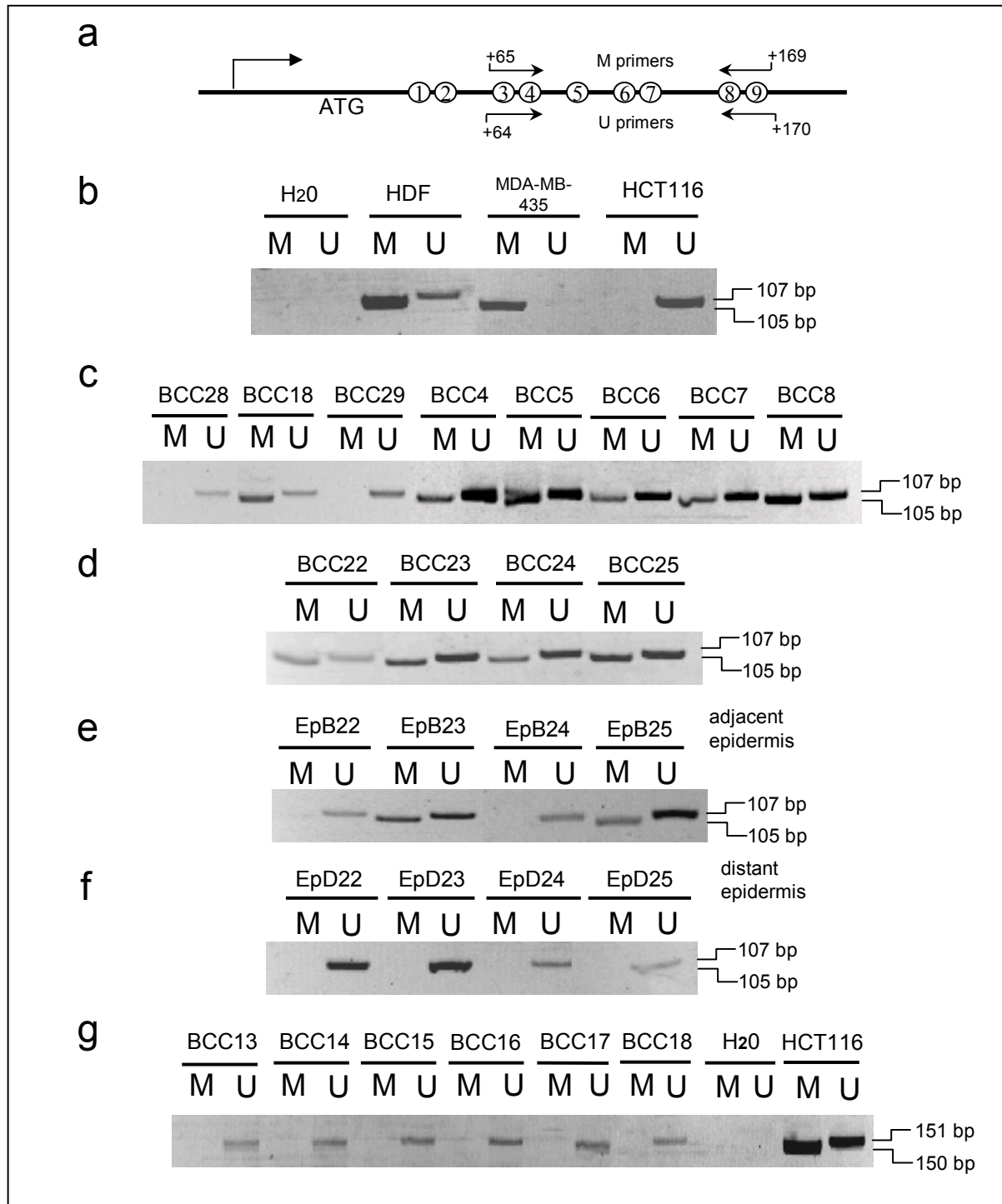


**Figure 15** Methylation status of the *14-3-3 $\sigma$*  and *p16<sup>INK4A</sup>* genes in BCC

(a) Location of the PCR primers employed for MSP analysis of *14-3-3 $\sigma$* . (b) Confirmation of specific MSP conditions for *14-3-3 $\sigma$* . Paired samples of bisulphite-treated genomic DNA derived from the indicated cell lines or primary human diploid fibroblasts (HDF) were subjected to PCR amplification with primers specific for unmethylated (U) and methylated (M) *14-3-3 $\sigma$*  alleles. (c) Exemplary MSP results from eight different BCC patients. (d) Detection of CpG methylation in the *14-3-3 $\sigma$*  gene in four BCC samples, (e) their corresponding adjacent epidermis and (f) epidermis samples adjacent to distant, naevocytic naevi from the same patients. (g) MSP analysis of *p16<sup>INK4A</sup>*. Exemplary results are shown. Genomic DNA was isolated from six microdissected BCC samples and the colorectal cancer cell line HCT116 (positive control for methylated and unmethylated *p16<sup>INK4A</sup>* alleles). For the analyses shown in (c)-(g) paraffin-embedded 6  $\mu$ m sections were laser-microdissected. PCR products were resolved on 8% polyacrylamide gels and stained with ethidium bromide.

**Table 4** 14-3-3 $\sigma$  and p63 protein expression in different types of hyperproliferative skin diseases

	14-3-3 $\sigma$ IHC			p63 IHC	
	Cases analysed (number)	14-3-3 $\sigma$ (positive)	Frequency (%)	Cases analysed (number)	p63 (positive)
<b>Actinic keratosis</b>	11	11	100	7	7
<b>Psoriasis vulgaris</b>	11	11	100	ND	ND
<b>Condylomata acuminata</b>	11	11	100	ND	ND
<b>Squamous cell carcinoma</b>	11	11	100	6	6
<b>Basal cell carcinoma</b>	41	12	29.3	20	20

IHC, immunohistochemical analysis. ND, not determined.

Surprisingly, keratinocytes derived from normal epidermis adjacent to the BCC lesions also showed methylation of CpG-residues at the 14-3-3 $\sigma$  locus in 7 of 20 (35%) cases analyzed (Table 5, column 3). The CpG-methylation detected in keratinocytes from adjacent, normal epidermis did not coincide with a reduced presence of 14-3-3 $\sigma$  protein as detected by immunohistochemistry (data not shown). However, epidermis isolated from distant sites adjacent to naevocytic naevi was negative for CpG methylation (Figure 15d-f, Table 5, column 4). In order to determine whether methylation of 14-3-3 $\sigma$  is a selective event in BCC or whether other genes encoding negative cell cycle regulators are also hypermethylated in BCC, the CpG methylation status of *p16<sup>INK4A</sup>* was analyzed by MSP as described (Herman et al., 1996) (Figure 15g). In 17 cases of BCC with methylated 14-3-3 $\sigma$ , no CpG methylation of *p16<sup>INK4A</sup>* was detected (Table 5, column 5). Only in one of 9 cases of BCC with un-methylated 14-3-3 $\sigma$  alleles, the *p16<sup>INK4A</sup>* promoter was found to be methylated (Table 5, column 5).

**Table 5** Analysis of 14-3-3 $\sigma$  protein expression and promoter methylation in BCC

Patient number	Location / Typ of analysis					
	BCC 14-3-3 $\sigma$ MSP (M/U)	BCC 14-3-3 $\sigma$ IHC	Adjacent epidermis 14-3-3 $\sigma$ MSP (M/U)	Distant epidermis 14-3-3 $\sigma$ MSP (M/U)	BCC p16 MSP (M/U)	BCC p63 IHC
1	+/+	+			-/+	
2	+/+	-			-/+	
3	+/+	-	+/-		-/+	
4	+/+	-/+	-/+		-/+	
5	+/+	-/+	-/+		-/+	
6	+/+	-/+	+/+		-/+	
7	+/+	-				
8	+/+	-/+				
9	+/+	+	-/+		-/+	+
10	+/+	-	+/+		-/+	
11	+/+	-/+			-/+	
12	+/+	+			-/+	+
13	+/+	+			-/+	+
14	+/+	+			-/+	+
15	+/+	-				+
16	+/+	+	-/+		-/+	+
17	+/+	-/+				
18	+/+	-	+/+		-/+	
19	+/+	-			-/+	
20	+/+	-	-/+		-/+	
21	+/+	-/+	-/+	-/+		
22	+/+	-	-/+	-/+		+
23	+/+	-	+/+	-/+		+
24	+/+	-	-/+	-/+		+
25	+/+	-	+/+	-/+		+
26	+/+	-	-/+			+
27	+/+	-	-/+			+
28	+/+	-	+/+			+
29	-/+	+				
30	-/+	+			-/+	
31	-/+	+			+/+	+
32	-/+	-/+			-/+	+
33	-/+	-			-/+	+
34	-/+	+			-/+	+
35	-/+	-	-/+		-/+	+
36	-/+	-				
37	-/+	+				
38	-/+	+				
39	-/+	-/+	-/+			+
40	-/+	-			-/+	+
41	-/+	-/+	-/+		-/+	

Keratinocytes representing BCC, adjacent normal epidermis or distant, normal epidermis derived from 41 patients (coded no. 1–41) were analysed as described in **Methods**. Parallel sections were stained with a 14-3-3 $\sigma$ -specific antiserum (third column). '+': staining similar to normal epidermal keratinocytes; '-/+': staining significantly reduced; '-': no staining (IHC=immunohistochemical analysis). Results obtained by MSP are represented by '+/+': (positive for methylated (M) and unmethylated (U) alleles) or '-/+': (negative for methylated and positive for unmethylated alleles). p63 protein expression was analysed in parallel sections obtained from BCC. Positive, nuclear p63 staining is indicated as '+' in the right column. Fields with no entries correspond to cases that were not analysed.



### 5.3 Identification of genes epigenetically silenced in prostate cancer by pharmacological unmasking

#### 5.3.1 Epigenetic analysis of PCa cell lines

Expression profiling of PCa cell lines treated with an inhibitor of DNA methyltransferases and/or histone deacetylases was exploited to identify genes potentially silenced by DNA methylation. Genes up-regulated by combined treatment were further validated in a panel of PCa and non-transformed prostate cell lines and primary PCa tissues (Figure 16). The immunohistochemical analysis of primary PCa and functional characterization in prostate cells were performed for a subset of identified genes.

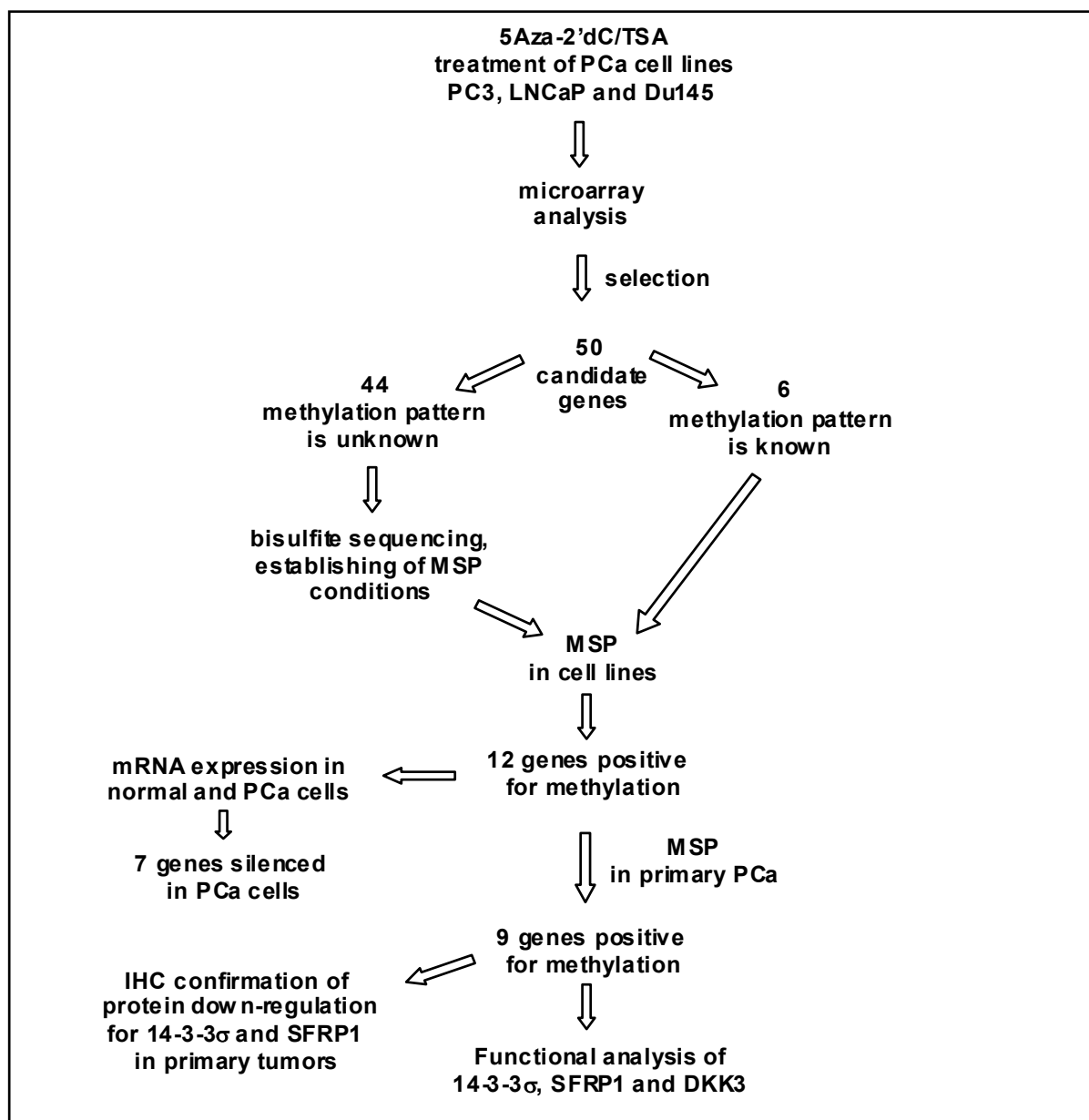


**Figure 16** Epigenetic analysis of PCa: the outline of the experimental procedure

Conditions for optimal re-expression after combined treatment with 5Aza-2'dC and TSA were determined by methylation-specific PCR of the promoter regions of *GSTP1*, *RASSF1A* and *p16* in several PCa cell lines. Thereby, the metastatic PCa cell lines PC3, LNCaP and DU-145 were identified as most suitable for this type of analysis (data not shown). For re-expression of silenced genes the cell lines were exposed to 1  $\mu$ M 5Aza-2'dC for 72 hours and to 300 nM TSA for the last 24 hours. Treatment with 300 nM TSA alone for 24 hours served as a control. Total RNA was isolated, converted to biotinylated cRNA and hybridized to oligonucleotide arrays representing ~22,000 individual transcripts. Each microarray analysis was performed in duplicates. Efficient demethylation of CpG-dinucleotides was confirmed by MSP analysis of several selected promoters (Figure 17a). The microarray analysis revealed that several hundred transcripts were induced in the cells exposed to 5Aza-2'dC and TSA when compared to cells treated with TSA alone (data not shown). *GSTP1*, a gene previously shown to be silenced by CpG methylation in PCa (Singal et al., 2001), was induced 1.87 fold in LNCaP cells. Therefore, an induction of at least 1.8 fold was chosen as the minimal requirement for further analysis of candidate genes. The induction of *GSTP1* was confirmed by RT-PCR (Figure 17b) and Northern blot analysis (data not shown). Exemplary confirmations of results obtained by microarray analysis were performed by RT-PCR for 10 different genes (Figure 17b). In addition, the expression of *RASSF1A* and *p16*, which are known to be induced after demethylation, was analyzed by RT-PCR (Figure 17b). The re-expression of several imprinted genes (e.g. *IGF2*) and of genes silenced by CpG methylation in somatic tissues (e.g. *MAGE*) could be detected. Furthermore, interferon-responsive genes, which have been previously reported to be activated by 5Aza-2'dC treatment (Karpf and Jones, 2002), were found to be induced (data not shown). Genes belonging to these three classes were excluded from further analysis. Re-expressed genes with known putative tumor suppressive functions (e.g. involvement in DNA-repair, negative cell cycle regulation, induction of apoptosis, detoxification, differentiation, transcriptional regulation) were examined for the presence of CpG-islands in their promoters. In total 50 genes met these criteria (listed in Table 6).

**Table 6** Candidate genes for epigenetic silencing identified by microarray analysis

Gene	Symbol	Chr. location	Induced by 5Aza2dC	Function	Methylation detected by		
					BS-seq. in cell lines	MSP	
					in cell lines	in primary tumors	
14-3-3sigma (stratifin)	<b>SFN</b>	1p35	L	G <sub>2</sub> /M transition		yes	41/41
secreted frizzled-related protein 1	<b>SFRP1</b>	<u>8p12</u>	P	Wnt signaling		yes	34/41
apolipoprotein D	<b>APOD</b>	3q26	L, P	HDL component		yes	n.d.
tissue factor pathway inhibitor 2	<b>TFPI2</b>	7q22	P, D	ECM proteases inhibitor		No	
thrombospondin 1	<b>THBS1</b>	15q15	L, P, D	angiogenesis inhibitor		No	
retinoblastoma protein-interacting zinc finger	<b>RIZ1</b>	1p36	P	methyltransferase		No	
caspase 7	<b>CASP7</b>	<u>10q25</u>	P, D	apoptosis	no		
apoptotic protease activating factor	<b>APAF1</b>	12q23	P, D	apoptosis	no		
apoptosis-inducing protein D	<b>APPD</b>	19q11	D	apoptosis	no		
tumor necrosis factor receptor 10b	<b>TNFRSF10B</b>	8p22	D	apoptosis	no		
cyclin-dependent kinase inhibitor 1C (p57, Kip2)	<b>CDKN1C</b>	11p15	L, P	cdk inhibitor	yes	yes	23/41
cyclin-dependent kinase inhibitor 2D (p19)	<b>CDKN2D</b>	19p13	P	cdk inhibitor	no		
cyclin-dependent kinase inhibitor 1A (p21, Cip1)	<b>CDKN1A</b>	6p21.2	L, P, D	cdk inhibitor	no		
retinoblastoma-like 2 (p130)	<b>RBL2</b>	16q12	D	cell cycle	no		
glutathione S-transferase M1	<b>GSTM1</b>	1p13	L	detoxification	yes	yes	24 <sup>§</sup> /41
glutathione peroxidase 3	<b>GPX3</b>	<u>5q23</u>	L, P	detoxification	yes	yes	38/41
HUS1	<b>HUS1</b>	7p13	D	DNA damage response	no		
meiotic recombination 11	<b>MRE11A</b>	11q21	D	DNA damage response	no		
xeroderma pigmentosum, complementation group C	<b>XPC</b>	3p25	L	DNA repair	no		
damage-specific DNA binding protein 2	<b>DDB2</b>	11p12	L	DNA repair	yes	yes	34/41
postmeiotic segregation increased 2	<b>FMS2</b>	7p22	D	DNA repair	no		
breast cancer 2, early onset	<b>BRCA2</b>	13q12.3	D	DNA repair, transcription	no		
cylindromatosis (turban tumor syndrome)	<b>CYLD</b>	16q11	P	deubiquitination	no		
bridging integrator 1	<b>BIN1</b>	2q14	D	differentiation	low	n.d.	n.d.
growth arrest and DNA-damage-inducible, alpha	<b>GADD45A</b>	1p31.2	P, D	growth arrest	low	n.d.	n.d.
connective tissue growth factor	<b>CTGF</b>	<u>6q23</u>	P, D	growth factor	no		
nerve growth factor receptor	<b>NGFR</b>	17q21	P, D	growth factor receptor	no		
interferon regulatory factor 1	<b>IRF1</b>	<u>5q31</u>	P, D	interferon response	no		
interferon regulatory factor 7	<b>IRF7</b>	11p15	L, P, D	interferon response	no		
hydroxyprostaglandin dehydrogenase 15-(NAD)	<b>HPGD</b>	4q34	L, P	prostaglandin signaling	yes	yes	30/41
Prostaglandin E receptor 4 (subtype EP4)	<b>PTGER4</b>	5p13	L, P, D	prostaglandin signaling	no		
cyclooxygenase 2	<b>PTGS2</b>	1q25	L, P	prostaglandin signaling	yes	yes	32/41
sequestosome 1	<b>SQSTM1</b>	<u>5q35</u>	L, P	protein degradation	no		
dual specificity phosphatase 1	<b>DUSP1</b>	<u>5q34</u>	P, D	signaling	no		
jun B proto-oncogene	<b>JUNB</b>	14q32	P, D	transcription factor	no		
cut-like 2	<b>CUTL2</b>	12q24	P	transcription factor	yes	n.d.	n.d.
zinc finger protein 36, C3H type, homolog	<b>ZFP36</b>	19q13	L, D	transcription factor	no		
Cbp/p300-interacting transactivator	<b>CITED2</b>	<u>6q23</u>	P, D	transcriptional control	no		
SWI/SNF related regulator of chromatin A1	<b>SMARCA1</b>	Xq25	D	transcriptional control	no		
inhibitor of DNA binding 3	<b>ID3</b>	1p36	L, P	transcriptional control	no		
serum-inducible kinase	<b>SNK</b>	<u>5q12</u>	L, P	signaling	no		
serum/glucocorticoid regulated kinase	<b>SGK</b>	<u>6q23</u>	L, P, D	signaling	no		
serine/threonine kinase 38 like	<b>STK38L</b>	12p12.3	L	signaling	no		
growth arrest-specific 2 like 1	<b>GAS2L1</b>	22q12.2	L	unknown	no		
deleted in liver cancer 1	<b>DLC1</b>	<u>8p22</u>	D	unknown	no		
ras-induced senescence 1	<b>RIS1</b>	3p.21	D	unknown	yes	yes	n.d.
B-cell translocation gene 1, anti-proliferative	<b>BTG1</b>	12q22	D	unknown	no		
B-cell translocation gene 3, anti-proliferative	<b>BTG3</b>	21q21	P, D	unknown	no		
dickkopf homolog 3	<b>DKK3</b>	11p15	P	Wnt signaling	yes	yes	28/41
dickkopf homolog 1	<b>DKK1</b>	<u>10q11</u>	D	Wnt signaling	no		

Experimental results for 50 selected, CpG-island containing genes induced upon treatment with 5Aza-2'dC and TSA in prostate carcinoma cell lines are summarized. Bold gene symbols, genes known to be silenced by CpG methylation in other types of human cancer (not PCa); underlined chromosomal locations, regions of frequent LOH in PCa; bold cell line abbreviations, genomic DNA used for bisulfite sequencing; L, LNCaP; P, PC3; D, Du-145; BS-seq., bisulfite sequencing analysis; MSP, methylation sensitive PCR; §, methylation-specific PCR product dominant over PCR product corresponding to unmethylated allele.

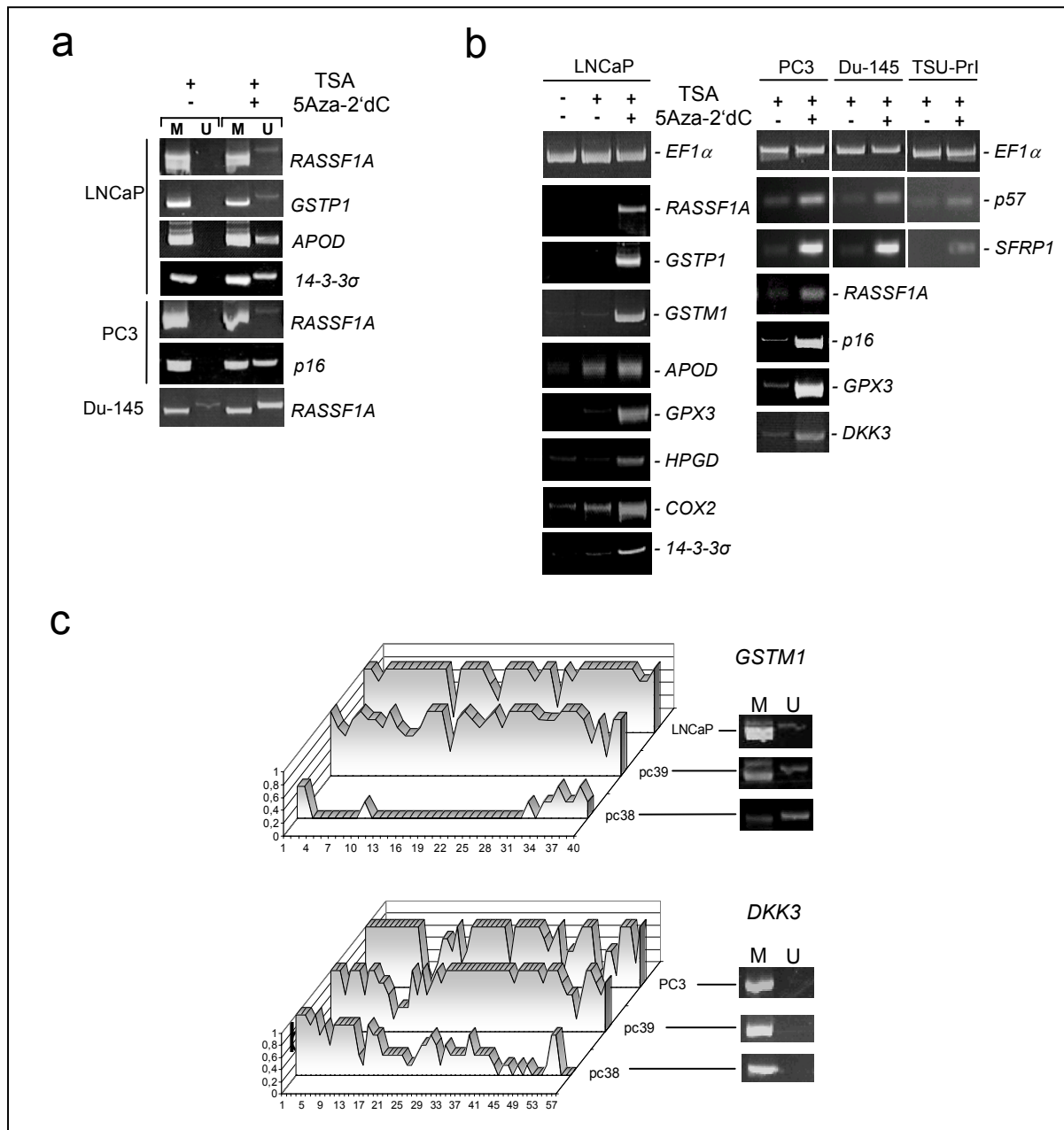


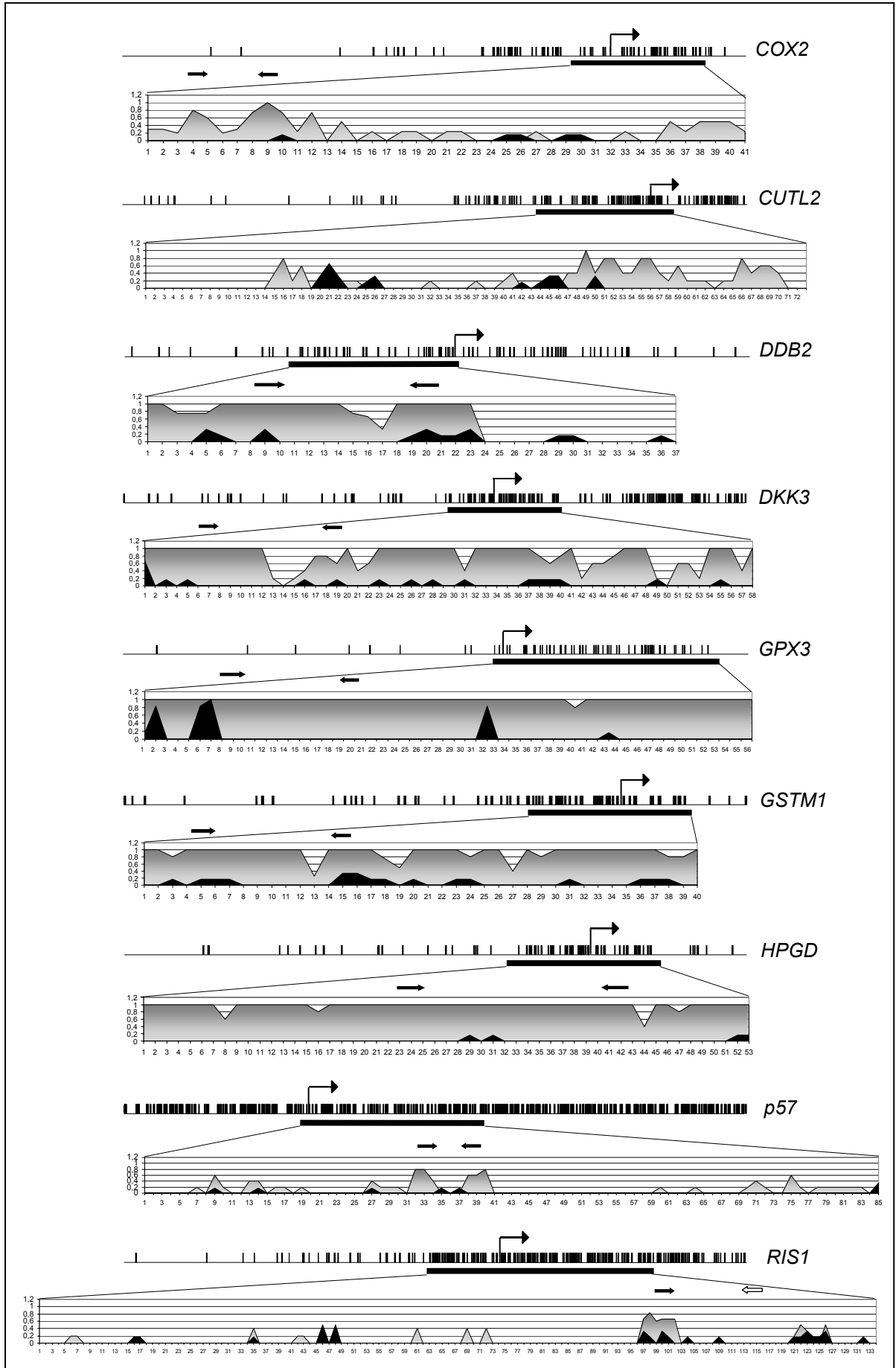
**Figure 17** Analysis of CpG methylation in PCa cell lines

(a) Pharmacological reversion of epigenetic silencing in prostate carcinoma cell lines. LNCaP, PC3 and Du-145 prostate cancer cell lines were treated with 5Aza-2'dC for 72 hours and with TSA for the last 24 hours, with TSA only for 24 hours or left untreated. After bisulfite treatment genomic DNA was subjected to MSP analysis with primers specific for the indicated genes. The PCR-products labelled with "M" were generated by methylation-specific primers, and those labeled with "U" by primers specific for unmethylated DNA. (b) mRNA expression of the indicated genes was analyzed by semi-quantitative RT-PCR. As a loading control and expression standard amplification of the house keeping gene *EF1 $\alpha$*  was used. (c) Comparison of *GSTM1* and *DKK3* CpG methylation pattern in cell lines vs. primary tumors. Tumor cells were laser microdissected from paraffin-embedded PCa sections and genomic DNA was isolated. Results of sequencing of at least 6 individual subclones for each area are shown: grey shaded chart areas represent frequencies of methylated CpG-dinucleotides within the respective fragments in PCa cell lines. Results of a parallel MSP-analysis of the genomic DNA employed for bisulfite sequencing are depicted.

### 5.3.2 The methylation pattern of candidate promoters

The CpG methylation pattern of *GSTM1* and *DKK3* was determined in the cell lines LNCaP and PC3 respectively and compared to the pattern found in primary PCa cells isolated by laser microdissection of paraffin-embedded prostate sections from two patients (Figure 17c). The CpG methylation pattern found in PCa cell lines reflected the pattern found in primary tumors and is therefore appropriate for the design of MSP primers used in the analysis of primary tumors. In total the promoters of 44 induced genes were subjected to analysis by bisulfite sequencing in PCa cell lines which have been used for the microarray analysis (Table 6). Extensive CpG methylation was detected in the 5' regions of *DDB2*, *DKK3*, *GPX3*, *GSTM1* and *HPGD*, whereas *COX2*, *CUTL2*, *p57* and *RIS1* displayed focal CpG methylation (Figure 18). In non-transformed PrECs these genes did not display significant CpG methylation (Figure 18). 35 of the 44 genes analyzed by bisulfite sequencing did not show detectable CpG methylation, although these genes were significantly up-regulated after the combined 5Aza-2'dC/TSA treatment (listed in Table 6). Presumably, these genes were induced secondary to the up-regulation of other genes silenced by CpG methylation or due to non-specific activation of transcriptional pathways by the combined 5Aza-2'dC/TSA treatment (Gius et al., 2004; Karpf et al., 2001). It is possible that the CpG dinucleotides responsible for the silencing of these genes were not in the region analyzed by bisulfite sequencing in this study. However, as indicated in Figure 18, the analyzed regions covered several hundred base-pairs around the transcription start site, which display a high CpG-content and are expected to be the main targets for CpG methylation.

**Figure 18** Determination of the CpG methylation patterns of candidate genes in PCa. Bisulfite sequencing was performed with genomic DNA derived from LNCaP (for *COX2*, *DDB2*, *GSTM1* and *HPGD*), PC3 (*CUTL2*, *DKK3*, *GPX3*, and *p57*) and Du-145 (*RIS1*) cells or PrECs (each gene). The distribution of CpGs and their methylation status are shown. The depicted areas correspond to genomic DNA sequences of 2.5 kbp. Vertical bars represent CpG-dinucleotides. The position of the transcription start site is indicated by an arrow. Horizontal, black rectangles indicate areas which were amplified and subcloned after bisulfite treatment. Results of sequencing of at least 6 individual subclones for each area are shown: grey shaded chart areas represent frequencies of methylated CpG-dinucleotides within the respective fragments in PCa cell lines. Black shaded areas show methylation patterns detected in PrECs. The y-axis corresponds to the relative amount of methylation of the CpG-dinucleotide at the indicated relative positions. The exact location of amplified fragments and CpG-dinucleotides is given in the supplemental Table 1



### 5.3.3 Validation of candidate genes for epigenetic silencing

One of the genes induced by demethylation in LNCaP cells was *14-3-3 $\sigma$* . Using MSP conditions described in section 5.2.2 it was confirmed that this gene is completely methylated in LNCaP cells and underwent partial demethylation upon treatment with 5Aza-2'dC resulting in mRNA induction detected by RT-PCR and Northern blot analysis (Figure 17, a and b; data not shown). Furthermore, detection of methylated cytosines with higher resolution by bisulfite sequencing demonstrated a minimal degree of CpG methylation of the *14-3-3 $\sigma$*  gene in PrECs, whereas dense methylation was evident in the DNA derived from the LNCaP cell line (Figure 19a).

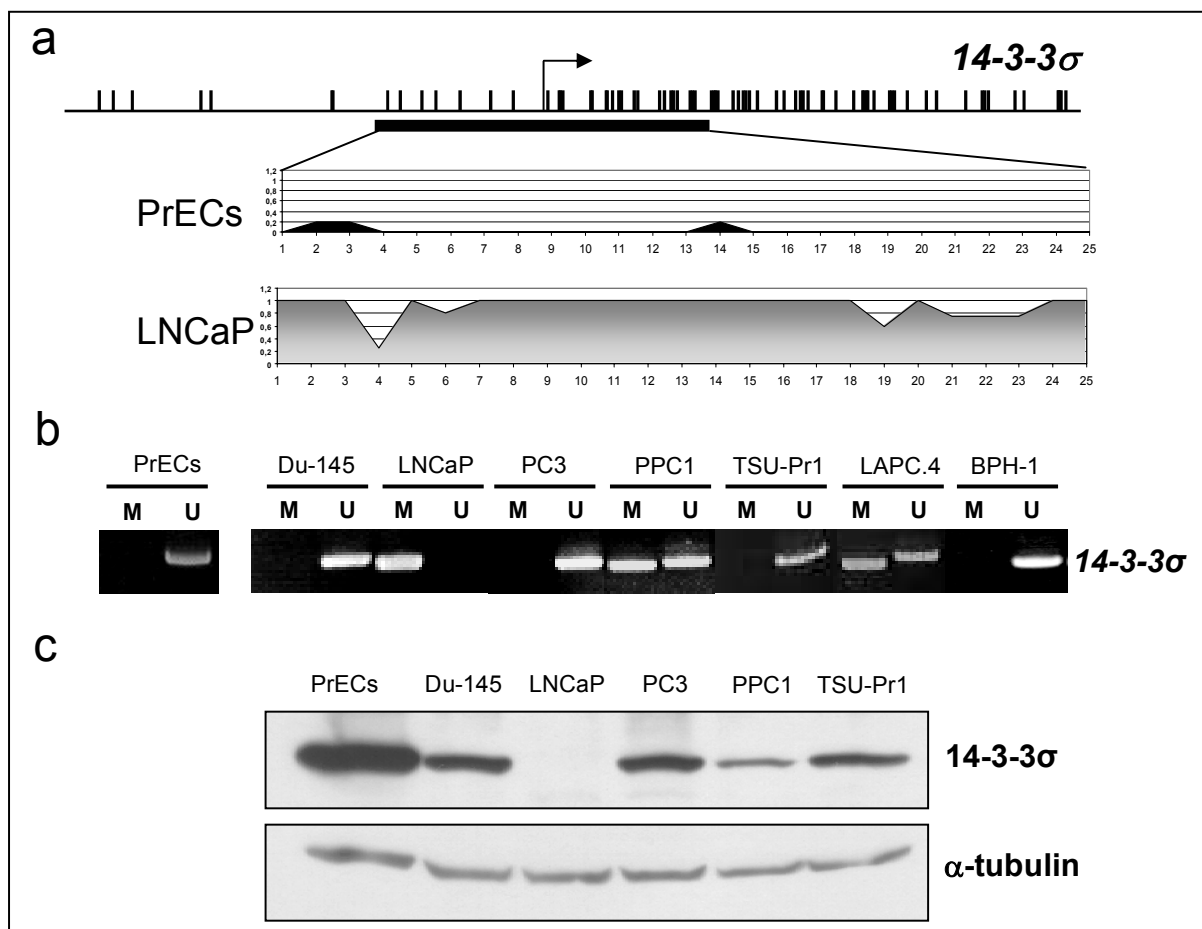


**Figure 19** Methylation status and protein expression of *14-3-3 $\sigma$*  in PCa cell lines

(a) The pattern of CpG methylation of the *14-3-3 $\sigma$*  locus as determined by bisulfite sequencing. Genomic DNA isolated from PrECs and PCa cell line LNCaP was treated with bisulfite and analysed as described in **Methods**. Depicted is a schematic representation of the CpG distribution around transcription start site of *14-3-3 $\sigma$* . The detailed description of the graphic features is given in the legend for Figure 18. (b) *14-3-3 $\sigma$* -specific MSP analysis of PrECs, PCa and BPH-1 cell lines. Genomic DNA was isolated from exponentially proliferating cells, treated with sodium bisulfite and used as a template for MSP analysis with primers specific for the methylated (M) and unmethylated (U) *14-3-3 $\sigma$*  allele. BPH-1: benign prostate hyperplasia cells immortalized with SV40 large T antigen; PrECs: human primary prostate epithelial cells. (c) Detection of *14-3-3 $\sigma$*  protein expression. Western blot analysis was performed with extracts from exponentially growing cells using an affinity-purified rabbit *14-3-3 $\sigma$*  antiserum. Detection of  $\alpha$ -tubulin was employed as a loading control.

MSP analysis extended to other cell lines revealed that *14-3-3 $\sigma$*  is also methylated in the PCa cell lines PPC1 and LAPC4, but not in a cell line established from a benign prostate hyperplasia (BPH1) or in primary prostate epithelial cells (Figure 19b). By Western blot analysis, an inverse correlation between the degree of CpG methylation and protein expression was identified (Figure 19c): LNCaP cells, which display complete CpG methylation of *14-3-3 $\sigma$* , were devoid of *14-3-3 $\sigma$*  expression; PPC1 cells, which have methylated and unmethylated *14-3-3 $\sigma$*  alleles, showed a significant down-regulation of *14-3-3 $\sigma$*  protein expression. The cell lines Du-145, PC3 and TSU-Pr1 did not reveal any CpG methylation in the *14-3-3 $\sigma$*  gene and showed relatively high levels of *14-3-3 $\sigma$*  protein expression. The highest level of *14-3-3 $\sigma$*  expression was detected in the PrECs, which lack CpG methylation of the *14-3-3 $\sigma$*  gene. Interestingly, the cell lines Du-145 and PC3 harbor *p53* mutations, whereas LNCaP cells express wild-type *p53*. This correlation suggests that silencing of *14-3-3 $\sigma$*  may potentially alleviate the requirement to inactivate *p53* in PCa.

In order to facilitate detection of aberrant methylation in a larger number of specimens the CpG methylation patterns obtained for other candidate genes were used to assign the positions of MSP-primers (indicated in Figure 18). The respective MSP-primers were tested for their specificity and sensitivity (data not shown). Only for *CUTL2* reliable MSP-conditions could not be established. For analysis of genes previously known to be silenced by CpG methylation in other tumor types, the respective published MSP-primers were tested and used for MSP analysis. In total 14 genes (including *14-3-3 $\sigma$* ) which displayed significant CpG methylation as determined by bisulfite sequencing or MSP in one of the cell lines PC3, LNCaP or Du-145 were examined by MSP in a panel of five prostate cancer cell lines, BPH1, PrECs and in the bladder carcinoma cell line TSU-Pr1 (Figure 20, left panel).

The analysis of candidates revealed, that the genes initially identified in selected PCa cell lines also displayed CpG methylation in other PCa cell lines and, occasionally in the cell line BPH1. 9 of the 14 analyzed genes did not display CpG methylation in primary prostate epithelial cells (PrECs). Therefore, CpG methylation of these 9 genes is a specific feature of cancerous prostate epithelial cells. *APOD*, *DDB2*, *GSTM1* and *RIS1* displayed partial CpG methylation in PrECs (Figure 20). However, the degree of CpG methylation of *DDB2*, *APOD* and *GSTM1* appeared to be significantly elevated in most of the PCa-cell lines when compared to normal PrECs (Figure 20), suggesting a PCa-specific increase in CpG methylation of these



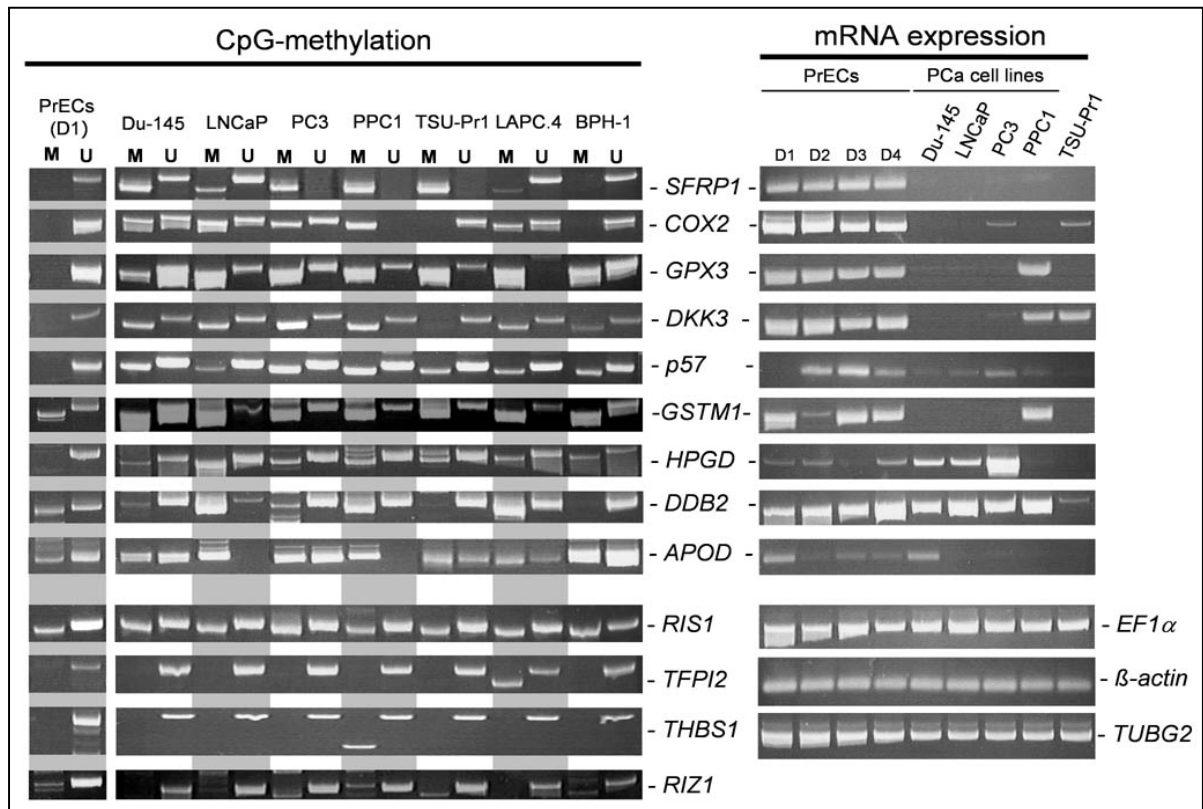


**Figure 20** Comparative analysis of CpG methylation and gene expression  
 Left panel: MSP analysis of a series of PCa cell lines and primary prostate epithelial cells (left panel). The MSP-analysis was done using two primers sets (M = methylated; U = unmethylated) specific for the indicated genes. BPH1 = benign prostate hyperplasia cells immortalized with SV40 large T antigen. Right panel: RT-PCR analysis of the indicated genes in non-transformed and tumor cells. D1-D4 samples represent primary prostate epithelial cells (PrECs) from four different donors.  $\beta$ -actin and  $\gamma$ -tubulin (*TUBG2*) were used as additional standards to *EF1 $\alpha$* .

genes and potential subsequent silencing. CpG methylation of *SFRP1*, *GPX3*, *GSTM1* and *APOD* was also detected in the bladder carcinoma cell line TSU-Pr1. The expression level of 9 genes which showed selective or preferential CpG methylation in PCa was analyzed in order to determine whether CpG methylation correlates with reduced or absent expression of the respective genes. RT-PCR analysis of cDNAs obtained from normal prostate epithelial cells derived from 4 healthy donors and 4 PCa cell lines revealed several distinct patterns of mRNA expression (Figure 20, right panel). The CpG methylation interrogated by the MSP-primers used here largely correlated with reduced gene expression in the case of *SFRP1*, *DKK3*, *GPX3*, *COX2*, *GSTM1*, *APOD* and *p57*, whereas the detected CpG methylation of *DDB2* and *HPGD* was not accompanied by decreased gene expression. In the case of *HPGD* the expression was even induced in 3 PCa samples, which clearly showed CpG methylation. These results indicate that CpG methylation of a promoter should not be interpreted as proof for its transcriptional repression.

### 5.3.4 Analysis of DNA methylation in primary PCa samples

The CpG methylation status of the genes showing CpG methylation mediated silencing in PCa cell lines was determined in 41 primary PCa samples obtained after radical (37 cases) or transurethral (4 cases) prostate resection. In addition, the genes *DDB2* and *HPGD* were included in this analysis, although no correlation between CpG methylation and down-regulation of mRNA expression for these genes has been detected. Nonetheless, the detection of PCa-specific CpG methylation in the promoter of these genes may be useful for diagnostic applications. Prostatic tissue samples contain several cell-types. Non-neoplastic epithelial cells, stromal cells, lymphocytic infiltrates and blood cells are present in close proximity to PCa cells. Therefore, laser microdissection was employed to isolate PCa cells. Similarly, non-neoplastic prostate epithelial cells were isolated from samples obtained from 9 patients with benign prostate hyperplasia, which did not represent PCa and were in the same age group as the 41 PCa patients. Genomic DNA was isolated from these samples and subjected to MSP analysis (Figures 21 and 22).

In the PCa cells, *14-3-3 $\sigma$*  showed CpG methylation at medium to high degrees (Figure 21a): in three cases, only the methylated allele was detected and, with the exception of one case, the PCR product representing the methylated allele was more prominent than the PCR product specific for the unmethylated allele. From prostatic paraffin sections of 36 PCa patients, enough adjacent epithelial cells with normal appearing morphology could be isolated by laser microdissection to allow MSP analysis. The four transurethral and one radical prostatectomy specimens did not yield enough DNA for MSP analysis. The adjacent, normal prostate epithelial cells did not show methylation of *14-3-3 $\sigma$*  in 31 cases (86.1% (31 of 36 cases); Figure 21b). Only five cases (pn1, pn19, pn23, pn25, pn30) showed CpG methylation of *14-3-3 $\sigma$*  in normal prostate epithelium, which may be caused by isolation of PCa-precursor cells displaying a normal morphology. In three cases, PCR products with aberrant sizes not corresponding to methylated *14-3-3 $\sigma$*  were detected (pn6, pn14, pn26). CpG methylation of *14-3-3 $\sigma$*  was previously detected in histologically normal epithelial cells adjacent to cancer cells in other types of cancer and may represent precursor lesions (Umbricht et al., 2001). The necessity of laser microdissection for epigenetic analysis was underscored by a prominent CpG methylation of *14-3-3 $\sigma$*  detected in stromal cells of the prostate (Figure 21c). Furthermore, hyperproliferative prostate epithelial cells obtained from five patients with BPH, which

did not present PCa and were in the same age group as the 41 PCa patients, were subjected to MSP analysis. The *14-3-3 $\sigma$*  promoter was not methylated in prostate epithelial cells in four cases of BPH (Figure 21d). In a fifth BPH specimen, a weak signal representing methylated *14-3-3 $\sigma$*  allele was detected (Figure 21d).

The other analyzed genes showed CpG methylation at medium to high frequencies in PCa cells. CpG methylation was detected for *SFRP1* in 34 (83%), *COX2* in 32 (78%), *DKK3* in 28 (68%), *GPX3* in 38 (93%), *p57* in 23 (56%), *HPGD* in 30 (73%) and *DDB2* in 34 (83%) of the 41 PCa samples analyzed (Figures 22 and 23). Predominant methylation of *GSTM1* was detected in 24 (58%) of 41 cases. For *SFRP1* and *COX2* no CpG methylation was detected in BPH derived from 9 different patients, suggesting that the CpG methylation of these genes is specific for neoplastic prostate epithelial cells. CpG methylation was detected for *GPX3* in two and for *DKK3* in one of 9 analyzed BPH samples (Figure 23). For *GSTM1* CpG methylation was detected in the 5 BPH samples analyzed (Figure 22). However, the CpG methylation of *GSTM1* was elevated in the majority of PCa samples, whereas in the non-neoplastic BPH cells equal signals for the PCR-products representing methylated and unmethylated *GSTM1* alleles were detected. Furthermore, the unmethylated *GSTM1* allele was not detected in several samples of PCa. No obvious correlation between staging information and CpG methylation was detected by cluster analysis (data not shown).

In order to evaluate the tumor-specificity of the CpG methylation detected in PCa, the CpG methylation status was examined in human diploid fibroblasts (HDF) derived from neonatal skin, in stroma isolated from 5 cancer-free prostate specimens and in peripheral blood mononuclear cells (PBMC) from 6 individuals (Figure 23). The *p57* gene did not show CpG methylation in stromal cells. Partial CpG methylation of *SFRP1* and *COX2* was evident only in one of five analyzed stroma samples. One of six PBMC samples showed partial methylation of *SFRP1* and *p57* genes. By contrast, *DKK3* and *GPX3* displayed CpG methylation in most of the stromal samples and blood cells.

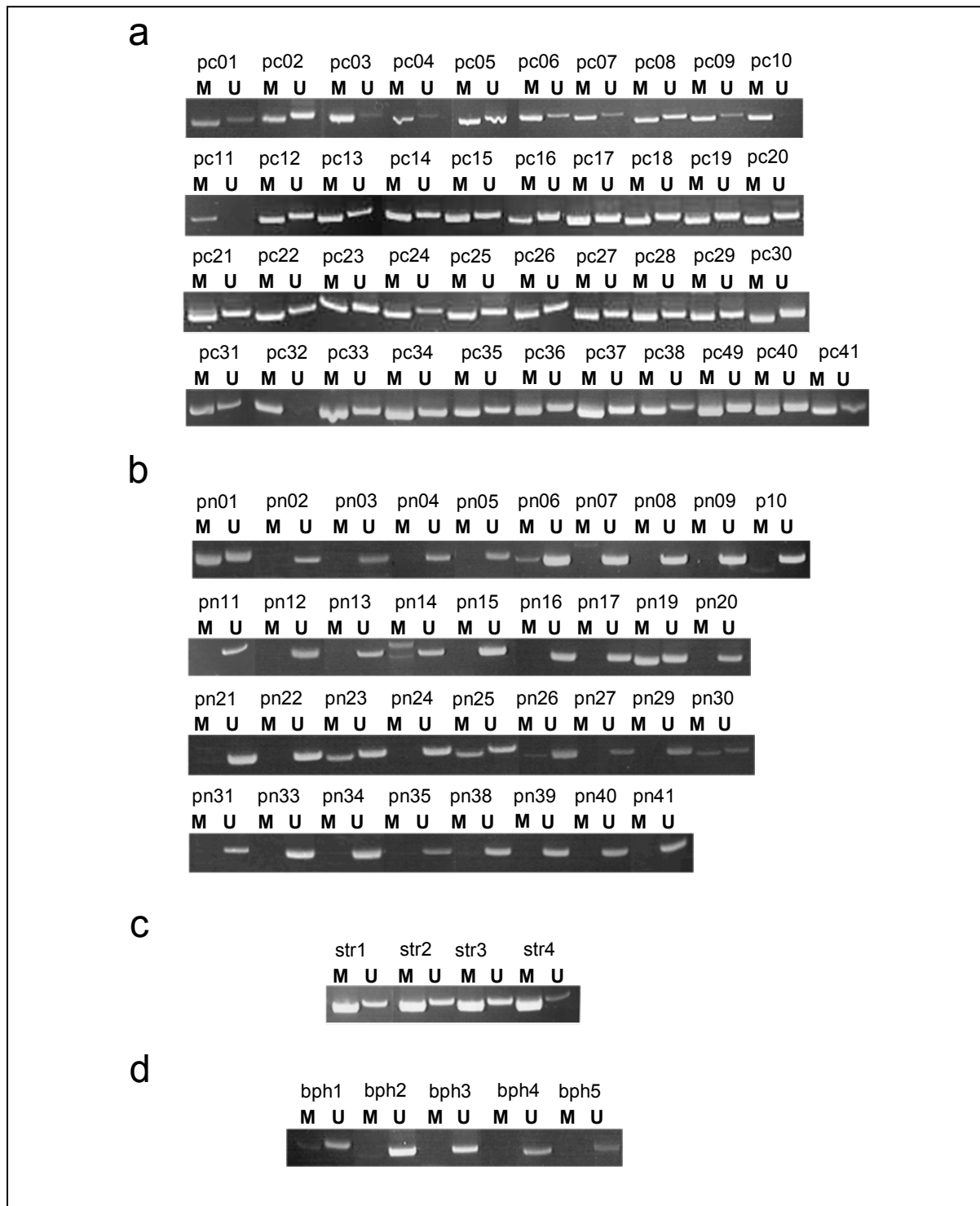


**Figure 21** 14-3-3 $\sigma$ -specific MSP analysis of *in vivo* CpG methylation in prostate tissue after laser microdissection.

Different neoplastic and non-neoplastic cell types were isolated from 5  $\mu$ m sections of archival formalin-fixed, paraffin-embedded samples using laser-pressure catapulting. MSP analysis was performed on (a) PCa cells (pc01 - pc41) and (b) normal prostate epithelial cells (pn01 - pn41), (c) prostate stromal cells (str1 - str4) and (d) prostate epithelial cells representing BPH (bph1 - bph5) obtained from five BPH patients.

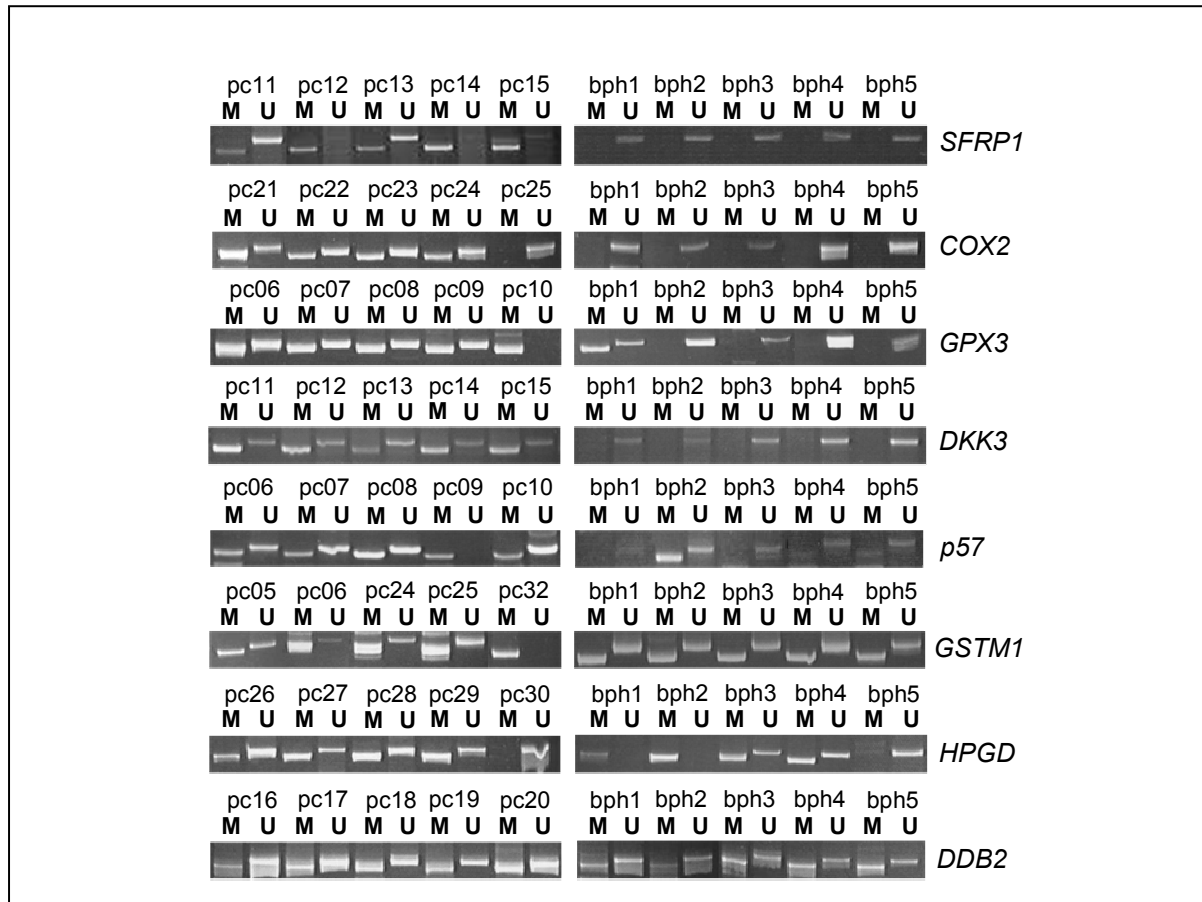


**Figure 22** Detection of CpG methylation after laser microdissection

Tumor cells or normal prostate epithelial cells were isolated from paraffin-embedded tumor sections derived from 41 different patients (pc01-pc41) using laser-pressure catapulting. Representative examples of MSP analysis of 5 tumor cell samples and 5 samples derived from normal epithelial cells (BPH) for the indicated genes are shown.

	SFRP1	COX2	GPX3	DKK3	p57	GSTM1	HPGD	DDB2	14-3-3 $\sigma$	Gleason	pT	pN
pc01												
pc02												
pc03										7	2a	0
pc04										6	3a	0
pc05										6	2c	0
pc06										7	2c	0
pc07										6	2a	0
pc08										5	2c	0
pc09										6	2a	0
pc10										6	3b	0
pc11										5	2c	0
pc12										5	2c	0
pc13										6	2a	0
pc14										7	2a	0
pc15										7	2a	1
pc16										7	2a	0
pc17										7	3a	0
pc18										9	x	x
pc19										7	3a	0
pc20										7	3b	0
pc21										7	2c	0
pc22										7	3a	0
pc23										6	2c	0
pc24										6	2c	0
pc25												
pc26										7	2b	0
pc27										6	2c	0
pc28										8	x	x
pc29										10	3b	0
pc30										6	2c	0
pc31										6	2c	0
pc32										6	2c	0
pc33										7	3b	0
pc34										6	2c	0
pc35										6	2c	0
pc36										9	x	x
pc37										10	x	
pc38										7	3b	0
pc39										7	3a	1
pc40										6	2c	0
pc41										7	2c	x
bph1												
bph2												
bph3												
bph4												
bph5												
bph6												
bph7												
bph8												
bph9												
str1												
str2												
str3												
str4												
str5												
HDF												
PBMC1												
PBMC2												
PBMC3												
PBMC4												
PBMC5												
PBMC6												

**Figure 23** Summary of MSP results in primary PCa

Gene names are indicated on the top. Each row represents a primary PCa tumor (pc01-41), non-neoplastic prostate epithelial cells (bph1-9) or prostate stroma samples (str1-5) isolated by laser microdissection. Human diploid fibroblasts (HDF) derived from skin and PBMC (peripheral blood mononuclear cells) were cultured *in vitro*. Color coding: white = no significant CpG methylation detected; grey = PCR-product representing CpG methylation has a similar intensity as the PCR-product specific for the unmethylated allele; black = allele with CpG methylation is dominant over the unmethylated allele or the unmethylated allele is absent.

### 5.3.5 Analysis of 14-3-3 $\sigma$ and SFRP1 protein expression in PCa

In order to determine whether CpG methylation of the 14-3-3 $\sigma$  gene affects the expression of the corresponding gene product *in vivo*, the level of 14-3-3 $\sigma$  protein expression was determined by immunohistochemistry in tissue sections of the prostate. PCa samples from 41 different patients were analysed with an affinity-purified antibody specific for the 14-3-3 $\sigma$  protein. In normal basal and luminal prostate epithelial cells and in prostate epithelial cells representing BPH and atrophic lesions, an intense cytoplasmic staining for 14-3-3 $\sigma$  protein was detected (Figure 24a-f). The expression of 14-3-3 $\sigma$  protein was down-regulated markedly (>50%) in neoplastic cells and glands of 26 PCa samples. Representative examples are shown in Figure 24a and b. A total of 12 specimens showed a moderate reduction (examples in Figure 24, d and e) and four cases showed a minor decrease in 14-3-3 $\sigma$  protein-specific staining (data not shown). The down-regulation of 14-3-3 $\sigma$  protein expression was also detected in PIN (prostatic intraepithelial neoplasia) lesions, which represent precursors of PCa (Figure 24, e and f). Loss of 14-3-3 $\sigma$  expression was restricted to luminal cells in the PIN lesions, whereas basal cells stained positive for 14-3-3 $\sigma$ . At present it is unclear whether the down-regulation of 14-3-3 $\sigma$  expression in PIN is due to CpG methylation, since the amount of DNA obtained after microdissection of PIN lesions was not sufficient to perform MSP analyses (data not shown).

In order to determine whether the CpG methylation of SFRP1 affects the expression of the respective gene product in primary tumors, the level of SFRP1 protein expression was determined by immunohistochemistry in PCa samples derived from 39 different patients (representative example shown in Figure 24, g and h). In non-neoplastic prostate glands most of the luminal cells were positive for SFRP1 with a characteristic granular cytoplasmic and apical membrane staining, whereas PCa cells were devoid of SFRP1 staining. A prominent down-regulation (> 50% of reduction) or complete loss of SFRP1 protein was detected in 29 of 39 PCa samples (data not shown).

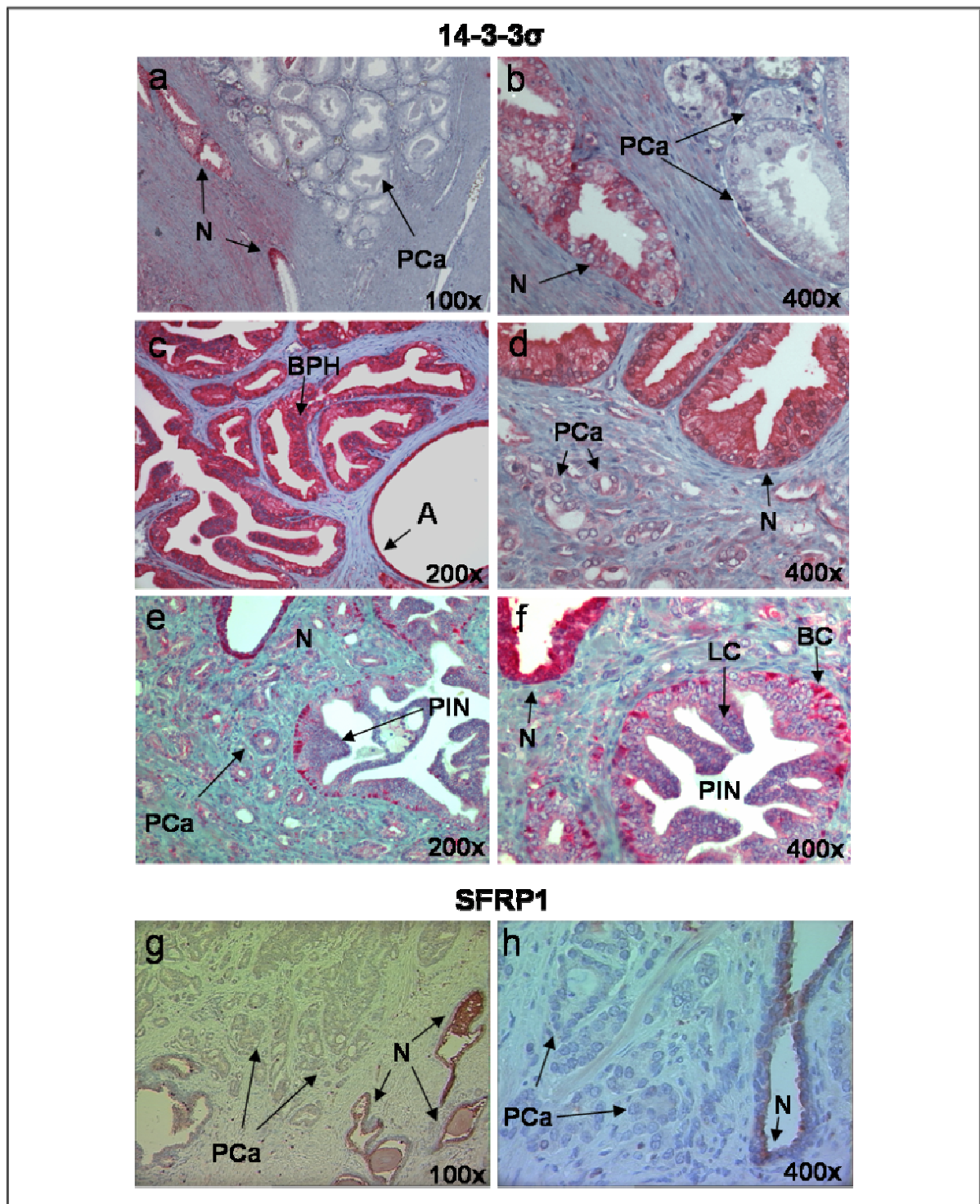


**Figure 24** Analysis of 14-3-3 $\sigma$  and SFRP1 protein expression in primary PCa tissues (a-f) Depicted are immunohistochemical detections of 14-3-3 $\sigma$  protein (red color) in paraffin-embedded prostate tissue obtained from PCa and BPH patients. (A: atrophic prostate epithelial cells; BC: basal PIN cells; BPH: benign prostate hyperplasia; LC: luminal PIN cells; N: non-neoplastic prostate epithelial cells; PCa: prostate cancer cells; PIN: prostatic intraepithelial neoplasia). (a, b, d) Sections containing normal prostate glands and PCa; (c) section with BPH and an atrophic gland; (e, f) section with PIN, PCa and normal prostate glands. The respective magnifications are indicated. (g, h) Immunohistochemical detections of SFRP1 (red) in primary PCa. Stainings and their evaluation were performed by members of the laboratory of Dr. Joachim Diebold (Institute of Pathology, LMU, Munich)



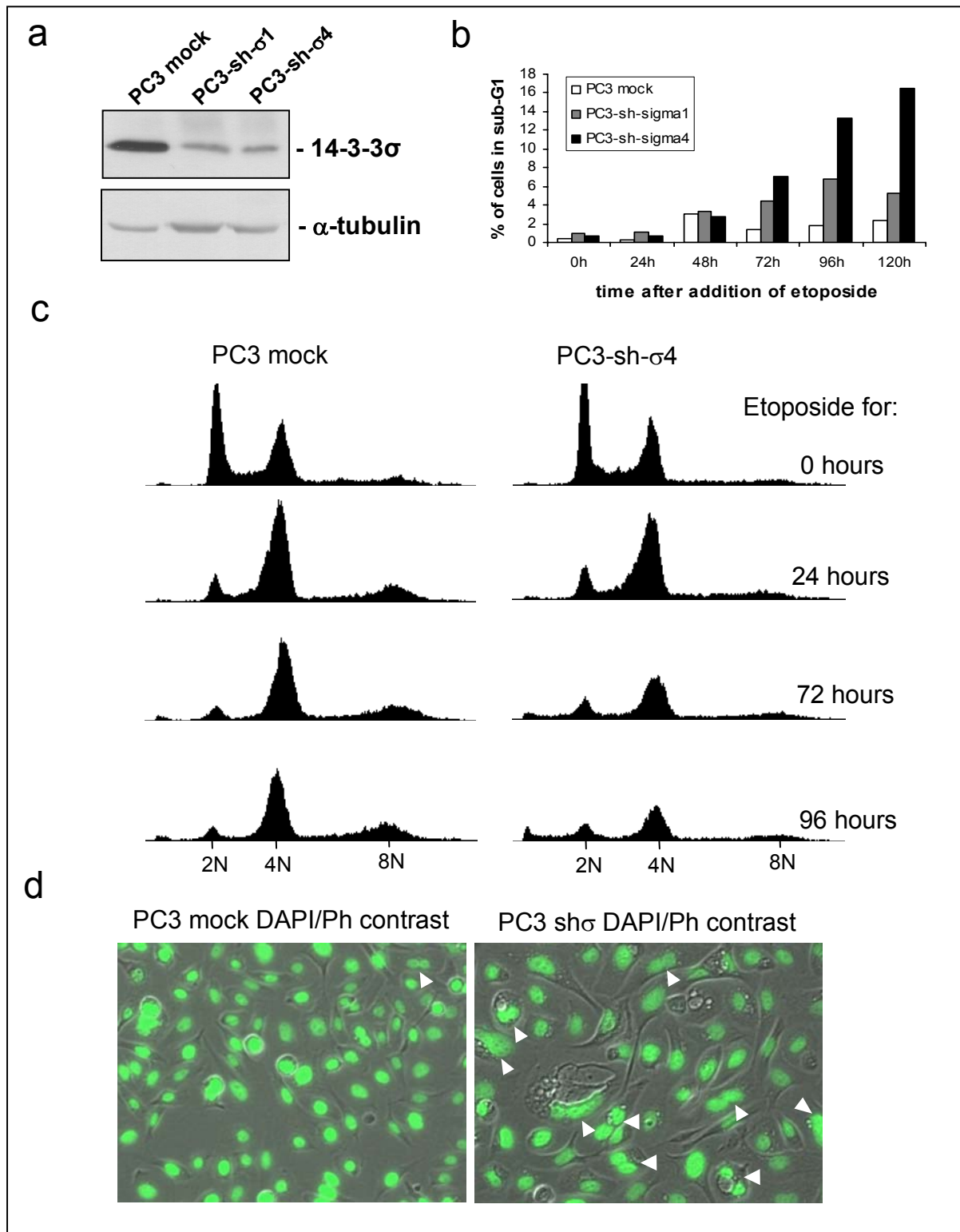
### 5.3.6 Functional analysis of *14-3-3 $\sigma$*

In order to assess the functional consequences of down-regulation of *14-3-3 $\sigma$*  expression in prostate epithelial cells, a retroviral vector expressing a short RNA hairpin specifically directed against the open reading frame of *14-3-3 $\sigma$*  was generated (see **Methods** for details). Two independent PC3 cell clones (PC3-sh- $\sigma$  1 and PC3-sh- $\sigma$  4) stably expressing this construct showed significant down-regulation of *14-3-3 $\sigma$*  protein (Figure 25a). After treatment with etoposide which induces DNA damage via inhibition of topoisomerases, PC3-sh- $\sigma$  1 and PC3-sh- $\sigma$  4 cells were unable to stably arrest. By contrast, PC3 cells transfected with the empty vector showed a stable arrest in the G<sub>2</sub>/M phase (Figure 25c). The PC3 cell lines showed a significant amount of cells with a >2*N* DNA content. The peak at 8*N* observed after DNA damage therefore corresponds to tetraploid cells in the G<sub>2</sub>/M phase (Figure 25c). The inability of the PC3-sh- $\sigma$  1 and PC3-sh- $\sigma$  4 cells to stably arrest was accompanied by an increased rate of apoptosis as evidenced by an elevated portion of cells with a sub-G<sub>1</sub> DNA content (Figure 25b).

In the absence of DNA-damaging treatment PC3-sh- $\sigma$  1 and PC3-sh- $\sigma$  4 cells have acquired a significant number of cells with an aberrant number of nuclei (Figure 25d). Two independent clones showed ~14% and ~22% of cells with two or multiple nuclei. PC3 cells infected with an empty vector, as well as a parental cell line, showed less than 2% of multinuclear cells. These results show that loss of *14-3-3 $\sigma$*  is sufficient to generate aneuploid cells, which may give rise to alterations in cancer-relevant genes and promote PCa progression.

#### **Figure 25** Effects of *14-3-3 $\sigma$* down-regulation on the DNA damage response.

(a) Western blot analysis of *14-3-3 $\sigma$*  protein expression in PC3 cell lines stably expressing short RNA hairpins directed against *14-3-3 $\sigma$*  (PC3-sh- $\sigma$  1 and PC3-sh- $\sigma$  4) and PC3 cells containing a pRetroSUPER vector not encoding an shRNA (PC3 mock). (b) Cell cycle distribution of PC3 cell lines differing in *14-3-3 $\sigma$*  expression. PC3 cells treated with the DNA-damaging agent etoposide (20  $\mu$ M) for the indicated periods of time were fixed, stained with propidium iodide and the DNA content was determined by FACS. (c) Representation of the sub-G<sub>1</sub> (=apoptotic) fraction of PC3 cell lines after addition of etoposide for the indicated periods as detected by FACS. (d) Effect of *14-3-3 $\sigma$*  loss on polyploidization. PC3 cells expressing short hairpin RNA targeting *14-3-3 $\sigma$*  and mock infected cells were stained with DAPI for visualization of nuclei. Depicted are the phase contrast images overlaid with fluorescent pseudocoloured (green) images of nuclei. Representative examples are shown. For the vector alone control 12 of 698 (2%), for the PC3 cells with *14-3-3 $\sigma$*  down-regulation 85 of 602 (14%) and for a second clone with *14-3-3 $\sigma$*  down-regulation 64 of 285 (22%) evaluated cells were multinucleated.



### 5.3.7 Functional analysis of *DKK3* and *SFRP1*

Epigenetic inactivation of the members of the *SFRP* gene family presumably contributes to activation of WNT signaling in colorectal cancer (Suzuki et al., 2004). *DKK3* negatively regulates the  $\beta$ -catenin pathway in osteosarcoma cells (Hoang et

al., 2004). Therefore, epigenetic silencing of *SFRP1* and/or *DKK3* expression in prostate carcinoma cells might be associated with constitutive activation of WNT/ $\beta$ -catenin signaling. To test this hypothesis the activity of the  $\beta$ -catenin/TCF pathway in PCa cells was investigated. Unexpectedly,  $\beta$ -catenin was localized at the cell membrane and absent from the nucleus in PC3 and Du145 cells (Figure 26a), which show significant silencing of *DKK3* and *SFRP1* (Figure 20). As nuclear  $\beta$ -catenin is a hallmark of an activated WNT/ $\beta$ -catenin pathway, this pathway is presumably not active in PCa. Furthermore, co-transfection with a *WNT1* expression construct did not result in activation of a TCF-reporter in PC3 and Du145 cells (Figure 26b). In contrast, HCT116 colon cancer cell lines, which harbor an activated WNT/APC/TCF4 pathway (Morin et al., 1997), showed nuclear  $\beta$ -catenin localization (data not shown) and strong activation of the wild-type but not the mutant TCF reporter by *WNT1* co-expression (Figure 26b).

Recently it has been reported that WNT1 activates the MAP kinase pathway (Civenni et al., 2003). Therefore, the WNT antagonists *DKK3* and *SFRP1* were tested for their ability to inhibit the MAP kinase pathway in PCa. PC3 cells were infected with retroviruses containing an expression cassette for *DKK3* or *SFRP1* fused to an IRES-EGFP. Expression of the respective protein product in GFP-positive pools was verified by immunoblotting (Figure 26c). In exponentially growing PC3 cells ectopically expressing *DKK3* the level of ERK1 and ERK2 phosphorylation, which is indicative of MAP kinase activity, was diminished (Figure 26d). Furthermore, PC3 cells ectopically expressing *DKK3* or *SFRP1* showed a significant decrease in colony formation (Figure 26e), which was due to a decrease in colony size. The rate of spontaneous apoptosis was not affected by ectopic expression of *DKK3* or *SFRP1* as determined by flow cytometry (data not shown). Therefore, loss of *DKK3* and *SFRP1* expression by epigenetic silencing presumably promotes the proliferation of prostate epithelial cells.

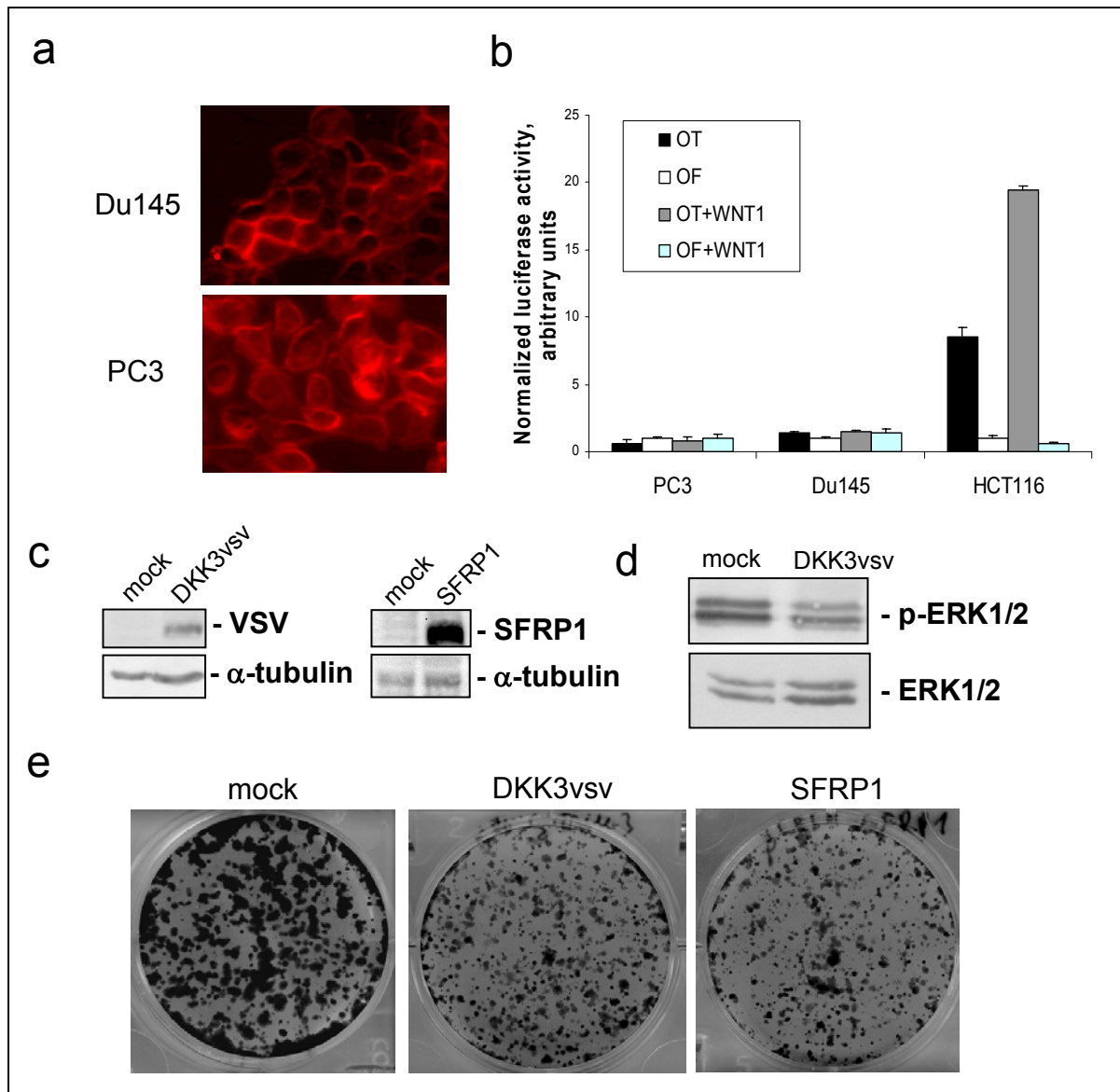


**Figure 26** Analysis of pathways downstream of DKK3 and SFRP1 in PCa cells

(a) Detection of  $\beta$ -catenin in PC3 and Du-145 PCa cells by immunofluorescence. (b) Analysis of TCF/LEF reporter activity in PCa (PC3, Du145) and colon (HCT116) cancer cell lines. Cells were transfected with a pGL3-OT (OT) TCF/LEF reporter construct, or with pGL3-OF (OF), a negative control containing a mutated TCF binding site. A WNT1 expression construct or its backbone construct were co-transfected. Luciferase activity was measured 36 hours after transfection. Transfection efficiency was normalized by co-transfection of a  $\beta$ -galactosidase encoding plasmid. The assays were performed in triplicates (standard deviation indicated). The values obtained for transfection of the OF-plasmid alone were set to one to visualize the differences among the three different cell lines. (c) Ectopic expression of *DKK3* and *SFRP1* in prostate carcinoma cells. PC3 cells were infected with bicistronic retroviruses encoding EGFP2, *DKK3*+EGFP2 or *SFRP1*+EGFP2; GFP-positive cells were isolated by flow cytometry and total protein lysates were subjected to Western blot analysis with anti-VSV or anti-SFRP1 antibodies. Equal loading was confirmed by detection of  $\alpha$ -tubulin. (d) Inhibition of ERK1/2 phosphorylation in PC3 cells ectopically expressing *DKK3*. Total protein lysates were analyzed using antibodies specific for ERK1 and ERK2 phosphorylated at the Thr202 and Tyr204 residues or anti-ERK1/2 antibodies. (e) Inhibition of cellular proliferation by *DKK3* and *SFRP1*. The equal number of PC3 cells transduced with the indicated constructs was plated at low density in 6-well plates, cultured for 10 days and colonies were stained with crystal violet. The analysis was performed in duplicates yielding identical results (data not shown).

## 6. Discussion

### 6.1 Induction of cellular senescence by LY83583

In the past decades the mainstay of cancer drug development was an empirical search for new cytotoxic compounds and their optimization (reviewed in Chabner and Roberts, 2005). For most of them the mechanism of action is the induction of DNA damage, which however also contributes to carcinogenesis. Apart from a limited efficacy, the genotoxic stress exerted by these drugs is also responsible for the major side effects of the current chemotherapeutic treatment of cancer in normal highly proliferating tissues. A new concept of targeted agent development emerged recently aiming to improve specificity and efficiency of cancer treatment (reviewed in Sawyers, 2004). The term 'targeted therapy' refers to a new generation of cancer drugs designed to interfere with a specific molecular target (typically a protein) that is believed to have a critical role in tumor growth or progression. The identification of appropriate targets is based on a detailed understanding of the molecular changes underlying cancer. This study focused on cellular senescence as a natural barrier for tumor development and potential target for pharmacological interference. Expression profiling of primary human cells undergoing replicative senescence was used to gain insight into underlying molecular pathways and to identify a drug-target which can be of use for the inhibition of tumor growth.

Several components of the cGMP signaling pathway were transcriptionally suppressed during replicative senescence in HDF. To test whether proliferation of early-passage fibroblasts is influenced by cGMP, the activity of the enzyme responsible for cGMP generation was pharmacologically modulated. For this purpose, LY83583 (LY) was selected, since it specifically inhibits soluble guanylate cyclase (Schmidt et al., 1985). LY was first described as an inhibitor of leukotriene release (Fleisch et al., 1984). Later, it was found to lower cGMP levels by inhibiting soluble guanylate cyclase (Mulsch et al., 1988). In the experiments presented here, LY was able to mimic cellular senescence in primary HDF and inhibited proliferation in several cancer cell lines. However, it is unclear whether inhibition of cGMP generation is the only pathway by which LY achieves its effects. It is possible that LY has additional, unknown properties that participate in the induction of cellular senescence and cell-cycle arrest. It has been proposed that the quinone structure of LY may lead to the generation of superoxide anions (Cherry et al., 1990). A recent

report that used the colorectal cancer cell line HCT116 and the isogenic *p21*- or *p53*-deficient cells also analyzed in the present study showed that reactive oxygen species (ROS) generated by hyperoxic conditions induce expression of *p21* in a *p53*-dependent manner (Helt et al., 2001). Furthermore, proliferation of HCT116 cells is inhibited by hyperoxic conditions in a *p21*- and *p53*-independent manner (Helt et al., 2001). In contrast to induction of *p21* by ROS, induction of *p21* by LY was not mediated by *p53*. Furthermore, inhibition of proliferation by LY was dependent on *p21*. These results suggest that LY does not act by generating ROS, which in turn mediate cell-cycle arrest or senescence.

The results described here demonstrate that LY induces cellular senescence in HDF and cell-cycle arrest in several human and murine cell types. One requirement for these effects of LY is the transcriptional induction of the CDK inhibitor *p21*, since *p21*-deficient cells are resistant to LY-induced arrest. Furthermore, in the absence of functional pocket proteins (*pRB*, *p107*, *p130*) which are downstream effectors of the *p21* cell-cycle the arrest is converted to induction of apoptosis in a *p53*-independent manner. In this case the apoptosis could be a cellular response to conflicting signals: negative signals due to LY-induced *p21* and resulting CDK inhibition versus cell-cycle-driving signals due to the lack of active pocket proteins, which allow high levels of active E2F transcription factors. The induction of *p21* is not mediated through the DNA-damage/*p53* pathway, since *p53*-deficient cells also show up-regulation of *p21* by LY and subsequent inhibition of cell proliferation. Many tumor cells lose *pRB* function, either through mutation of *pRB* (Horowitz et al., 1990) or through expression of viral proteins. For example, in cervical cancer, expression of *E7* by HPV16/18 leads to inactivation of *pRB* (reviewed in zur Hausen, 2001). In HPV16/18-infected cells, treatment with LY would presumably induce apoptosis. Since LY induces *p21*, cell-cycle arrest, and apoptosis in a *p53*-independent manner, it may prove useful for the treatment of cancers harboring *p53* mutations, which represent more than half of all human cancers (reviewed in Hollstein et al., 1999).

In the future, it will be important to analyze whether LY or derived substances can be used to prevent tumor growth *in vivo* using animal models. The results provided in this study may serve as a basis for further characterization and optimization of LY derived drugs as therapeutic agents for the treatment of tumors. An obvious advantage of LY is its ability to interfere with cellular proliferation and to induce apoptosis in *pRB*-negative cells without inducing DNA damage. These effects

of LY are not mediated by the CDK inhibitor p16, which is an advantage given the frequent inactivation of  $p16^{INK4A}$  in human cancer. On the other hand, the  $p21$  gene, which presumably mediates the effects of LY, has not been reported to be inactivated in human cancer. Commonly used chemotherapeutic agents, like adriamycin, generate DNA damage and thereby induce apoptosis in cancer cells, which lack cell-cycle checkpoints (reviewed in Hartwell et al., 1997). However, DNA-damaging substances have several adverse effects (Batchelor, 2001; Dropcho, 2004) and may induce further mutations in precancerous and healthy cells, which lead to secondary cancer (Felix, 1998; Travis, 2002). The strategy used in this study — that is, identification of pathways that are repressed during senescence and their inhibition in tumor cells by synthetic drugs — may also prove useful for the identification of other inhibitors of tumor cell proliferation.

## 6.2 Epigenetic inactivation of $14-3-3\sigma$ in basal cell carcinoma

Inactivation of  $14-3-3\sigma$  in primary human keratinocytes promotes immortalization (Dellambra et al., 2000), suggesting that this protein may play a tumor suppressive role in human epidermis. Immunohistochemical analysis of benign (psoriasis, genital warts and actinic keratoses) and malignant (squamous cell carcinoma) hyperproliferative skin diseases revealed no reduction in  $14-3-3\sigma$  protein expression. These results demonstrate that down-regulation of the  $14-3-3\sigma$  protein is not a general requirement for hyperproliferation of keratinocytes. They further suggest that  $14-3-3\sigma$  may have additional functions that contribute to the expansion of keratinocytes. One function of  $14-3-3\sigma$  could be the prevention of apoptosis by cytoplasmic sequestration of the pro-apoptotic factor BAX, which has been observed in colorectal cancer cells (Samuel et al., 2001).

In contrast to other analyzed pathological conditions, basal cell carcinoma of the skin showed a prominent reduction or complete loss of  $14-3-3\sigma$  in 71% of patients. These results suggest, that inactivation of  $14-3-3\sigma$  may be the preferred mechanism to evade senescence in BCC. Further it was demonstrated, that down-regulation of the antiproliferative  $14-3-3\sigma$  protein is a characteristic feature of BCC, which is associated with CpG-methylation of the  $14-3-3\sigma$  promoter. Morphologically normal epidermis adjacent to BCC also displayed methylation of this gene in a considerable number of cases. However, epidermis isolated from distant sites adjacent to

naevocytic naevi from the identical patient was negative for CpG-methylation. Recent studies showed that *14-3-3 $\sigma$*  is also methylated in epithelial cells derived from histologically normal tissue surrounding breast carcinomas (Umbricht et al., 2001) or hepatocellular carcinoma (Iwata et al., 2000). However, methylation of *14-3-3 $\sigma$*  was never detected in breast epithelial tissue derived from cancer-free donors (Umbricht et al., 2001). Therefore, it has been suggested that CpG-methylation of *14-3-3 $\sigma$*  represents a precursor lesion, which precedes any morphological change in tissue architecture. Several other genes, which are inactivated during tumor development, show CpG-methylation in tissue adjacent to tumor tissue (Ivanova et al., 2002; Li et al., 2002; Tokugawa et al., 2002). CpG-methylation of *14-3-3 $\sigma$*  in the normal epidermis may indicate the presence BCC precursor cells. However, it will be necessary to further characterize the relation of these neighboring cells to BCCs to conclude that *14-3-3 $\sigma$*  methylation is a marker for BCC precursor cells.

In a fraction of BCC, *14-3-3 $\sigma$*  expression was lost in the absence of CpG-methylation. This could be due to mutational inactivation of *14-3-3 $\sigma$* . However, although the *14-3-3 $\sigma$*  gene is localized on chromosome 1p35, a region frequently deleted in cancer, mutational inactivation of *14-3-3 $\sigma$*  has not been observed yet. In colorectal cancer, analysis of 40 tumors with LOH at the *14-3-3 $\sigma$*  locus revealed no mutations in the remaining *14-3-3 $\sigma$*  allele (Hermeking et al., unpublished results). Similarly, rare cases of LOH at the *14-3-3 $\sigma$*  locus have been observed in oral squamous cell carcinomas (Gasco et al., 2002). However, the remaining *14-3-3 $\sigma$*  allele was not mutated. One potential mechanism of *14-3-3 $\sigma$*  down-regulation could be a  $\Delta$ Np63 $\alpha$ -dependent transcriptional repression. However, it is unlikely to be involved in basalioma development, since no direct correlation between the absence of *14-3-3 $\sigma$*  expression and the presence of  $\Delta$ Np63 $\alpha$  was detected by immunohistochemical analysis in BCC and other lesions. Recently, an alternative mechanism for loss of *14-3-3 $\sigma$*  protein has been identified: the ubiquitin E3-ligase EFP targets the *14-3-3 $\sigma$*  protein for proteasomal degradation (Urano et al., 2002). Therefore, up-regulation of the *EFP* could potentially account for the loss of *14-3-3 $\sigma$*  protein in those cases of BCC where no CpG methylation is detected.

Until now it has been impossible to cultivate BCC cells *in vitro*. Therefore, the functional consequences of *14-3-3 $\sigma$*  down-regulation were not amenable to functional analysis in this study. In several tumor cell lines, demethylation of *14-3-3 $\sigma$*  by 5-aza-



2'-deoxycytidine leads to re-expression of the *14-3-3 $\sigma$*  mRNA (e.g. Ferguson et al., 2000, see also epigenetic analysis of PCa in this study), showing that CpG-methylation is causally involved in silencing of *14-3-3 $\sigma$* . In breast cancer cells, silencing of *14-3-3 $\sigma$*  is associated with a defect in the G<sub>2</sub>/M checkpoint (Ferguson et al., 2000). It is likely that the CpG methylation of *14-3-3 $\sigma$*  detected here in BCC has similar functional consequences.

With 750,000 newly diagnosed cases each year, BCC is the most common malignancy in the US (Miller, 1991). BCCs rarely metastasize, but may lead to significant morbidity because of local tissue destruction (Schubert and Muller, 1997). The finding, that *14-3-3 $\sigma$*  expression is lost in the majority of BCC, provides an opportunity to devise selective therapeutic means, since loss of *14-3-3 $\sigma$*  sensitizes epithelial cells to DNA-damaging agents (Chan et al., 1999; Samuel et al., 2001) and may explain the effectiveness of radiotherapy for treatment of BCC.

### **6.3 Functional epigenomic analysis of prostate carcinoma cell lines**

In the present study epigenetic changes characteristic for prostate cancer were identified by pharmacological unmasking. This approach takes advantage of the fact, that the inhibition of DNA methyltransferase activity by 5-aza-2'-deoxycytidine (5-Aza-2'dC) can reverse the silencing of genes hypermethylated in tumor cell lines. Genome-wide transcriptional changes exerted by genomic demethylation were determined using microarray analysis of gene expression. Several hundred mRNAs were up-regulated after combined treatment with 5Aza-2'dC and TSA. Many of these transcripts may have been induced secondary to the demethylation or by cellular stress evoked by the 5Aza-2'dC. Consistent with this assumption, subsequent analysis of CpG methylation by bisulfite sequencing and MSP revealed the presence of CpG methylation in the promoters of only about 25% of selected candidate genes. This underscores the necessity of the validation of the expression data at the genomic level when using this approach. For the majority of genes positive for CpG methylation the differential methylation inversely correlated with differential expression in tumor/normal cells.

The sensitivity of the microarray hybridization was not sufficient to detect induction of *p16* and *RASSF1A* genes which are known to be hypermethylated in PCa cell lines used here, although their up-regulation following genomic

demethylation was confirmed by RT-PCR. In addition, the induction of uncharacterized ESTs and genes coding for putative proteins was not investigated in this study. Thus, it is possible that the analysis presented here has missed some hypermethylated genes which are expressed at low levels.

Nevertheless, the applied strategy resulted in the identification of more than ten novel targets for epigenetic silencing in PCa, validating the efficiency of the functional epigenomic analysis. The high frequency of CpG methylation observed in primary tumors suggests that the differences in CpG methylation which were initially detected in PCa cell lines did not occur during *in vitro* cultivation of PCa cell lines. Whether the CpG methylation of distinct genes is the cause or consequence of their down-regulation during prostate cancer initiation or progression remains to be shown. In addition, the functional relevance of the down-regulation of these genes has to be determined in the future. However, the high frequency of the epigenetic silencing events identified in this study suggests that these genes may be causally involved in prostate cancer development. Potential functional consequences of the epigenetic silencing events detected here will be discussed in the following paragraphs.

#### **6.4 Frequent epigenetic silencing of *14-3-3 $\sigma$* in prostate cancer**

The high frequency of CpG methylation (100%) at the *14-3-3 $\sigma$*  locus observed in primary PCa shows that the CpG methylation initially detected in PCa cell lines did not result from prolonged *in vitro* passaging of PCa cell lines, but reflects a carcinoma-specific event. This notion is further supported by the finding that benign but hyperproliferative benign prostatic hyperplasia (BPH) shows no significant *14-3-3 $\sigma$*  silencing. The presence of CpG methylation in all PCa samples analysed may indicate an absolute requirement of *14-3-3 $\sigma$*  down-regulation for PCa formation. The strategy used to identify *14-3-3 $\sigma$*  as a gene specifically silenced in PCa, that is, reversion of CpG methylation-mediated gene repression in PCa cell lines, clearly argues for a role of CpG methylation in the down-regulation of *14-3-3 $\sigma$*  at the level of mRNA and protein expression. Previously, ectopic expression of *14-3-3 $\sigma$*  by adenoviral infection was shown to cause a G<sub>2</sub>/M arrest in PrECs (Hermeking et al., 1997). In line with an involvement of *14-3-3 $\sigma$*  in the regulation of G<sub>2</sub>/M progression, RNA interference-mediated down-regulation of *14-3-3 $\sigma$*  in the PCa cell line PC3

facilitated an escape from a stable G<sub>2</sub>/M cell cycle arrest after DNA damage. This study shows that prostate carcinoma cells with constitutively decreased level of *14-3-3 $\sigma$*  expression spontaneously acquire nuclear aberrations, which presumably arise due to aberrant mitosis in the presence of DNA-damage and the subsequent failure to complete cytokinesis. Therefore, silencing of *14-3-3 $\sigma$*  in pre-neoplastic prostate epithelial cells may result in tetra- or polyploidization, which, in turn, allows the loss of chromosomal fragments affecting other genes critical for PCa progression.

During the early phases of PCa progression, a DNA damage signal is presumably generated, as telomere shortening has been detected in PIN lesions (Meeker et al., 2002). Interestingly, the shortening of telomeres in PIN was restricted to luminal cells, which also show down-regulation of *14-3-3 $\sigma$*  expression as detected here. It is therefore possible that telomere shortening promotes the selection of cells that have lost *14-3-3 $\sigma$*  expression due to CpG methylation. The silencing of *14-3-3 $\sigma$*  expression observed here may contribute to PCa formation by promoting the escape from the telomere checkpoint. Subsequent cell proliferation with unprotected telomeres would contribute to genetic instability and accelerate the inactivation of additional tumor suppressive genes or activation of oncogenes (Artandi et al., 2000).

From other types of cancer, it is known that CpG methylation of *14-3-3 $\sigma$*  is often an early event during tumor progression. For example, in breast cancer it has been shown that CpG methylation of *14-3-3 $\sigma$*  occurs during the transition from atypical hyperplastic lesions to carcinoma *in situ* (Umbricht et al., 2001). The loss of *14-3-3 $\sigma$*  protein expression in PIN lesions indicates that *14-3-3 $\sigma$*  inactivation is an early event during PCa progression.

The CpG methylation of *14-3-3 $\sigma$*  may be used to detect PCa in the future. Since *14-3-3 $\sigma$*  is also hypermethylated in a number of other carcinomas, a combination of this marker with PCa-specific CpG methylation markers may allow the development of a highly sensitive and specific diagnostic assay in the future. As changes in DNA methylation seem to occur early in carcinogenesis, this assay may be suited to detect cells or free DNA released from early PCa lesions in body fluids. A potential obstacle to the use of *14-3-3 $\sigma$*  CpG methylation as a diagnostic marker may be the presence of CpG-methylated *14-3-3 $\sigma$*  alleles in stromal cells and lymphocytes (Bhatia et al., 2003; Umbricht et al., 2001). However, preliminary studies with other CpG marker genes show that these cell types may not interfere with CpG methylation-based diagnostic approaches (reviewed in Laird, 2003).

## 6.5 CpG methylation and down-regulation of *SFRP1* and *DKK3* in prostate cancer

SFRP1 negatively regulates the WNT pathway, which is frequently activated in cancer by mutations in the *APC* and *β-catenin* genes (Giles et al., 2003; Kinzler and Vogelstein, 1996). Recently, *SFRP1* was shown to undergo both genetic and epigenetic alterations in colon and bladder cancer (Caldwell et al., 2004; Stoehr et al., 2004). Frequent hypermethylation of *SFRP1* was recently detected in colorectal cancer (Suzuki et al., 2002), where the loss of SFRP1 correlated with an increased  $\beta$ -catenin/TCF4 activity and ectopic expression of SFRP1 led to reduced  $\beta$ -catenin/TCF4 activity. However, activation of the  $\beta$ -catenin/TCF4 pathway was not detected in PCa in this study. Therefore, loss of *SFRP1* may contribute to activation of other oncogenic signaling pathways in PCa. The *SFRP1* gene is located on chromosome 8p12, a region which frequently undergoes LOH in PCa. An induction of *SFRP1* mRNA was detected in human primary fibroblasts undergoing replicative senescence (data not shown), suggesting a possible role of SFRP1 in the terminal proliferation arrest of senescent cells.

Dickkopf 3 (*DKK3*) negatively regulates the WNT-pathway. The zonal distribution of *DKK3* expression in the adrenal gland suggests that *DKK3* is involved in zonal differentiation or growth (Suwa et al., 2003). *DKK3* was identified as a gene which is down-regulated upon immortalization of primary human cells (Tsuji et al., 2000). Reduced expression of *DKK3* was also found in non-small cell lung cancer and renal clear cell carcinoma (Kurose et al., 2004; Tsuji et al., 2001). Overexpression of *DKK3* inhibited growth, invasion and motility of Saos-2 osteosarcoma cells and non-small cell lung cancer cells by modulating WNT-signaling (Hoang et al., 2004; Tsuji et al., 2001). Interestingly, the *DKK3* transcript was shown to be up-regulated in senescent primary prostate epithelial cells (Untergasser et al., 2002). The epigenetic silencing of *DKK3* by CpG methylation observed here might therefore contribute to de-differentiation and immortalization of PCa cells.

The analysis of PCa cell lines suggests that the WNT/ $\beta$ -catenin pathway is not activated in Du-145 and PC3 cells with silenced *SFRP1* and *DKK3* genes. This is in agreement with a recent comprehensive study of 101 cases of primary PCa: none of

the tumors showed nuclear  $\beta$ -catenin staining (Bismar et al., 2004). However, genetic alterations of  *$\beta$ -catenin* or *APC* were detected in a subset of advanced PCa and were associated with an resistance to apoptosis and hormone-refractory phenotype (Chesire et al., 2000; de la Taille et al., 2003). Loss of *SFRP1* and *DKK3* expression may activate alternative signaling pathways (Figure 27). Recently, it was reported that transactivation of the EGF receptor by WNT ligands, which results in MAP-kinase activation, is inhibited by *SFRP1* and *DKK1* (Civenni et al., 2003). The data of this work indicate that *DKK3* may also have an inhibitory effect on MAP kinase signaling.

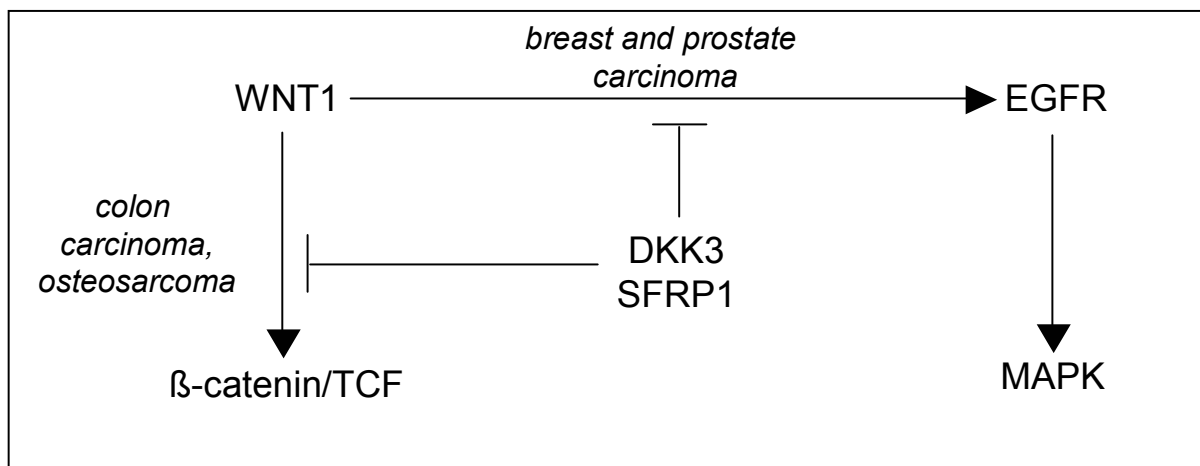


**Figure 27** Modulation of WNT effects by *DKK3* and *SFRP1*

In colon cancer epigenetic silencing of *SFRP1* contributes to the deregulation of WNT signaling and results in the activation of  $\beta$ -catenin. Similarly, *DKK3* antagonizes the  $\beta$ -catenin/TCF pathway in osteosarcoma cells. In breast cancer, and presumably in PCa cells the WNT ligands can transactivate the EGF receptor and the downstream MAPK pathway. *DKK3* and *SFRP1* inhibit this transactivation and negatively affect proliferation. Thus, the frequent silencing of *DKK3* and *SFRP1* in PCa may lead to an aberrant activation of MAPK cascade.

## 6.6 Hypermethylation of *p57*, *GPX3*, *GSTM1* and *COX2* genes in prostate cancer

*p57/KIP2* belongs to a family of conserved CDK inhibitors, which negatively regulate the cell cycle. Ectopic expression of *p57* suppresses cell transformation, whereas cells lacking *p57* show increased cell proliferation and decreased differentiation (Watanabe et al., 1998; Yan et al., 1997; Zhang et al., 1997). *p57* expression is decreased in PCa cell lines and primary prostate epithelial cells immortalized by HPV16 E7 (Schwarze et al., 2001). Expression of *p57* induces a senescence-like phenotype in PCa cells (Schwarze et al., 2001), suggesting that down-regulation of *p57* may be required for immortalization of prostate cells. The *p57* gene is located on chromosome 11p15.5, a region implicated in both sporadic

cancers and the Beckwith-Wiedemann cancer syndrome. Mutations of *p57* have rarely been detected in human tumors (Tokino et al., 1996). Epigenetic silencing of *p57* was also detected in gastric, hepatocellular, pancreatic carcinomas and acute myeloid leukaemia (Kikuchi et al., 2002b; Shin et al., 2000). The down-regulation of *p57* in bladder cancer involves several mechanisms including LOH and hypermethylation (Hoffmann et al., 2004). The *p57* gene is located in the vicinity of imprinted genes (*IGF2* and *H19*) and itself displays features of an imprinted gene as the maternal allele is preferentially expressed. However, the imprinting is not absolute, as the paternal allele is also expressed at low levels in most tissues (Matsuoka et al., 1996). Furthermore, the relevance of DNA methylation for the imprinting of *p57* is not clear, as CpG-methylation has not been detected in the 5' region of *p57* in normal tissue (Chung et al., 1996; Kikuchi et al., 2002b). Here CpG methylation of *p57* was not detected in normal PrECs and stromal cells and is therefore a specific feature of PCa progression.

Glutathione peroxidase 3 (GPX3) catalyzes the reduction of peroxides by glutathione and protects cells against oxidative damage. The PCa-specific silencing of *GPX3* may lead to an impaired defence against endogenous and exogenous genotoxic compounds, which could potentially result in an increased rate of mutations in critical genes. Down-regulation of *GPX3* expression upon transition from normal to neoplastic prostate tissue was recently detected by microarray analysis of microdissected primary PCa (Ashida et al., 2004). Presumably, this down-regulation of *GPX3* in PCa is caused by the epigenetic silencing of *GPX3* detected here.

Glutathione S-transferase  $\mu$  1 (*GSTM1*) belongs to a family of enzymes that catalyze the conjugation of reduced glutathione to a variety of electrophiles. Thereby, *GSTM1* detoxifies mutagenic substances mainly epoxides formed from common carcinogens such as polycyclic aromatic hydrocarbons, and thus may play a protective role for the genome, as was proposed for *GSTP1* and also for *GPX* (this study). The common null-allele of *GSTM1* shows a weak association with lung cancer (reviewed in (Mohr et al., 2003)). However, no significant association of *GSTM1* polymorphisms or deletion with PCa has been reported. The tumor-specific hypermethylation of *GSTM1* identified here may explain the decreased expression of *GSTM1* in PCa detected in three previous studies (Ashida et al., 2004; Chetcuti et al., 2001; Vanaja et al., 2003). Down-regulation of *GSTM1* was also shown in colorectal

carcinoma in individuals with *GSTM1* positive genotype, but was not associated with CpG methylation (Barker et al., 2002).

Cyclooxygenase 2 (COX2) catalyzes the synthesis of prostaglandin H<sub>2</sub>, a precursor of other prostanoids, and has been implicated in inflammation and carcinogenesis (reviewed in Dannenberg and Subbaramaiah, 2003). COX2 inhibitors, like nonsteroidal anti-inflammatory drugs (NSAIDs), decrease the risk of developing PCa (Nelson and Harris, 2000) and inhibit the growth of PCa in a xenograft model (Liu et al., 2000). However, the effects of NSAIDs on cancer cells may not be caused by inhibition of COX2. The published data on COX2 expression in tumors is not uniform: over-expression of COX2 was found in several tumor types including PCa (Gupta et al., 2000). However, no consistent over-expression of COX2 in PCa or high-grade prostatic intraepithelial neoplasia compared to adjacent normal prostate tissue was found in another study (Zha et al., 2001). Furthermore, the high COX2 levels were detected in areas of proliferative inflammatory atrophy, which presumably represents an early precursor of PCa (Nelson et al., 2003). Expression of COX2 protein was not detected in the PCa cell lines LNCaP, PC3 and Du-145 (Zha et al., 2001), which is consistent with silencing of the COX2 gene by CpG-methylation reported here. Epigenetic silencing of COX2 was also detected in a subset of gastric (Kikuchi et al., 2002a) and colorectal cancers (Toyota et al., 2000).

While this study was in progress, CpG methylation of the COX2 gene in PCa was reported independently (Kang et al., 2004; Yegnasubramanian et al., 2004). In the study by Kang *et al.* the CpG methylation of COX2 was detected in 22 % of primary PCa, while Yegnasubramanian *et al.* detected hypermethylation of COX2 in 88% of PCa when they applied a quantitative method to analyze a larger collection of samples. Interestingly, the hypermethylation of COX2 was associated with a higher risk of recurrence of PCa (Yegnasubramanian et al., 2004), proving the prognostic potential of methylation markers in PCa.

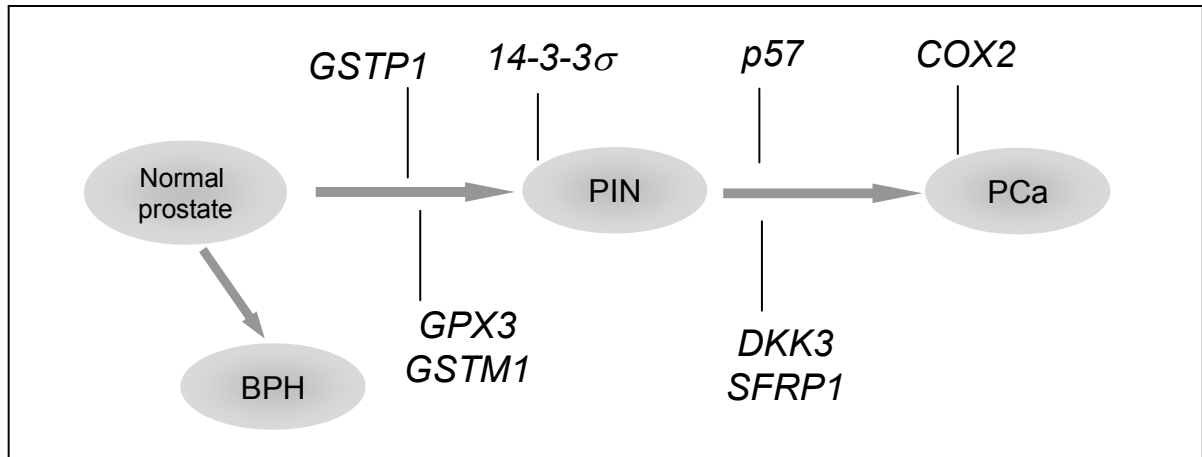


**Figure 28** Aberrant DNA methylation in the development of prostate carcinoma

Since *GSTP1*, *GSTM1* and *GPX3* are involved in the protection of the cells from potentially carcinogenic substances, their epigenetic inactivation may contribute to an acquisition of oncogenic mutations in the prostate at the very beginning of the transformation process. Epigenetic silencing of *14-3-3σ* can compromise genomic stability of aberrantly proliferating cells and occurs already at the PIN stage. Epigenetic inactivation of the CDK inhibitor *p57* may contribute to abrogation of the senescence state and promote the immortalization of prostate cells. A frequent hypermethylation of the *DKK3* and *SFRP1* genes indicates the role of the WNT signaling in prostate carcinogenesis.

The lack of a correlation between CpG methylation and grade or stage of the PCa is in agreement with other recent studies (Florl et al., 2004; Kang et al., 2004; Yegnasubramanian et al., 2004). Taken together the data suggest that silencing of genes by CpG methylation occurs at an early stage of prostate cancer development (Figure 28). This may have implications for the use of these CpG methylation events for the early diagnostics of PCa lesions. Tumor-specific CpG methylation can be detected with high sensitivity and specificity in biopsies and body fluids (Laird, 2003). The CpG methylation of *SFRP1*, *COX2* and *p57* has the highest specificity for PCa and is therefore of higher relevance for potential diagnostic applications. However, this conclusion will require validation on larger cohort of patients in the future.



## 7. Summary

Pharmacological induction of the senescence program in tumor cells could be of benefit for the treatment of cancer. cDNA microarray analysis of the transcriptional changes associated with replicative senescence in primary human diploid fibroblasts revealed coordinated down-regulation of the cGMP signaling pathway. A specific inhibitor of soluble guanylate cyclase, LY83583 (LY) induced premature senescence in HDF and inhibited proliferation of tumor cell lines in a dose-dependent manner. Expression profiling of LY-treated fibroblasts revealed a common trend for 114 genes differentially expressed upon activation of the replicative and premature senescence program. LY treatment resulted in rapid transcriptional induction of the CDK inhibitor *p21* in the absence of p53 accumulation. Moreover, the inhibitory effect of LY on proliferation required the function of p21 but not p53, as shown by analysis of isogenic knock-out cell lines. Functional inactivation of pocket proteins converted LY-induced growth arrest to apoptosis.

Since the inactivation of *14-3-3 $\sigma$*  is sufficient to immortalize primary human keratinocytes *ex vivo*, the expression of *14-3-3 $\sigma$*  protein was studied in human skin diseases, which display hyperproliferation of the epidermis. Basal cell carcinomas of the skin showed prominent reduction or loss of *14-3-3 $\sigma$*  expression in 71% of analyzed cases. MSP analysis of microdissected BCC tissue showed the presence of CpG methylation of *14-3-3 $\sigma$*  in 68%, being a likely mechanism of *14-3-3 $\sigma$*  silencing. CpG methylation of *14-3-3 $\sigma$*  may be an early event in BCC formation since it was detected in morphologically normal epidermis adjacent to BCC, but not in distant epidermis.

Genes abnormally methylated in cancer may represent tumor-suppressive factors or serve as tumor markers, facilitating diagnosis and prognosis. In order to identify such genes, global transcriptional changes induced by genomic demethylation in three prostate carcinoma cell lines were analyzed using microarrays. Several hundred mRNAs were up-regulated upon combined treatment with 5Aza-2'dC and TSA. Based on their biological function and presence of CpG-island in the promoter region, 50 genes were selected for bisulfite sequencing and MSP analysis. Seven genes turned out to be epigenetically silenced in PCa cell lines. Interestingly, four of those (*14-3-3 $\sigma$* , *DKK3*, *SFRP1* and *p57*) were previously implicated in cellular senescence. The frequencies of CpG methylation in 41 microdissected primary PCa

were: *14-3-3 $\sigma$* :100%, *GPX3*: 93%, *SFRP1*: 83%, *COX2*: 78%, *DKK3*: 68%, *GSTM1*: 58% and *KIP2/p57*: 56%. Tumor-specific down-regulation of protein expression in primary PCa was confirmed immunohistochemically for *14-3-3 $\sigma$*  and *SFRP1*. Depletion of *14-3-3 $\sigma$*  by RNA interference in PC3 cells resulted in an impaired G<sub>2</sub>/M arrest after DNA damage and spontaneous acquisition of aberrant nuclei. Ectopic expression of *DKK3* or *SFRP1* inhibited growth of PCa cells. In case of *DKK3* this effect presumably was mediated through the attenuation of the MAPK signaling. Since *COX2*, *SFRP1* and *p57* genes showed only a minor methylation in benign prostate hyperplasia, prostate stroma and blood cells, detection of CpG methylation in those genomic regions may prove useful for the diagnosis of PCa.

## 8. References

- Abate-Shen, C., and Shen, M. M. (2000). Molecular genetics of prostate cancer. *Genes Dev* 14, 2410-2434.
- Abdulkadir, S. A., Magee, J. A., Peters, T. J., Kaleem, Z., Naughton, C. K., Humphrey, P. A., and Milbrandt, J. (2002). Conditional loss of Nkx3.1 in adult mice induces prostatic intraepithelial neoplasia. *Mol Cell Biol* 22, 1495-1503.
- Alcorta, D. A., Xiong, Y., Phelps, D., Hannon, G., Beach, D., and Barrett, J. C. (1996). Involvement of the cyclin-dependent kinase inhibitor p16 (INK4a) in replicative senescence of normal human fibroblasts. *Proc Natl Acad Sci U S A* 93, 13742-13747.
- American Cancer Society. Cancer Facts and Figures, 2005. American Cancer Society, Atlanta, GA, 2005 <http://www.cancer.org>
- Aprelikova, O., Pace, A. J., Fang, B., Koller, B. H., and Liu, E. T. (2001). BRCA1 is a selective co-activator of 14-3-3 sigma gene transcription in mouse embryonic stem cells. *J Biol Chem* 276, 25647-25650.
- Artandi, S. E., Chang, S., Lee, S. L., Alson, S., Gottlieb, G. J., Chin, L., and DePinho, R. A. (2000). Telomere dysfunction promotes non-reciprocal translocations and epithelial cancers in mice. *Nature* 406, 641-645.
- Ashida, S., Nakagawa, H., Katagiri, T., Furihata, M., Iizumi, M., Anazawa, Y., Tsunoda, T., Takata, R., Kasahara, K., Miki, T., *et al.* (2004). Molecular features of the transition from prostatic intraepithelial neoplasia (PIN) to prostate cancer: genome-wide gene-expression profiles of prostate cancers and PINs. *Cancer Res* 64, 5963-5972.
- Bachman, K. E., Park, B. H., Rhee, I., Rajagopalan, H., Herman, J. G., Baylin, S. B., Kinzler, K. W., and Vogelstein, B. (2003). Histone modifications and silencing prior to DNA methylation of a tumor suppressor gene. *Cancer Cell* 3, 89-95.
- Bakin, A. V., and Curran, T. (1999). Role of DNA 5-methylcytosine transferase in cell transformation by fos. *Science* 283, 387-390.

- Barker, H. J., Alpert, L. C., Compton, C. C., Maslen, A., and Kirby, G. M. (2002). Loss of glutathione S-transferase (GST) mu phenotype in colorectal adenocarcinomas from patients with a GSTM1 positive genotype. *Cancer Lett* 177, 65-74.
- Batchelor, D. (2001). Hair and cancer chemotherapy: consequences and nursing care--a literature study. *Eur J Cancer Care (Engl)* 10, 147-163.
- Bender, J. (2001). A vicious cycle: RNA silencing and DNA methylation in plants. *Cell* 106, 129-132.
- Benzinger, A., Popowicz, G. M., Joy, J. K., Majumdar, S., Holak, T. A. and Hermeking, H. (2005). The crystal structure of the non-liganded 14-3-3 $\sigma$  protein: insights into determinants of isoform specific ligand binding and oligomerization. *Cell Research* 15, 219-227.
- Bhatia, K., Siraj, A. K., Hussain, A., Bu, R., and Gutierrez, M. I. (2003). The tumor suppressor gene 14-3-3 sigma is commonly methylated in normal and malignant lymphoid cells. *Cancer Epidemiol Biomarkers Prev* 12, 165-169.
- Bhatia-Gaur, R., Donjacour, A. A., Sciavolino, P. J., Kim, M., Desai, N., Young, P., Norton, C. R., Gridley, T., Cardiff, R. D., Cunha, G. R., *et al.* (1999). Roles for Nkx3.1 in prostate development and cancer. *Genes Dev* 13, 966-977.
- Bird, A. (2002). DNA methylation patterns and epigenetic memory. *Genes Dev* 16, 6-21.
- Bismar, T. A., Humphrey, P. A., Grignon, D. J., and Wang, H. L. (2004). Expression of beta-catenin in prostatic adenocarcinomas: a comparison with colorectal adenocarcinomas. *Am J Clin Pathol* 121, 557-563.
- Boulanger, C. A., and Smith, G. H. (2001). Reducing mammary cancer risk through premature stem cell senescence. *Oncogene* 20, 2264-2272.
- Brenner, C., Deplus, R., Didelot, C., Lorient, A., Vire, E., De Smet, C., Gutierrez, A., Danovi, D., Bernard, D., Boon, T., *et al.* (2005). Myc represses transcription through recruitment of DNA methyltransferase corepressor. *Embo J* 24, 336-346.

Brummelkamp, T. R., Bernards, R., and Agami, R. (2002a). Stable suppression of tumorigenicity by virus-mediated RNA interference. *Cancer Cell* 2, 243-247.

Brummelkamp, T. R., Bernards, R., and Agami, R. (2002b). A system for stable expression of short interfering RNAs in mammalian cells. *Science* 296, 550-553.

Bunz, F., Dutriaux, A., Lengauer, C., Waldman, T., Zhou, S., Brown, J. P., Sedivy, J. M., Kinzler, K. W., and Vogelstein, B. (1998). Requirement for p53 and p21 to sustain G2 arrest after DNA damage. *Science* 282, 1497-1501.

Caldwell, G. M., Jones, C., Gensberg, K., Jan, S., Hardy, R. G., Byrd, P., Chughtai, S., Wallis, Y., Matthews, G. M., and Morton, D. G. (2004). The Wnt antagonist sFRP1 in colorectal tumorigenesis. *Cancer Res* 64, 883-888.

Chabner, B. A., and Roberts, T. G., Jr. (2005). Timeline: Chemotherapy and the war on cancer. *Nat Rev Cancer* 5, 65-72.

Chan, T. A., Hermeking, H., Lengauer, C., Kinzler, K. W., and Vogelstein, B. (1999). 14-3-3Sigma is required to prevent mitotic catastrophe after DNA damage. *Nature* 401, 616-620.

Chan, T. A., Hwang, P. M., Hermeking, H., Kinzler, K. W., and Vogelstein, B. (2000). Cooperative effects of genes controlling the G(2)/M checkpoint. *Genes Dev* 14, 1584-1588.

Cherry, P. D., Omar, H. A., Farrell, K. A., Stuart, J. S., and Wolin, M. S. (1990). Superoxide anion inhibits cGMP-associated bovine pulmonary arterial relaxation. *Am J Physiol* 259, H1056-1062.

Chesire, D. R., Ewing, C. M., Sauvageot, J., Bova, G. S., and Isaacs, W. B. (2000). Detection and analysis of beta-catenin mutations in prostate cancer. *Prostate* 45, 323-334.

Chetcuti, A., Margan, S., Mann, S., Russell, P., Handelsman, D., Rogers, J., and Dong, Q. (2001). Identification of differentially expressed genes in organ-confined prostate cancer by gene expression array. *Prostate* 47, 132-140.

Chung, W. Y., Yuan, L., Feng, L., Hensle, T., and Tycko, B. (1996). Chromosome 11p15.5 regional imprinting: comparative analysis of KIP2 and H19 in human tissues and Wilms' tumors. *Hum Mol Genet* 5, 1101-1108.

Civenni, G., Holbro, T., and Hynes, N. E. (2003). Wnt1 and Wnt5a induce cyclin D1 expression through ErbB1 transactivation in HC11 mammary epithelial cells. *EMBO Rep* 4, 166-171.

Classon, M., and Harlow, E. (2002). The retinoblastoma tumour suppressor in development and cancer. *Nat Rev Cancer* 2, 910-917.

Costello, J. F., Fruhwald, M. C., Smiraglia, D. J., Rush, L. J., Robertson, G. P., Gao, X., Wright, F. A., Feramisco, J. D., Peltomaki, P., Lang, J. C., *et al.* (2000). Aberrant CpG-island methylation has non-random and tumour-type-specific patterns. *Nat Genet* 24, 132-138.

Cristofalo, V. J., Volker, C., Francis, M. K., and Tresini, M. (1998). Age-dependent modifications of gene expression in human fibroblasts. *Crit Rev Eukaryot Gene Expr* 8, 43-80.

Dahia, P. L. (2000). PTEN, a unique tumor suppressor gene. *Endocr Relat Cancer* 7, 115-129.

Dannenberg, A. J., and Subbaramaiah, K. (2003). Targeting cyclooxygenase-2 in human neoplasia: rationale and promise. *Cancer Cell* 4, 431-436.

Dannenberg, J. H., van Rossum, A., Schuijff, L., and te Riele, H. (2000). Ablation of the retinoblastoma gene family deregulates G(1) control causing immortalization and increased cell turnover under growth-restricting conditions. *Genes Dev* 14, 3051-3064.

de la Taille, A., Rubin, M. A., Chen, M. W., Vacherot, F., de Medina, S. G., Burchardt, M., Buttyan, R., and Chopin, D. (2003). Beta-catenin-related anomalies in apoptosis-resistant and hormone-refractory prostate cancer cells. *Clin Cancer Res* 9, 1801-1807.

De Marzo, A. M., Marchi, V. L., Epstein, J. I., and Nelson, W. G. (1999a). Proliferative inflammatory atrophy of the prostate: implications for prostatic carcinogenesis. *Am J Pathol* 155, 1985-1992.

De Marzo, A. M., Marchi, V. L., Yang, E. S., Veeraswamy, R., Lin, X., and Nelson, W. G. (1999b). Abnormal regulation of DNA methyltransferase expression during colorectal carcinogenesis. *Cancer Res* 59, 3855-3860.

DeCaprio, J. A., Ludlow, J. W., Figge, J., Shew, J. Y., Huang, C. M., Lee, W. H., Marsilio, E., Paucha, E., and Livingston, D. M. (1988). SV40 large tumor antigen forms a specific complex with the product of the retinoblastoma susceptibility gene. *Cell* 54, 275-283.

Dellambra, E., Golisano, O., Bondanza, S., Siviero, E., Lacal, P., Molinari, M., D'Atri, S., and De Luca, M. (2000). Downregulation of 14-3-3sigma prevents clonal evolution and leads to immortalization of primary human keratinocytes. *J Cell Biol* 149, 1117-1130.

Dhar, S., Squire, J. A., Hande, M. P., Wellinger, R. J., and Pandita, T. K. (2000). Inactivation of 14-3-3sigma influences telomere behavior and ionizing radiation-induced chromosomal instability. *Mol Cell Biol* 20, 7764-7772.

Dimri, G. P., Lee, X., Basile, G., Acosta, M., Scott, G., Roskelley, C., Medrano, E. E., Linskens, M., Rubelj, I., and Pereira-Smith, O. (1995). A biomarker that identifies senescent human cells in culture and in aging skin in vivo. *Proc Natl Acad Sci U S A* 92, 9363-9367.

Donehower, L. A., Harvey, M., Slagle, B. L., McArthur, M. J., Montgomery, C. A., Jr., Butel, J. S., and Bradley, A. (1992). Mice deficient for p53 are developmentally normal but susceptible to spontaneous tumours. *Nature* 356, 215-221.

Dropcho, E. J. (2004). Neurotoxicity of cancer chemotherapy. *Semin Neurol* 24, 419-426.

Eads, C. A., Nickel, A. E., and Laird, P. W. (2002). Complete genetic suppression of polyp formation and reduction of CpG-island hypermethylation in *Apc*(Min/+) *Dnmt1*-hypomorphic Mice. *Cancer Res* 62, 1296-1299.

Eden, A., Gaudet, F., Waghmare, A., and Jaenisch, R. (2003). Chromosomal instability and tumors promoted by DNA hypomethylation. *Science* 300, 455.

el-Deiry, W. S., Tokino, T., Velculescu, V. E., Levy, D. B., Parsons, R., Trent, J. M., Lin, D., Mercer, W. E., Kinzler, K. W., and Vogelstein, B. (1993). WAF1, a potential mediator of p53 tumor suppression. *Cell* 75, 817-825.

Ercole, C. J., Lange, P. H., Mathisen, M., Chiou, R. K., Reddy, P. K., and Vessella, R. L. (1987). Prostatic specific antigen and prostatic acid phosphatase in the monitoring and staging of patients with prostatic cancer. *J Urol* 138, 1181-1184.

Feinberg, A. P., and Tycko, B. (2004). The history of cancer epigenetics. *Nat Rev Cancer* 4, 143-153.

Felix, C. A. (1998). Secondary leukemias induced by topoisomerase-targeted drugs. *Biochim Biophys Acta* 1400, 233-255.

Ferguson, A. T., Evron, E., Umbricht, C. B., Pandita, T. K., Chan, T. A., Hermeking, H., Marks, J. R., Lambers, A. R., Futreal, P. A., Stampfer, M. R., and Sukumar, S. (2000). High frequency of hypermethylation at the 14-3-3 sigma locus leads to gene silencing in breast cancer. *Proc Natl Acad Sci U S A* 97, 6049-6054.

Fleisch, J. H., Haisch, K. D., Spaethe, S. M., Rinkema, L. E., Cullinan, G. J., Schmidt, M. J., and Marshall, W. S. (1984). Pharmacologic analysis of two novel inhibitors of leukotriene (slow reacting substance) release. *J Pharmacol Exp Ther* 229, 681-689.

Florl, A. R., Steinhoff, C., Muller, M., Seifert, H. H., Hader, C., Engers, R., Ackermann, R., and Schulz, W. A. (2004). Coordinate hypermethylation at specific genes in prostate carcinoma precedes LINE-1 hypomethylation. *Br J Cancer* 91, 985-994.

Gasco, M., Bell, A. K., Heath, V., Sullivan, A., Smith, P., Hiller, L., Yulug, I., Numico, G., Merlano, M., Farrell, P. J., *et al.* (2002). Epigenetic inactivation of 14-3-3 sigma in oral carcinoma: association with p16(INK4a) silencing and human papillomavirus negativity. *Cancer Res* 62, 2072-2076.

Gaudet, F., Hodgson, J. G., Eden, A., Jackson-Grusby, L., Dausman, J., Gray, J. W., Leonhardt, H., and Jaenisch, R. (2003). Induction of tumors in mice by genomic hypomethylation. *Science* 300, 489-492.



Giles, R. H., van Es, J. H., and Clevers, H. (2003). Caught up in a Wnt storm: Wnt signaling in cancer. *Biochim Biophys Acta* 1653, 1-24.

Giulii, G., Roechel, N., Scholl, U., Mattei, M. G., and Guellaen, G. (1993). Colocalization of the genes coding for the alpha 3 and beta 3 subunits of soluble guanylyl cyclase to human chromosome 4 at q31.3-q33. *Hum Genet* 91, 257-260.

Giulii, G., Scholl, U., Bulle, F., and Guellaen, G. (1992). Molecular cloning of the cDNAs coding for the two subunits of soluble guanylyl cyclase from human brain. *FEBS Lett* 304, 83-88.

Gius, D., Cui, H., Bradbury, C. M., Cook, J., Smart, D. K., Zhao, S., Young, L., Brandenburg, S. A., Hu, Y., Bisht, K. S., *et al.* (2004). Distinct effects on gene expression of chemical and genetic manipulation of the cancer epigenome revealed by a multimodality approach. *Cancer Cell* 6, 361-371.

Grana, X., Garriga, J., and Mayol, X. (1998). Role of the retinoblastoma protein family, pRB, p107 and p130 in the negative control of cell growth. *Oncogene* 17, 3365-3383.

Gupta, S., Srivastava, M., Ahmad, N., Bostwick, D. G., and Mukhtar, H. (2000). Over-expression of cyclooxygenase-2 in human prostate adenocarcinoma. *Prostate* 42, 73-78.

Harper, J. W., Adami, G. R., Wei, N., Keyomarsi, K., and Elledge, S. J. (1993). The p21 Cdk-interacting protein Cip1 is a potent inhibitor of G1 cyclin-dependent kinases. *Cell* 75, 805-816.

Harper, J. W., Elledge, S. J., Keyomarsi, K., Dynlacht, B., Tsai, L. H., Zhang, P., Dobrowolski, S., Bai, C., Connell-Crowley, L., Swindell, E., and *et al.* (1995). Inhibition of cyclin-dependent kinases by p21. *Mol Biol Cell* 6, 387-400.

Hartwell, L. H., Szankasi, P., Roberts, C. J., Murray, A. W., and Friend, S. H. (1997). Integrating genetic approaches into the discovery of anticancer drugs. *Science* 278, 1064-1068.

He, T. C., Sparks, A. B., Rago, C., Hermeking, H., Zawel, L., da Costa, L. T., Morin, P. J., Vogelstein, B., and Kinzler, K. W. (1998). Identification of c-MYC as a target of the APC pathway. *Science* 281, 1509-1512.

Helt, C. E., Rancourt, R. C., Staversky, R. J., and O'Reilly, M. A. (2001). p53-dependent induction of p21(Cip1/WAF1/Sdi1) protects against oxygen-induced toxicity. *Toxicol Sci* 63, 214-222.

Herman, J. G., Civin, C. I., Issa, J. P., Collector, M. I., Sharkis, S. J., and Baylin, S. B. (1997). Distinct patterns of inactivation of p15INK4B and p16INK4A characterize the major types of hematological malignancies. *Cancer Res* 57, 837-841.

Herman, J. G., Graff, J. R., Myohanen, S., Nelkin, B. D., and Baylin, S. B. (1996). Methylation-specific PCR: a novel PCR assay for methylation status of CpG islands. *Proc Natl Acad Sci U S A* 93, 9821-9826.

Hermeking, H. (2003). The 14-3-3 cancer connection. *Nat Rev Cancer* 3, 931-943.

Hermeking, H., Lengauer, C., Polyak, K., He, T. C., Zhang, L., Thiagalingam, S., Kinzler, K. W., and Vogelstein, B. (1997). 14-3-3 sigma is a p53-regulated inhibitor of G2/M progression. *Mol Cell* 1, 3-11.

Hermeking, H., Wolf, D. A., Kohlhuber, F., Dickmanns, A., Billaud, M., Fanning, E., and Eick, D. (1994). Role of c-myc in simian virus 40 large tumor antigen-induced DNA synthesis in quiescent 3T3-L1 mouse fibroblasts. *Proc Natl Acad Sci U S A* 91, 10412-10416.

Hoang, B. H., Kubo, T., Healey, J. H., Yang, R., Nathan, S. S., Kolb, E. A., Mazza, B., Meyers, P. A., and Gorlick, R. (2004). Dickkopf 3 inhibits invasion and motility of Saos-2 osteosarcoma cells by modulating the Wnt-beta-catenin pathway. *Cancer Res* 64, 2734-2739.

Hoffmann, M. J., Florl, A. R., Seifert, H. H., and Schulz, W. A. (2004). Multiple mechanisms downregulate CDKN1C in human bladder cancer. *Int J Cancer* 114, 406-413.

Hofmann, F., Ammendola, A., and Schlossmann, J. (2000). Rising behind NO: cGMP-dependent protein kinases. *J Cell Sci* 113 ( Pt 10), 1671-1676.

Hollstein, M., Hergenhahn, M., Yang, Q., Bartsch, H., Wang, Z. Q., and Hainaut, P. (1999). New approaches to understanding p53 gene tumor mutation spectra. *Mutat Res* 431, 199-209.

Hopkins-Donaldson, S., Ziegler, A., Kurtz, S., Bigosch, C., Kandioler, D., Ludwig, C., Zangemeister-Wittke, U., and Stahel, R. (2003). Silencing of death receptor and caspase-8 expression in small cell lung carcinoma cell lines and tumors by DNA methylation. *Cell Death Differ* 10, 356-364.

Horowitz, J. M., Park, S. H., Bogenmann, E., Cheng, J. C., Yandell, D. W., Kaye, F. J., Minna, J. D., Dryja, T. P., and Weinberg, R. A. (1990). Frequent inactivation of the retinoblastoma anti-oncogene is restricted to a subset of human tumor cells. *Proc Natl Acad Sci U S A* 87, 2775-2779.

Hayflick, L., and Moorhead, P. S. (1961) The limited in vitro lifetime of human diploid cell strains. *Exp Cell Res* 25, 585-621.

Ivanova, T., Petrenko, A., Gritsko, T., Vinokourova, S., Eshilev, E., Kobzeva, V., Kisseljov, F., and Kisseljova, N. (2002). Methylation and silencing of the retinoic acid receptor-beta 2 gene in cervical cancer. *BMC Cancer* 2, 4.

Iwata, N., Yamamoto, H., Sasaki, S., Itoh, F., Suzuki, H., Kikuchi, T., Kaneto, H., Iku, S., Ozeki, I., Karino, Y., *et al.* (2000). Frequent hypermethylation of CpG islands and loss of expression of the 14-3-3 sigma gene in human hepatocellular carcinoma. *Oncogene* 19, 5298-5302.

Jackson, J. P., Lindroth, A. M., Cao, X., and Jacobsen, S. E. (2002). Control of CpNpG DNA methylation by the KRYPTONITE histone H3 methyltransferase. *Nature* 416, 556-560.

Jaenisch, R., and Bird, A. (2003). Epigenetic regulation of gene expression: how the genome integrates intrinsic and environmental signals. *Nat Genet* 33 *Suppl*, 245-254.

Jones, P. A., and Baylin, S. B. (2002). The fundamental role of epigenetic events in cancer. *Nat Rev Genet* 3, 415-428.

Kahlem, P., Dorken, B., and Schmitt, C. A. (2004). Cellular senescence in cancer treatment: friend or foe? *J Clin Invest* 113, 169-174.

Kamijo, T., Bodner, S., van de Kamp, E., Randle, D. H., and Sherr, C. J. (1999). Tumor spectrum in ARF-deficient mice. *Cancer Res* 59, 2217-2222.

Kamijo, T., Zindy, F., Roussel, M. F., Quelle, D. E., Downing, J. R., Ashmun, R. A., Grosveld, G., and Sherr, C. J. (1997). Tumor suppression at the mouse INK4a locus mediated by the alternative reading frame product p19ARF. *Cell* 91, 649-659.

Kang, G. H., Lee, S., Lee, H. J., and Hwang, K. S. (2004). Aberrant CpG island hypermethylation of multiple genes in prostate cancer and prostatic intraepithelial neoplasia. *J Pathol* 202, 233-240.

Karan, D., Lin, M. F., Johansson, S. L., and Batra, S. K. (2003). Current status of the molecular genetics of human prostatic adenocarcinomas. *Int J Cancer* 103, 285-293.

Karpf, A. R., and Jones, D. A. (2002). Reactivating the expression of methylation silenced genes in human cancer. *Oncogene* 21, 5496-5503.

Karpf, A. R., Moore, B. C., Ririe, T. O., and Jones, D. A. (2001). Activation of the p53 DNA damage response pathway after inhibition of DNA methyltransferase by 5-aza-2'-deoxycytidine. *Mol Pharmacol* 59, 751-757.

Kawasaki, H., and Taira, K. (2004). Induction of DNA methylation and gene silencing by short interfering RNAs in human cells. *Nature* 431, 211-217.

Kikuchi, T., Itoh, F., Toyota, M., Suzuki, H., Yamamoto, H., Fujita, M., Hosokawa, M., and Imai, K. (2002a). Aberrant methylation and histone deacetylation of cyclooxygenase 2 in gastric cancer. *Int J Cancer* 97, 272-277.

Kikuchi, T., Toyota, M., Itoh, F., Suzuki, H., Obata, T., Yamamoto, H., Kakiuchi, H., Kusano, M., Issa, J. P., Tokino, T., and Imai, K. (2002b). Inactivation of p57KIP2 by regional promoter hypermethylation and histone deacetylation in human tumors. *Oncogene* 21, 2741-2749.

Kimura, F., Franke, K. H., Steinhoff, C., Golka, K., Roemer, H. C., Anastasiadis, A. G., and Schulz, W. A. (2000). Methyl group metabolism gene polymorphisms and susceptibility to prostatic carcinoma. *Prostate* 45, 225-231.

Kinzler, K. W., and Vogelstein, B. (1996). Lessons from hereditary colorectal cancer. *Cell* 87, 159-170.

Kinzler, K. W., and Vogelstein, B. (1997). Cancer-susceptibility genes. Gatekeepers and caretakers. *Nature* 386, 761, 763.

Kote-Jarai, Z., Easton, D., Edwards, S. M., Jefferies, S., Durocher, F., Jackson, R. A., Singh, R., Ardern-Jones, A., Murkin, A., Dearnaley, D. P., *et al.* (2001). Relationship between glutathione S-transferase M1, P1 and T1 polymorphisms and early onset prostate cancer. *Pharmacogenetics* 11, 325-330.

Krimpenfort, P., Quon, K. C., Mooi, W. J., Loonstra, A., and Berns, A. (2001). Loss of p16Ink4a confers susceptibility to metastatic melanoma in mice. *Nature* 413, 83-86.

Krishnamurthy, J., Torrice, C., Ramsey, M. R., Kovalev, G. I., Al-Regaiey, K., Su, L., and Sharpless, N. E. (2004). Ink4a/Arf expression is a biomarker of aging. *J Clin Invest* 114, 1299-1307.

Kurose, K., Sakaguchi, M., Nasu, Y., Ebara, S., Kaku, H., Kariyama, R., Arao, Y., Miyazaki, M., Tsushima, T., Namba, M., *et al.* (2004). Decreased expression of REIC/Dkk-3 in human renal clear cell carcinoma. *J Urol* 171, 1314-1318.

Kuzmin, I., Gillespie, J. W., Protopopov, A., Geil, L., Dreijerink, K., Yang, Y., Vocke, C. D., Duh, F. M., Zabarovsky, E., Minna, J. D., *et al.* (2002). The RASSF1A tumor suppressor gene is inactivated in prostate tumors and suppresses growth of prostate carcinoma cells. *Cancer Res* 62, 3498-3502.

Laird, P. W. (2003). The power and the promise of DNA methylation markers. *Nat Rev Cancer* 3, 253-266.

Lehnertz, B., Ueda, Y., Derijck, A. A., Braunschweig, U., Perez-Burgos, L., Kubicek, S., Chen, T., Li, E., Jenuwein, T., and Peters, A. H. (2003). Suv39h-mediated histone H3 lysine 9 methylation directs DNA methylation to major satellite repeats at pericentric heterochromatin. *Curr Biol* 13, 1192-1200.

Li, E. (2002). Chromatin modification and epigenetic reprogramming in mammalian development. *Nat Rev Genet* 3, 662-673.

Li, L. C., Carroll, P. R., and Dahiya, R. (2005). Epigenetic changes in prostate cancer: implication for diagnosis and treatment. *J Natl Cancer Inst* 97, 103-115.

Li, Z., Meng, Z. H., Chandrasekaran, R., Kuo, W. L., Collins, C. C., Gray, J. W., and Dairkee, S. H. (2002). Biallelic inactivation of the thyroid hormone receptor beta1 gene in early stage breast cancer. *Cancer Res* 62, 1939-1943.

Lin, X., Tascilar, M., Lee, W. H., Vles, W. J., Lee, B. H., Veeraswamy, R., Asgari, K., Freije, D., van Rees, B., Gage, W. R., *et al.* (2001). GSTP1 CpG island hypermethylation is responsible for the absence of GSTP1 expression in human prostate cancer cells. *Am J Pathol* 159, 1815-1826.

Liu, X. H., Kirschenbaum, A., Yao, S., Lee, R., Holland, J. F., and Levine, A. C. (2000). Inhibition of cyclooxygenase-2 suppresses angiogenesis and the growth of prostate cancer in vivo. *J Urol* 164, 820-825.

Ly, D. H., Lockhart, D. J., Lerner, R. A., and Schultz, P. G. (2000). Mitotic misregulation and human aging. *Science* 287, 2486-2492.

Matsuoka, S., Thompson, J. S., Edwards, M. C., Bartletta, J. M., Grundy, P., Kalikin, L. M., Harper, J. W., Elledge, S. J., and Feinberg, A. P. (1996). Imprinting of the gene encoding a human cyclin-dependent kinase inhibitor, p57KIP2, on chromosome 11p15. *Proc Natl Acad Sci U S A* 93, 3026-3030.

Matzke, M., Matzke, A. J., and Kooter, J. M. (2001). RNA: guiding gene silencing. *Science* 293, 1080-1083.

Meeker, A. K., Hicks, J. L., Platz, E. A., March, G. E., Bennett, C. J., Delannoy, M. J., and De Marzo, A. M. (2002). Telomere shortening is an early somatic DNA alteration in human prostate tumorigenesis. *Cancer Res* 62, 6405-6409.

Miller, S. J. (1991). Biology of basal cell carcinoma (Part I). *J Am Acad Dermatol* 24, 1-13.

Mohr, L. C., Rodgers, J. K., and Silvestri, G. A. (2003). Glutathione S-transferase M1 polymorphism and the risk of lung cancer. *Anticancer Res* 23, 2111-2124.

Morin, P. J., Sparks, A. B., Korinek, V., Barker, N., Clevers, H., Vogelstein, B., and Kinzler, K. W. (1997). Activation of beta-catenin-Tcf signaling in colon cancer by mutations in beta-catenin or APC. *Science* 275, 1787-1790.

Morris, K. V., Chan, S. W., Jacobsen, S. E., and Looney, D. J. (2004). Small interfering RNA-induced transcriptional gene silencing in human cells. *Science* 305, 1289-1292.

Mulsch, A., Busse, R., Liebau, S., and Forstermann, U. (1988). LY 83583 interferes with the release of endothelium-derived relaxing factor and inhibits soluble guanylate cyclase. *J Pharmacol Exp Ther* 247, 283-288.

Myohanen, S. K., Baylin, S. B., and Herman, J. G. (1998). Hypermethylation can selectively silence individual p16ink4A alleles in neoplasia. *Cancer Res* 58, 591-593.

Nacht, M., Ferguson, A. T., Zhang, W., Petroziello, J. M., Cook, B. P., Gao, Y. H., Maguire, S., Riley, D., Coppola, G., Landes, G. M., *et al.* (1999). Combining serial analysis of gene expression and array technologies to identify genes differentially expressed in breast cancer. *Cancer Res* 59, 5464-5470.

Nakayama, T., Watanabe, M., Yamanaka, M., Hirokawa, Y., Suzuki, H., Ito, H., Yatani, R., and Shiraishi, T. (2001). The role of epigenetic modifications in retinoic acid receptor beta2 gene expression in human prostate cancers. *Lab Invest* 81, 1049-1057.

Narita, M., Nunez, S., Heard, E., Lin, A. W., Hearn, S. A., Spector, D. L., Hannon, G. J., and Lowe, S. W. (2003). Rb-mediated heterochromatin formation and silencing of E2F target genes during cellular senescence. *Cell* 113, 703-716.

Nelson, J. E., and Harris, R. E. (2000). Inverse association of prostate cancer and non-steroidal anti-inflammatory drugs (NSAIDs): results of a case-control study. *Oncol Rep* 7, 169-170.

Nelson, W. G., De Marzo, A. M., and Isaacs, W. B. (2003). Prostate cancer. *N Engl J Med* 349, 366-381.

Noda, A., Ning, Y., Venable, S. F., Pereira-Smith, O. M., and Smith, J. R. (1994). Cloning of senescent cell-derived inhibitors of DNA synthesis using an expression screen. *Exp Cell Res* 211, 90-98.

Paz, M. F., Fraga, M. F., Avila, S., Guo, M., Pollan, M., Herman, J. G., and Esteller, M. (2003). A systematic profile of DNA methylation in human cancer cell lines. *Cancer Res* 63, 1114-1121.

- Pellegrini, G., Dellambra, E., Golisano, O., Martinelli, E., Fantozzi, I., Bondanza, S., Ponzin, D., McKeon, F., and De Luca, M. (2001). p63 identifies keratinocyte stem cells. *Proc Natl Acad Sci U S A* 98, 3156-3161.
- Pfaffl, M. W. (2001). A new mathematical model for relative quantification in real-time RT-PCR. *Nucleic Acids Res* 29, e45.
- Ramirez, R. D., Morales, C. P., Herbert, B. S., Rohde, J. M., Passons, C., Shay, J. W., and Wright, W. E. (2001). Putative telomere-independent mechanisms of replicative aging reflect inadequate growth conditions. *Genes Dev* 15, 398-403.
- Rhee, I., Bachman, K. E., Park, B. H., Jair, K. W., Yen, R. W., Schuebel, K. E., Cui, H., Feinberg, A. P., Lengauer, C., Kinzler, K. W., *et al.* (2002). DNMT1 and DNMT3b cooperate to silence genes in human cancer cells. *Nature* 416, 552-556.
- Robertson, K. D., Keyomarsi, K., Gonzales, F. A., Velicescu, M., and Jones, P. A. (2000). Differential mRNA expression of the human DNA methyltransferases (DNMTs) 1, 3a and 3b during the G(0)/G(1) to S phase transition in normal and tumor cells. *Nucleic Acids Res* 28, 2108-2113.
- Sage, J., Miller, A. L., Perez-Mancera, P. A., Wysocki, J. M., and Jacks, T. (2003). Acute mutation of retinoblastoma gene function is sufficient for cell cycle re-entry. *Nature* 424, 223-228.
- Sage, J., Mulligan, G. J., Attardi, L. D., Miller, A., Chen, S., Williams, B., Theodorou, E., and Jacks, T. (2000). Targeted disruption of the three Rb-related genes leads to loss of G(1) control and immortalization. *Genes Dev* 14, 3037-3050.
- Samuel, T., Weber, H. O., Rauch, P., Verdoodt, B., Eppel, J. T., McShea, A., Hermeking, H., and Funk, J. O. (2001). The G2/M regulator 14-3-3sigma prevents apoptosis through sequestration of Bax. *J Biol Chem* 276, 45201-45206.
- Sansom, O. J., Berger, J., Bishop, S. M., Hendrich, B., Bird, A., and Clarke, A. R. (2003). Deficiency of Mbd2 suppresses intestinal tumorigenesis. *Nat Genet* 34, 145-147.
- Sawyers, C. (2004). Targeted cancer therapy. *Nature* 432, 294-297.



Schmidt, M. J., Sawyer, B. D., Truex, L. L., Marshall, W. S., and Fleisch, J. H. (1985). LY83583: an agent that lowers intracellular levels of cyclic guanosine 3',5'-monophosphate. *J Pharmacol Exp Ther* 232, 764-769.

Schmitt, C. A., Fridman, J. S., Yang, M., Lee, S., Baranov, E., Hoffman, R. M., and Lowe, S. W. (2002). A senescence program controlled by p53 and p16INK4a contributes to the outcome of cancer therapy. *Cell* 109, 335-346.

Schubert, J., and Muller, A. (1997). [Basaliomas with invasion of bone: problems and prognosis]. *Mund Kiefer Gesichtschir* 1, 44-46.

Schulz, W. A., Burchardt, M., and Cronauer, M. V. (2003). Molecular biology of prostate cancer. *Mol Hum Reprod* 9, 437-448.

Schwarze, S. R., Shi, Y., Fu, V. X., Watson, P. A., and Jarrard, D. F. (2001). Role of cyclin-dependent kinase inhibitors in the growth arrest at senescence in human prostate epithelial and uroepithelial cells. *Oncogene* 20, 8184-8192.

Serrano, M., and Blasco, M. A. (2001). Putting the stress on senescence. *Curr Opin Cell Biol* 13, 748-753.

Serrano, M., Lee, H., Chin, L., Cordon-Cardo, C., Beach, D., and DePinho, R. A. (1996). Role of the INK4a locus in tumor suppression and cell mortality. *Cell* 85, 27-37.

Serrano, M., Lin, A. W., McCurrach, M. E., Beach, D., and Lowe, S. W. (1997). Oncogenic ras provokes premature cell senescence associated with accumulation of p53 and p16INK4a. *Cell* 88, 593-602.

Sharpless, E., and Chin, L. (2003). The INK4a/ARF locus and melanoma. *Oncogene* 22, 3092-3098.

Sharpless, N. E., Bardeesy, N., Lee, K. H., Carrasco, D., Castrillon, D. H., Aguirre, A. J., Wu, E. A., Horner, J. W., and DePinho, R. A. (2001). Loss of p16Ink4a with retention of p19Arf predisposes mice to tumorigenesis. *Nature* 413, 86-91.

Sharpless, N. E., and DePinho, R. A. (2004). Telomeres, stem cells, senescence, and cancer. *J Clin Invest* 113, 160-168.

Shelton, D. N., Chang, E., Whittier, P. S., Choi, D., and Funk, W. D. (1999). Microarray analysis of replicative senescence. *Curr Biol* 9, 939-945.

Shin, J. Y., Kim, H. S., Park, J., Park, J. B., and Lee, J. Y. (2000). Mechanism for inactivation of the KIP family cyclin-dependent kinase inhibitor genes in gastric cancer cells. *Cancer Res* 60, 262-265.

Singal, R., van Wert, J., and Bashambu, M. (2001). Cytosine methylation represses glutathione S-transferase P1 (GSTP1) gene expression in human prostate cancer cells. *Cancer Res* 61, 4820-4826.

Smith, D. S., and Catalona, W. J. (1995). Interexaminer variability of digital rectal examination in detecting prostate cancer. *Urology* 45, 70-74.

Soengas, M. S., Capodiceci, P., Polsky, D., Mora, J., Esteller, M., Opitz-Araya, X., McCombie, R., Herman, J. G., Gerald, W. L., Lazebnik, Y. A., *et al.* (2001). Inactivation of the apoptosis effector Apaf-1 in malignant melanoma. *Nature* 409, 207-211.

Stein, G. H., Drullinger, L. F., Soulard, A., and Dulic, V. (1999). Differential roles for cyclin-dependent kinase inhibitors p21 and p16 in the mechanisms of senescence and differentiation in human fibroblasts. *Mol Cell Biol* 19, 2109-2117.

Steinert, S., Shay, J. W., and Wright, W. E. (2000). Transient expression of human telomerase extends the life span of normal human fibroblasts. *Biochem Biophys Res Commun* 273, 1095-1098.

Steinhoff, C., Franke, K. H., Golka, K., Thier, R., Romer, H. C., Rotzel, C., Ackermann, R., and Schulz, W. A. (2000). Glutathione transferase isozyme genotypes in patients with prostate and bladder carcinoma. *Arch Toxicol* 74, 521-526.

Stoehr, R., Wissmann, C., Suzuki, H., Knuechel, R., Krieg, R. C., Klopocki, E., Dahl, E., Wild, P., Blaszyk, H., Sauter, G., *et al.* (2004). Deletions of chromosome 8p and loss of sFRP1 expression are progression markers of papillary bladder cancer. *Lab Invest*.

Suter, C. M., Martin, D. I., and Ward, R. L. (2004). Germline epimutation of MLH1 in individuals with multiple cancers. *Nat Genet* 36, 497-501.

Suwa, T., Chen, M., Hawks, C. L., and Hornsby, P. J. (2003). Zonal expression of dickkopf-3 and components of the Wnt signalling pathways in the human adrenal cortex. *J Endocrinol* 178, 149-158.

Suzuki, H., Freije, D., Nusskern, D. R., Okami, K., Cairns, P., Sidransky, D., Isaacs, W. B., and Bova, G. S. (1998). Interfocal heterogeneity of PTEN/MMAC1 gene alterations in multiple metastatic prostate cancer tissues. *Cancer Res* 58, 204-209.

Suzuki, H., Gabrielson, E., Chen, W., Anbazhagan, R., van Engeland, M., Weijnenberg, M. P., Herman, J. G., and Baylin, S. B. (2002). A genomic screen for genes upregulated by demethylation and histone deacetylase inhibition in human colorectal cancer. *Nat Genet* 31, 141-149.

Suzuki, H., Watkins, D. N., Jair, K. W., Schuebel, K. E., Markowitz, S. D., Dong Chen, W., Pretlow, T. P., Yang, B., Akiyama, Y., Van Engeland, M., *et al.* (2004). Epigenetic inactivation of SFRP genes allows constitutive WNT signaling in colorectal cancer. *Nat Genet* 36, 417-422.

Tamaru, H., and Selker, E. U. (2001). A histone H3 methyltransferase controls DNA methylation in *Neurospora crassa*. *Nature* 414, 277-283.

te Poele, R. H., Okorokov, A. L., Jardine, L., Cummings, J., and Joel, S. P. (2002). DNA damage is able to induce senescence in tumor cells in vitro and in vivo. *Cancer Res* 62, 1876-1883.

Tokino, T., Urano, T., Furuhashi, T., Matsushima, M., Miyatsu, T., Sasaki, S., and Nakamura, Y. (1996). Characterization of the human p57KIP2 gene: alternative splicing, insertion/deletion polymorphisms in VNTR sequences in the coding region, and mutational analysis. *Hum Genet* 97, 625-631.

Tokugawa, T., Sugihara, H., Tani, T., and Hattori, T. (2002). Modes of silencing of p16 in development of esophageal squamous cell carcinoma. *Cancer Res* 62, 4938-4944.

Tokumaru, Y., Harden, S. V., Sun, D. I., Yamashita, K., Epstein, J. I., and Sidransky, D. (2004). Optimal use of a panel of methylation markers with GSTP1 hypermethylation in the diagnosis of prostate adenocarcinoma. *Clin Cancer Res* 10, 5518-5522.

Toyota, M., Shen, L., Ohe-Toyota, M., Hamilton, S. R., Sinicrope, F. A., and Issa, J. P. (2000). Aberrant methylation of the Cyclooxygenase 2 CpG island in colorectal tumors. *Cancer Res* 60, 4044-4048.

Travis, L. B. (2002). Therapy-associated solid tumors. *Acta Oncol* 41, 323-333.

Tsuji, T., Miyazaki, M., Sakaguchi, M., Inoue, Y., and Namba, M. (2000). A REIC gene shows down-regulation in human immortalized cells and human tumor-derived cell lines. *Biochem Biophys Res Commun* 268, 20-24.

Tsuji, T., Nozaki, I., Miyazaki, M., Sakaguchi, M., Pu, H., Hamazaki, Y., Iijima, O., and Namba, M. (2001). Antiproliferative activity of REIC/Dkk-3 and its significant down-regulation in non-small-cell lung carcinomas. *Biochem Biophys Res Commun* 289, 257-263.

Umbricht, C. B., Evron, E., Gabrielson, E., Ferguson, A., Marks, J., and Sukumar, S. (2001). Hypermethylation of 14-3-3 sigma (stratifin) is an early event in breast cancer. *Oncogene* 20, 3348-3353.

Untergasser, G., Koch, H. B., Menssen, A., and Hermeking, H. (2002). Characterization of epithelial senescence by serial analysis of gene expression: identification of genes potentially involved in prostate cancer. *Cancer Res* 62, 6255-6262.

Urano, T., Saito, T., Tsukui, T., Fujita, M., Hosoi, T., Muramatsu, M., Ouchi, Y., and Inoue, S. (2002). Efp targets 14-3-3 sigma for proteolysis and promotes breast tumour growth. *Nature* 417, 871-875.

Vanaja, D. K., Cheville, J. C., Iturria, S. J., and Young, C. Y. (2003). Transcriptional silencing of zinc finger protein 185 identified by expression profiling is associated with prostate cancer progression. *Cancer Res* 63, 3877-3882.

Vogelstein, B., Lane, D., and Levine, A. J. (2000). Surfing the p53 network. *Nature* 408, 307-310.

Voorhoeve, P. M., and Agami, R. (2003). The tumor-suppressive functions of the human INK4A locus. *Cancer Cell* 4, 311-319.

- Voorhoeve, P. M., and Agami, R. (2004). Unraveling human tumor suppressor pathways: a tale of the INK4A locus. *Cell Cycle* 3, 616-620.
- Waldman, T., Lengauer, C., Kinzler, K. W., and Vogelstein, B. (1996). Uncoupling of S phase and mitosis induced by anticancer agents in cells lacking p21. *Nature* 381, 713-716.
- Watanabe, H., Pan, Z. Q., Schreiber-Agus, N., DePinho, R. A., Hurwitz, J., and Xiong, Y. (1998). Suppression of cell transformation by the cyclin-dependent kinase inhibitor p57KIP2 requires binding to proliferating cell nuclear antigen. *Proc Natl Acad Sci U S A* 95, 1392-1397.
- Weinberg, R. A. (1995). The retinoblastoma protein and cell cycle control. *Cell* 81, 323-330.
- West, M. D., Shay, J. W., Wright, W. E., and Linskens, M. H. (1996). Altered expression of plasminogen activator and plasminogen activator inhibitor during cellular senescence. *Exp Gerontol* 31, 175-193.
- Westfall, M. D., Mays, D. J., Sniezek, J. C., and Pietenpol, J. A. (2003). The Delta Np63 alpha phosphoprotein binds the p21 and 14-3-3 sigma promoters in vivo and has transcriptional repressor activity that is reduced by Hay-Wells syndrome-derived mutations. *Mol Cell Biol* 23, 2264-2276.
- Wilker, E. W., Grant, R. A., Artim, S. C., and Yaffe, M. B. (2005). A structural basis for 14-3-3 sigma functional specificity. *J Biol Chem*.
- Yaffe, M. B. (2002). How do 14-3-3 proteins work?-- Gatekeeper phosphorylation and the molecular anvil hypothesis. *FEBS Lett* 513, 53-57.
- Yamashita, K., Upadhyay, S., Osada, M., Hoque, M. O., Xiao, Y., Mori, M., Sato, F., Meltzer, S. J., and Sidransky, D. (2002). Pharmacologic unmasking of epigenetically silenced tumor suppressor genes in esophageal squamous cell carcinoma. *Cancer Cell* 2, 485-495.
- Yan, Y., Frisen, J., Lee, M. H., Massague, J., and Barbacid, M. (1997). Ablation of the CDK inhibitor p57Kip2 results in increased apoptosis and delayed differentiation during mouse development. *Genes Dev* 11, 973-983.

Yegnasubramanian, S., Kowalski, J., Gonzalgo, M. L., Zahurak, M., Piantadosi, S., Walsh, P. C., Bova, G. S., De Marzo, A. M., Isaacs, W. B., and Nelson, W. G. (2004). Hypermethylation of CpG islands in primary and metastatic human prostate cancer. *Cancer Res* *64*, 1975-1986.

Zha, S., Gage, W. R., Sauvageot, J., Saria, E. A., Putzi, M. J., Ewing, C. M., Faith, D. A., Nelson, W. G., De Marzo, A. M., and Isaacs, W. B. (2001). Cyclooxygenase-2 is up-regulated in proliferative inflammatory atrophy of the prostate, but not in prostate carcinoma. *Cancer Res* *61*, 8617-8623.

Zhang, H., Pan, K. H., and Cohen, S. N. (2003). Senescence-specific gene expression fingerprints reveal cell-type-dependent physical clustering of up-regulated chromosomal loci. *Proc Natl Acad Sci U S A* *100*, 3251-3256.

Zhang, P., Liegeois, N. J., Wong, C., Finegold, M., Hou, H., Thompson, J. C., Silverman, A., Harper, J. W., DePinho, R. A., and Elledge, S. J. (1997). Altered cell differentiation and proliferation in mice lacking p57KIP2 indicates a role in Beckwith-Wiedemann syndrome. *Nature* *387*, 151-158.

zur Hausen, H. (2001). Oncogenic DNA viruses. *Oncogene* *20*, 7820-7823.

## 9. Abbreviations

**5Aza-2'dC** – 5-aza-2'-deoxycytidine

**BCC** – basal cell carcinoma of the skin

**BPH** – benign prostate hyperplasia

**BrdU** - 5-bromo-2-deoxyuridine

**cDNA** – complementary DNA

**cGMP** - 3'5'-cyclic-guanosinmonophosphate

**CDK** – cyclin-dependent kinase

**CMV** – cytomegalovirus (promoter)

**CpG** - cytidine-phosphate-guanidin

**DMSO** – dimethylsulfoxide

**EF1 $\alpha$**  - elongation factor 1 alpha

**EGFP** - enhanced green fluorescent protein

**EGFR** – epidermal growth factor receptor

**EYFP** - enhanced yellow fluorescent protein

**EST** - expression sequence tag

**FACS** - fluorescence-activated cell scanning

**GTP** - guanosintriphosphate

**HDACs** – histone deacetylases

**HDF** - human diploid fibroblasts

**HPV** – human papilloma virus

**hTERT** – human telomerase reverse transcriptase

**IHC** – immunohistochemistry

**IRES** – internal ribosomal entry site

**MAPK** – mitogen-activated protein kinases

**MSP** – methylation-specific PCR

**PBMC** – peripheral blood mononuclear cells

**PBS** - phosphate buffered saline

**PCa** – prostate carcinoma

**PCR** – polymerase chain reaction

**PIN** – prostate intraepithelial neoplasia

**PrEGM** – prostate epithelium growth medium

**PrECs** – primary prostate epithelial cells

**qPCR** - quantitative real-time PCR

**RT-PCR** – reverse transcription PCR

**SA- $\beta$ -gal** – senescence associated beta-galactosidase

**SAGE** – serial analysis of gene expression

**SAHF**- senescence-associated heterochromatic foci

**SCC**- squamous cell carcinoma

**SDS**- sodium dodecyl sulfate

**SDS-PAGE**-sodium dodecyl sulfate polyacrylamide gel electrophoresis

**SNP** - sodium nitroprusside

**SV40** – simian virus 40

**TSA** – trichostatin A

**VSV** – vesicular stomatitis virus (tag)

## 10. Supplemental tables

**Supplemental Table 1** Oligonucleotides used for bisulfite sequencing

Gene		forward sequence 5'→3'	reverse sequence 5'→3'	Product size	Annealing T
<b>APAF1</b>	genomic sequence	ATAGTTCCCCTAGGAGAGGTGGG	CAGCCTGACCCCACAGTCCC	682	60°
	bisulfite converted	ATAGTTTTTTTAGGAGAGGTGGG	CAACCTAACCCACAAATCCC		
<b>APPD</b>	genomic sequence	GCTGAGGGTGACTGTGCTGTGAGGC	CCCAGGCTCCCAGGTTACCCC	665	60°
	bisulfite converted	GTTGAGGGTGATTGTGTTGTGAGGT	CCCAAACTCCCACAAATTCACCCC		
<b>BIN1</b>	genomic sequence	GGTGAGCCCCTGGAAAAGGAGGGGG	CCCTTTACTGCCCATCTCTGCCATC	633	60°
	bisulfite converted	GGTGAGTTTTTGGAAAAGGAGGGGG	CCCTTTACTACCCATCTCTACCATC		
<b>BRCA2</b>	genomic sequence	TGGCCTGGGACTCTTAAGGGTCAG	TTGGCAGAGACAAAAGGGCAAGAAGCC	517	62°
	bisulfite converted	TGGTTTGGGATTTTTAAGGGTTAG	TTAAACAACAACAAAAAACAAAAAACC		
<b>BTG1</b>	genomic sequence	CCCCTAGGGTGGAAACAGAAATGGCT	ATCTCAATAGCTGCATTTCCAGCTC	771	65°
	bisulfite converted	TTTTTAGGGTGGAAATAGAAATGGTT	ATCTCAATAACTACATTTCCAATC		
upstream	genomic sequence	GAGCTGGAAATGCAGCTATTGAGAT	CCA <del>CG</del> GCTCCTTTGTCCCCAAATCC	771	65°
	bisulfite converted	GAGTTGGAAATGTAGTTATTGAGAT	CCA <del>CR</del> ACTCCTTTATCCCCAAATCC		
<b>BTG3</b>	genomic sequence	GGTCTAGAGAGCTGGGTCTAGAACT	CCCCTGCCCTCCCCTGTCCCC	785	60°
	bisulfite converted	GGTTTAGAGAGTTGGGTTTAGAATT	CCCCTACCCCTCCCCTATCCCC		
<b>CASP7</b>	genomic sequence	GGTACTTCCTTCAAAGCTGAGGGAG	CAACCAGGCTCCCCTAGACCAC	883	65°
	bisulfite converted	GGTATTTTTTTTAAAGTTGAGGGAG	CAACCAAACTCCCCTAAACCAC		
<b>CITED2</b>	genomic sequence	GAGGCACAAGGGCACTCTGGAGGG	CAGCACATAGAGGGACCTTCCCTGGC	630	60°
	bisulfite converted	GAGGTATAAGGGTATTTTGGAGGG	CAACACATAAAAAAACCTTAAAC		
<b>CTGF</b>	genomic sequence	GTGTAGGACTCCATTCAGCTCATTGG	C <del>CG</del> AAGTGACAGAATAGGCCCTTGTGC	648	60°
	bisulfite converted	GTGTAGGATTTTATTTAGTTTATTGG	CCR <del>AA</del> ATAACA <del>AA</del> ATA <del>AA</del> CCCTTATAC		
<b>CUTL2</b>	genomic sequence	GGAGCTGGGGGTAGACAGGTGCAAG	CAATGGCTGCACTCAATATC <del>CG</del> GGCTGGAC	548	62°
	bisulfite converted	GGAGTTGGGGGTAGATAGGTGTAAG	CAATAACTCACTCAATATC <del>CR</del> AACTAAAC		
<b>CYLD</b>	genomic sequence	GAGGAAGGTCTGTACAGGGAGG	<del>CG</del> CCATTAACAAGGCCAGAACCCC	806	65°
	bisulfite converted	GAGGAAGGTGTGTTATAGGGAGG	<del>CR</del> CCATTAACA <del>AA</del> CCA <del>AA</del> ACCCC		
<b>DDB2</b>	genomic sequence	GAAAGGCACTAGCTCTCTACAAAGC	GGGCTTGTTCAAACCAGCTTGGAGC	665	57°
	bisulfite converted	GAAAGGTATTAGTTTTTTATAAAGT	<del>AA</del> ACTTATTCAAACCA <del>AA</del> CTT <del>AA</del> AAAC		
<b>DKC1</b>	genomic sequence	GAAAGCAAAGAAAGAGGTACTGTTTA	CTGGCAGCAGCACAGACACTGCCAC	764	65°
	bisulfite converted	GAAAGTAAAGAAAGAGGTATTGTTTA	CT <del>AA</del> CA <del>AA</del> CA <del>AA</del> CACA <del>AA</del> CACT <del>AA</del> CCAC		
<b>DKK1</b>	genomic sequence	AGGCAAGGGCACCCAAGTTCCAGAGT	CTGACTGCAGAGCCTGGGTGCCCC	631	64°
	bisulfite converted	AGGTAAGGGTATTTAAGTTTTAGAGT	CT <del>AA</del> ACT <del>AA</del> CA <del>AA</del> ACCT <del>AA</del> AT <del>AA</del> CCCC		



## Supplemental Table 1 (continued)

<b>DKK3</b>	genomic sequence	GCAGGCAGTGAAGGAGATGGCTG	TACCTGGGGTGGACCAAGCACAGGTCA		
	upstream (a) bisulfite converted	G <b>T</b> AGG <b>T</b> AGTGAAGGAGATGG <b>T</b> TG	TACCT <b>AAAA</b> T <b>AA</b> ACCA <b>AA</b> CACA <b>AA</b> TCA	505	64°
	genomic sequence	TGAGGAGCAGAGCTCAGCTTGTGC	CATCTCATTGAGGGTGGCCCTCCTCC		
	downstream (b) bisulfite converted	TGAGGAG <b>T</b> AGAG <b>T</b> TAG <b>T</b> TGTGT	CATCTCATT <b>AAAA</b> T <b>AA</b> CCCTCCTCC	436	64°
<b>DLC1</b>	genomic sequence	GCTCAAGGCACACTAGGGTCCAGGC	GCTTCTTTCTGCACATCAAGCAC		
	bisulfite converted	G <b>T</b> T <b>T</b> AA <b>G</b> G <b>T</b> ATAT <b>T</b> AGGG <b>T</b> T <b>T</b> AG <b>G</b> T	<b>A</b> CTTCTTTCT <b>A</b> CACATCAA <b>A</b> CAC	759	60°
<b>DUSP1</b>	genomic sequence	GGAGGGAGAGAGGGAGGAG	CCCACCTCCATGACCATGGC		
	bisulfite converted	GGAGGGAGAGAGGGAGGAG	CCCACCTCCAT <b>A</b> CCAT <b>A</b> AC	666	61°
<b>GADD45A</b>	genomic sequence	AAGACATGAAAAGATAATAAGAAAAAAGTG	CTTCCTCCCCTGCAAGCCTTCCACAGCCC		
	bisulfite converted	AAGAT <b>A</b> TGAAAAGATAATAAGAAAAAAGTG	CTTCCTCCCCT <b>A</b> CAA <b>A</b> CCTTCCACA <b>A</b> CCC	813	65°
<b>GAS2L1</b>	genomic sequence	TCCCCAGGAGACCAAAGAGGTTGGA	TGGGGCTCTGGGCCAGAGAGGGTG		
	bisulfite converted	<b>T</b> T <b>T</b> T <b>T</b> AGGAGAT <b>T</b> AAAGAGGTTGGA	<b>T</b> AAA <b>A</b> CTCT <b>AA</b> CCCA <b>AAAA</b> AA <b>A</b> T <b>A</b>	549	57°
<b>GPX3</b>	genomic sequence	GCCCCCTTGCCCTGGCTGTAATGGAGAC	CTGGGAACCTGCACAGCCCACCCAGAC		
	bisulfite converted	G <b>T</b> T <b>T</b> T <b>T</b> T <b>T</b> T <b>T</b> GG <b>T</b> TGTAATGGAGAT	CT <b>AAAA</b> ACT <b>T</b> A <b>C</b> ACA <b>CCC</b> ACCC <b>A</b> AC	860	65°
<b>GSTM1</b>	genomic sequence	GTTAGGATCTGGCTGGTGTCTCAAG	CCAGGGAAGCCCCAGTTTACTACTGC		
	bisulfite converted	GTTAGGAT <b>T</b> GG <b>T</b> TGGTGT <b>T</b> T <b>A</b> AG	CCA <b>AAAA</b> ACC <b>CC</b> CA <b>A</b> TTTACTACT <b>A</b> C	596	60°
<b>HPGD</b>	genomic sequence	AGCCAGAGGCTGAGGGGAGGCTTTG	TGAGGTGTGCTCACAGCCTCAGCTTC		
	bisulfite converted	AG <b>T</b> TAGAG <b>G</b> TGAGGGGAGG <b>T</b> TTT <b>G</b>	<b>T</b> AAA <b>A</b> T <b>A</b> ACTCACA <b>CC</b> TCA <b>A</b> CTT <b>C</b>	514	66°
<b>HUS1</b>	genomic sequence	TTAAAAAACACTTGAAATAGGTGTCA	CCTTCATCCCCACAAGTGCCCTCC		
	bisulfite converted	TTAAAA <b>A</b> AT <b>T</b> TTGAAATAGGTGT <b>A</b>	CCTTCATCCCCACA <b>A</b> T <b>ACC</b> CTCC	655	60°
<b>ICAM1</b>	genomic sequence	GAGGGGCATCCCTCAGTGGAGGGAGC	CTACCTAAGCATGCATGACCTGACCC		
	bisulfite converted	GAGGGG <b>T</b> AT <b>T</b> T <b>T</b> T <b>T</b> AGTGGAGGGAG <b>T</b>	CTACCTAA <b>A</b> CAT <b>A</b> CAT <b>AA</b> CC <b>T</b> A <b>ACC</b> CC	725	64°
<b>ID3</b>	genomic sequence	AGTCTGGAGGTGAG <b>C</b> GAACAGCAAATTGG	CATCCTTGCCCTGGGTGTTTACGCCCTGTC		
	bisulfite converted	AG <b>T</b> TGGAGG <b>T</b> TAG <b>A</b> Y <b>G</b> AATAG <b>T</b> AAATTGG	CATCCT <b>A</b> CC <b>T</b> AA <b>A</b> T <b>A</b> TTCA <b>ACC</b> CT <b>A</b> TC	916	65°
<b>IRF1</b>	genomic sequence	GAAAAGATGGCCCCAGGAGCCAG	CCCCCCTTCCCTGGTGCCC		
	bisulfite converted	GAAAAGATGG <b>T</b> T <b>T</b> T <b>T</b> AGGAG <b>T</b> T <b>A</b> G	CCCCCCTTCC <b>T</b> AA <b>A</b> ACC <b>C</b>	666	61°
<b>IRF7</b>	genomic sequence	TGTCCCCTGGGCTGTAGTGGAGTGGC	CAGGTGTGGACTGAGGGCTTGTAGCCACC		
	bisulfite converted	TGT <b>T</b> T <b>T</b> T <b>T</b> TGGG <b>T</b> TGTAGTGGAGTGG <b>T</b>	CA <b>AA</b> T <b>A</b> T <b>AA</b> ACT <b>AA</b> AA <b>ACT</b> T <b>A</b> T <b>A</b> CCACC	665	58°
<b>JUNB</b>	genomic sequence	TGAAACCCCTCACTCATGTGCCTGGG	AGGGCTGTTCCATTTTAGTGCACATC		
	bisulfite converted	TGAAA <b>T</b> T <b>T</b> T <b>T</b> AT <b>T</b> TATGT <b>T</b> TGGG	<b>A</b> AA <b>A</b> CT <b>A</b> TTCCATTT <b>A</b> AT <b>A</b> CACATC	590	60°
<b>MRE11</b>	genomic sequence	GGAGGGAGAGGGGATCCAGCTC	CCAGGACCCCTCCCTGCCCACTC		
	bisulfite converted	GGAGGGAGAGGGGAT <b>T</b> TAG <b>T</b> T <b>T</b>	CCA <b>AA</b> ACCCCTCCCT <b>A</b> CCCACTC	714	64°
<b>NGFR</b>	genomic sequence	GATGGGTAAGAGAGTGAACCCTGTGG	CTCACCCCCAGAAGCAGCAACAGCAGC		
	bisulfite converted	GATGGGTAAGAGAGTGA <b>A</b> T <b>T</b> TGTGG	CTCACCCCC <b>A</b> AA <b>A</b> CA <b>A</b> CA <b>A</b> CA <b>A</b> CA <b>A</b> C	529	64°

## Supplemental Table 1 (continued)

<b>p19 (CDKN2D)</b>	genomic sequence	TTGCCACACTCTGACCAATCAGGAG	ACCAGAGAGGAGCTCTGGGGTCTC	792	58°
	bisulfite converted	TTG <b>T</b> TATATTTT <b>G</b> ATTAAT <b>T</b> AGGAG	ACCA <b>A</b> AAAA <b>A</b> ACTCT <b>A</b> AAATCTC		
<b>p21 (CDKN1A)</b>	genomic sequence	GGGACCGGCTGGCCTGCTGGAAC <b>T</b>	CTTCCTGGGCCCTCCAGGGACAC	697	65°
	bisulfite converted	GGGAT <b>T</b> GGTTGG <b>T</b> TT <b>G</b> TTGGAAT <b>T</b>	CTTCCT <b>A</b> AA <b>C</b> CCCTCC <b>A</b> AA <b>A</b> ACAC		
<b>p57 (CDKN1C)</b>	genomic sequence	GGCTGGG <b>C</b> GTTCACAGGCCAAGT <b>G</b>	<b>C</b> CGGGACACTAGGCAGCTGCT <b>C</b>	718	63°
	bisulfite converted	GG <b>T</b> TTGGG <b>Y</b> G <b>T</b> TTTTATAGG <b>T</b> TAAGT <b>G</b>	<b>C</b> CR <b>A</b> AA <b>C</b> ACT <b>A</b> AA <b>C</b> ACT <b>A</b> CT <b>C</b>		
<b>p130 (RBL2)</b>	genomic sequence	TTCACCCCTGGTGA <b>A</b> ACTAGGGGAG	CAGAGGAAGTCCCACCCCTCTC	621	65°
	bisulfite converted	TT <b>T</b> AT <b>T</b> TTTGGTGA <b>A</b> ATAGGGGAG	CA <b>A</b> AAAA <b>A</b> ATCCCACCCCTCTC		
<b>PMS2</b>	genomic sequence	CATAAAAGTCTGAGTGAGTCCCTGGC	GCCATGTTCCCCCATTTCCAGGG	749	64°
	bisulfite converted	<b>T</b> ATAAAAG <b>T</b> TTGAGTGAG <b>T</b> TTTTGG <b>T</b>	<b>A</b> CCAT <b>A</b> TTCCCCCATTTCC <b>A</b> AAA		
<b>PTGER4</b>	genomic sequence	AGAAAAGTTTGTACAGAGGGTGGAA	TCAGTGAAGAATGGTGTGGATTTC	355	53°
	bisulfite converted	AGAAAAGTTTGT <b>A</b> TAGAGGGTGGAA	TC <b>A</b> ATAAAAA <b>A</b> TA <b>A</b> ACT <b>A</b> AA <b>T</b> TC		
<b>PTGS2 b</b>	genomic sequence	TCAGTCTTATAAAAAAGGAGTTCT	TGCTTGTGGGAAAGCTGGAATATCC	413	52°
	bisulfite converted	TTAG <b>T</b> TTTATAAAAAAGGAGTT <b>T</b>	<b>T</b> ACT <b>T</b> ATAAAAA <b>A</b> ACT <b>A</b> AA <b>A</b> TATCC		
<b>PTGS2 a</b>	genomic sequence	ATCAGACAGGAGAGTGGGGAC	AGCTCCACAGCCAGACGCCCTCAGA	331	55°
	bisulfite converted	AT <b>T</b> AG <b>A</b> TAGGAGAGTGGGG <b>A</b> T	<b>A</b> ACTCCACA <b>A</b> CC <b>A</b> AA <b>C</b> RCCCT <b>C</b> AAA		
<b>RIS1</b>	genomic sequence	GGGCCCTGGAGCCTCCCTCTGAGAA	AGCAGTAGGT <b>C</b> GCACTGGAAGCCCC	850	64°
	bisulfite converted	GGG <b>T</b> TTTGGAG <b>T</b> TTTTTTT <b>G</b> AGAA	<b>A</b> CA <b>A</b> TAA <b>A</b> T <b>C</b> R <b>C</b> ACT <b>A</b> AAAA <b>C</b> CCC		
<b>SGK</b>	genomic sequence	TGGGGGCTTGGCTCACTTCCCCAGA	GGACTTTCAAAAAATTTCCACTTTG	855	60°
	bisulfite converted	TGGGGG <b>T</b> TTGG <b>T</b> TTATTT <b>T</b> TTTAGA	<b>A</b> AACTTTCAAAAAATTTCCACT <b>T</b> TA		
<b>SMARCA1</b>	genomic sequence	AAAGAGCAGATTTAAGGGAAAGAGG	CCACCACACACACACCCCTTCCT	659	64°
	bisulfite converted	AAAGAG <b>T</b> AGATTTAAGGGAAAGAGG	CCACCACACACACACCCCTTCCT		
<b>SNK</b>	genomic sequence	TTTAGTACTAGTAACTGTCAAAGGC	GGCGGCTGGCTGGTAGGTGATAGT	1084	52°
	bisulfite converted	TTTAGT <b>A</b> TTAGT <b>A</b> AT <b>T</b> GT <b>T</b> AAAG <b>T</b>	<b>A</b> ACA <b>A</b> CT <b>A</b> ACT <b>A</b> ATA <b>A</b> ATA <b>A</b> T		
<b>SQSTM1</b>	genomic sequence	GGAAGGGGAGAGTAGTGAAGGGG	CCTTGGTCACCACTCCAGTCACCA	593	65°
	bisulfite converted	GGAAGGGGAGAGTAGTGAAGGGG	CCT <b>T</b> AATCACCACCTCCAGTCACCA		
<b>STK38L</b>	genomic sequence	CCACTCTCAAGAGAGGCCTGAACAG	ACCTAAAATCTCCTCCTGCTCCTGC	493	60°
	bisulfite converted	TTAT <b>T</b> TTTAAGAGAGG <b>T</b> TTGAAT <b>A</b> G	ACCTAAAATCTCCTCCT <b>A</b> CTCCT <b>A</b> C		
<b>TNFRSF10B</b>	genomic sequence	CCCTGGGAAGGGGAGAAGATCAAGA	CCCTCTCTCCCTGCCCTCTCCAGGC	744	65°
	bisulfite converted	TTT <b>T</b> GGGAAGGGGAGAAGAT <b>T</b> AAGA	CCCTCTCTCCCT <b>A</b> CCCTCTCC <b>A</b> AA <b>C</b>		
<b>XPC</b>	genomic sequence	GGAAAAAGCAGCCTAGTACAAGAAGCT	CTCTTGGCCTTGGATTTCTGGCTGC	445	62°
	bisulfite converted	GGAAAAAG <b>T</b> AGTTTAGT <b>A</b> TAAGAAG <b>T</b>	CTCTT <b>A</b> AC <b>T</b> TA <b>A</b> ATTTCT <b>A</b> ACT <b>A</b> C		
<b>ZFP36</b>	genomic sequence	AGTCTCCAGCTTTGAAA <b>A</b> CTGGGCAGG	CCTCCAAATCACC <b>A</b> AGCTGGTCTGAGC	536	65°
	bisulfite converted	AG <b>T</b> TT <b>T</b> AGTTT <b>T</b> GAAA <b>A</b> TTGGG <b>T</b> AGG	CCTCCAAATCACC <b>A</b> AA <b>A</b> CT <b>A</b> AT <b>T</b> CT <b>A</b> AA <b>C</b>		

Sequence information obtained from the human genome draft sequence (NCBI) is shown for PCR primers specific for DNA sequences converted by bisulfite treatment. Sequence alterations caused bisulfite conversion are shown in colour; R = A or G, Y = C or T bases.

**Supplemental Table 2** Oligonucleotides used for methylation-specific PCR

Gene		forward sequence 5'→3'	reverse sequence 5'→3'	Product size	Ta	Reference
<i>SFRP1</i>	MSP (M)	TGTAGTTTTCGGAGTTAGTGT <b>CGCGC</b>	CCTACGATCGAAAACGACGC <b>GAAACG</b>	127	65°	Suzuki et al., 2002 Nat Genet 31(2): 141-9.
	MSP (U)	GTTTTGTAGTTTT <b>TGGAGTTAGTGTGTGT</b>	CTCAACCTAC <b>CAATCAAAAACAACACAACA</b>	136	65°	
<i>APOD</i>	MSP (M)	CACAC <b>CGCG</b> AAAACAATAT	TATGTATGTTAC <b>GTTCGT</b> CG		59°	Yamashita et al. 2002Cancer Cell 2(6): 485-95.
	MSP (U)	<b>CACACA</b> AAAACAATATCTCATTCT	TTTTTTATGTATGTTAT <b>GTGTGT</b> TG		55°	
<i>RASSF1A</i>	MSP (M)	GGGTTTTG <b>CGAGAGCGCG</b>	<b>GCTA</b> ACAAAC <b>CGCA</b> ACCG	169	64°	Liu et al., 2002 Oncogene 21(44): 6835-40.
	MSP (U)	GGGGTTTTG <b>TGAGAGTGT</b> GTTTAG	TAAAC <b>ACTA</b> ACAAAC <b>ACAA</b> ACCAAC	175	62°	
<i>14-3-3σ</i>	MSP (M)	TGGTAGTTTTTATGAAAGG <b>CGTC</b>	CCTCTAAC <b>CGCC</b> ACCACG	105	65°	Ferguson et al., 2000 Proc Natl Acad Sci U S A 97(11): 6049-54.
	MSP (U)	ATGGTAGTTTTTATGAAAGG <b>TGTT</b>	CCCTCTAAC <b>ACCC</b> ACCACA	107	65°	
<i>p16 (CDKN2A)</i>	MSP (M)	TTATTAGAGGGTGGGG <b>CGGATCGC</b>	<b>GACCCCGA</b> ACCG <b>CGACCGTAA</b>	150	65°	Herman al., 1996 Proc Natl Acad Sci U S A 93(18): 9821-6.
	MSP (U)	TTATTAGAGGGTGGGG <b>TGGATGT</b>	<b>CAACCCAA</b> AC <b>ACA</b> ACCATAA	151	60°	
<i>GSTP1</i>	MSP (M)	*GGTTTTTT <b>CGGTTAGTTGCGCGCGG</b>	CCAAC <b>GAAA</b> ACCT <b>CGCG</b> ACCTCCG	206	60°	Singal et al., 2001 Cancer Res 61(12): 4820-6.
	MSP (U)	AAAGAGGGAAAGGTTTTTT <b>TGGTTAGTTGTGTGGTG</b>	AAACTCCAAC <b>AAAA</b> ACCT <b>ACA</b> ACCTCCA	222	64°	
<i>RIZ1</i>	MSP (M)	GTGGTGGTTATTGGG <b>CGACGGC</b>	GCTATTT <b>CGCCG</b> ACCC <b>CGACG</b>	127	68°	Du et al., 2001 Cancer Res 61(22): 8094-9.
	MSP (U)	TGGTGGTTATTGGG <b>TGATGGT</b>	ACTATTT <b>CAACA</b> ACCC <b>CAAGA</b>	126	60°	
<i>THBS1</i>	MSP (M)	TG <b>CGAGCG</b> TTTTTTTAAATGC	TAAACT <b>CGCAA</b> ACCAACTCG	74	62°	Kang et al., 2001 Cancer Res 61(7): 2847-51.
	MSP (U)	GTTTGGTTGTTGTTTATTGGTTG	CCTAAACT <b>CACAA</b> ACCAACTCA	115	62°	
<i>TFPI2</i>	MSP (M)	CACAATTTACAAC <b>GCGAAAACGACGAA</b>	TTTTGTTTTAGG <b>CGGTT</b> CGGGTGTTC	135	65°	Konduri et al., 2003 Oncogene 22(29): 4509-16.
	MSP (U)	CTTACACAATTTACAAC <b>ACAAAAACAACAAA</b>	GTTTTTTGTTTTAGG <b>TGGTT</b> TGGGTGTTT	142	65°	
<i>PTGS2</i>	genomic	TAAAAAACCCCTGCCCCACCGGGCTTACG	AGTCGTATGACAATTGGTCGCTAACCGAG			
	MSP (M)	AAAATTTTGTTTTAT <b>CGGGTTTAC</b>	<b>CGTATA</b> ACAATTAAT <b>CGCTA</b> ACCG	165	60°	
	MSP (U)	AAAAAATTTTGTTTTAT <b>TGGGTTTAT</b>	AATC <b>ATATA</b> ACAATTAAT <b>CACTA</b> ACCA	170	60°	
<i>GPX3</i>	genomic	TGGGGAGCTGAGGGCAAGTCGCGCCCGCC	GCTGCCTGATCCCTGGCCACCGTCCGT			
	MSP (M)	GGAGTTGAGGGTAAGT <b>CGCGTTC</b>	ACCTAATCCCTAACCACC <b>GTCCG</b>	156	65°	
	MSP (U)	GGGGAGTTGAGGGTAAGT <b>TGTGTTT</b>	CTACCTAATCCCTAACCACC <b>ATCCA</b>	160	65°	
<i>DDB2</i>	genomic	GACCCGAGAGGCCTGGCAGCGCCCGGTT	TACAAGCGTACGCCACCACGCCCGGC			
	MSP (M)	GTAGAGGTTTGGTAG <b>CGTCGC</b>	<b>GTACGCC</b> ACCACGCC <b>CGCCG</b>	175	t/d	
	MSP (U)	TT <b>TGT</b> AGAGGTTTGGTAG <b>TGTGT</b>	AACA <b>TAC</b> ACCACCAC <b>ACCCA</b>	181	t/d	
<i>GSTM1</i>	genomic	TAGGGAAGCTGGCGAGGCCGAGCCCGCC	CTCGGCCCGCCACAACCCGAAAGGCGCC			
	MSP (M)	GAAGTTGG <b>CGAGGT</b> CGAGTTT <b>C</b>	ACCC <b>GCC</b> CACAACCC <b>GAAAAACG</b>	157	t/d	
	MSP (U)	GGGAAGTTGGT <b>GAGGT</b> TGAGTTT <b>T</b>	<b>CAACCC</b> ACCACAACCC <b>AAAAACA</b>	161	t/d	

**Supplemental Table 2 (continued)**

<b>DKK3</b>	genomic	GTGAGGTGGCCGGCGCCCGGCTGGC	CCCACCAGGCTCCCTCTCCGCCCCCGCC		
<b>upstream (a)</b>	MSP (M)	AGGTGGT <b>CGGC</b> GTTCGGTTGG	CCTAACTCCCTCTCC <b>GCCCCG</b>	109	t/d
	MSP (U)	TGAGGTGGT <b>TGGT</b> GTTCGGTTGG	CACCAAACCTCCTCCTCC <b>ACCCCA</b>	113	t/d
<b>downstream (b)</b>	genomic	GCCAGGGGCGGGCGGGGGCGG	CGCTGCATCTCCGCTCTGCGCCCGC		
	MSP (M)	GGGG <b>CGGG</b> CGGGCGGGG	ACATCTCC <b>GCTCTACG</b> CCCCG	120	t/d
	MSP (U)	TTAGGGG <b>TGGT</b> GGTGGGGT	CTACATCTCC <b>ACTCTAC</b> ACCCA	125	t/d
<b>RIS1</b>	genomic	CCCGTCCGCGGGCGGGCCGCGACGCGCC	GGGGCCGCGAGGCCAGCAGCC		
	MSP (M)	<b>TCCGGCGGGGT</b> CGCGAC <b>CGCG</b>	AAAAC <b>RC</b> CRAAACCAACAACC	113	t/d
	MSP (U)	<b>GTTTGTGGT</b> GGGGT <b>TGTG</b> AT <b>GTG</b>	AAAAC <b>RC</b> CRAAACCAACAACC	115	t/d
<b>p57 (CDKN1C)</b>	genomic	GCTGCCCGCTTTGCGCAGCCCCGGG	GGGAAGGTCCCACGGGCGACAAGACGCT		
	MSP (M)	TTGTTYGYGTTT <b>CGTAGTTTC</b>	AAATCCCAC <b>RAACG</b> ACAAA <b>ACG</b>	88	62°
	MSP (U)	TTGTTYGYGTTT <b>TGTAGTTTT</b>	AAAAATCCCAC <b>RAACA</b> ACAAA <b>ACA</b>	91	62°
<b>HPGD</b>	genomic	GGGGCATAAAAGCCGCGCCGCGCGG	GCAGAGAAATTTCCGCGGCTGGGCGCCGGG		
	MSP (M)	GTATAAAAGT <b>CGCGGT</b> CGCGC	AAATTTCC <b>CGG</b> ACTAAAC <b>GCCG</b>	189	65°
	MSP (U)	GGGTATAAAAGT <b>TGTGGT</b> TGTGT	AAAAAATTTCC <b>ACA</b> ACTAAAC <b>ACCA</b>	195	65°

Sequence alterations caused bisulfite conversion are shown in colour; R = A or G; Ta = annealing temperature; t/d = touch down PCR with 2 cycles at 68°C, 2 cycles at 66°C, N cycles at 65°C; \* = error in the reference: one extra T in the M forward primer sequence

**Supplemental Table 3** Oligonucleotides used for RT-PCR

Gene	forward sequence 5'->3'	reverse sequence 5'->3'	Product size	Ta	Cycle number	Reference
<b>14-3-3σ</b>	CCAGGCTACTTCTCCCTC	CTGTCCAGTTCTCAGCCACA	99	60°	31	NM_006142
<b>APOD</b>	AAAAGCTCCAGGTCCCTTC	AGGGTTTCTTGCCAAGATCC	498	58°	25	Kao et al., 2002 Endocrinology 143(6): 2119-38.
<b>DKK3</b>	AAGGCAGAAGGAGCCACGAGTGC	GGCCATTTTGGTGCAGTGACCCCA	179	60°	34	NM_013253
<b>GSTM1</b>	ACTTTCCCAATCTGCCTAC	TTCTGGATTGTAGCAGATCA	191	55°	32	Hurteau et al., 2002 Anal Biochem 307(2): 304-15.
<b>GSTP1</b>	TCACTCAAAGCCTCCTGCCTAT	CAGTGCCTTCACATAGTCATCC	242	60°	33	Singal et al. 2001 Cancer Res 61(12): 4820-6.
<b>GPX3</b>	CTTCTACCCTCAAGTATGTCCG	GAGGTGGGAGGACAGGAGTTCTT	134	65°	33	NM_002084
<b>EF1A</b>	CACACGGCTCACATTGCAT	CACGAACAGCAAAGCGACC	192	60°	18	Menssen and Hermeking, 2002 PNAS 99(9): 6274-9.
<b>HPGD</b>	CTCTGCAAATTAATTTGGTTTCTGT	ACAGAAACCAAATTAATTTGCAGAG	149	64°	26	NM_000860
<b>RASSF1A</b>	TGGTGCACCTCTGTGGCGACTT	TCCTGCAAGGAGGGTGGCTTC	239	60°	37	Schagdarsurengin et al., 2003 Oncogene 22(12): 1866-71.
<b>p57</b>	CTGACCAGCTGCACTCGGGGATTTT	GCCGCCGTTGTCTGCTACATGA	341	60°	31	Kikuchi et al., 2002 Oncogene 21(17): 2741-9.
<b>p16</b>	AGCCTTCGGCTGACTGGCTGG	CTGCCCATCATGACCTGGA	139	60°	40	Suzuki et al., 2002 Nat Genet 31(2): 141-9.
<b>PTGS2</b>	TAAACAGACATTTATTCCAGAC	GAAAGAAATAGTCAATATGCTTG	193	60°	33	Suzuki et al., 2002 Nat Genet 31(2): 141-9.
<b>SFRP1</b>	TTGTAGTTATCTTAGAAGATAGCATGG	ACGGGAATTACTATTAACATAAGCG	532	65°	31	Suzuki et al., 2002 Nat Genet 31(2): 141-9.

## Acknowledgement

I would like to express my especial gratefulness to my supervisor Dr. Heiko Hermeking for offering me an opportunity to do my PhD thesis work in his laboratory, for accompanying the projects with his scientific interest and support, for helpful discussions and for the organizing a fruitful collaboration with other scientists. I am also grateful to Heiko for his support in presenting my data at the scientific conferences.

I want to thank Prof. Dr. Thomas Cremer for participating in my thesis committee.

Prof. Dr. Joachim Diebold for the great collaboration in the prostate cancer project, selection and evaluation of clinical samples and also for his expert introduction in histopathology of the prostate. I also would like to acknowledge technical assistants Anja Heyer and Andrea Sendelhofert who were involved in immunohistochemical analysis of prostate cancer.

Alex Epantchintsev for his contribution to the bisulfite sequencing analysis of PCa cell lines.

Dr. Amir Yazdi, Dr. Thomas Herzinger and Dr. Christian Sander for their indispensable contribution to the analysis of 14-3-3 $\sigma$  in diseased and normal human skin.

Dr. Reinhard Hoffmann for his help in the experiments with Affymetrix microarray. I would like also to thank Dr. Jorg Mages for his assistance in the processing of microarray data.

Dr. Wolfgang Klinkert for assistance with flow cytometry.

I am grateful to all my lab colleagues for their daily help and communication with regard to research and beyond. I want to express my special gratitude to my fellow PhD students Alex, Anne, Heike and Henrike.

### **Parts of this work were published:**

Peer-reviewed, research articles:

Lodygin, D., Menssen, A., and Hermeking, H. (2002). Induction of the Cdk inhibitor p21 by LY83583 inhibits tumor cell proliferation in a p53-independent manner. *J Clin Invest* 110, 1717-1727.

Lodygin, D., Yazdi, A. S., Sander, C. A., Herzinger, T., and Hermeking, H. (2003). Analysis of 14-3-3sigma expression in hyperproliferative skin diseases reveals selective loss associated with CpG-methylation in basal cell carcinoma. *Oncogene* 22, 5519-5524.

Lodygin, D., Diebold, J., and Hermeking, H. (2004). Prostate cancer is characterized by epigenetic silencing of 14-3-3sigma expression. *Oncogene* 23, 9034-9041.

Mhawech, P., Benz, A., Cerato, C., Greloz, V., Assaly, M., Desmond, J. C., Koeffler, H. P., Lodygin, D., Hermeking, H., Herrmann, F., and Schwaller, J. (2005). Downregulation of 14-3-3sigma in ovary, prostate and endometrial carcinomas is associated with CpG island methylation. *Mod Pathol* 18, 340-348.

Lodygin, D., Epanchintsev, A., Menssen, A., Diebold, J., and Hermeking, H. (2005). Functional epigenomics identifies genes frequently silenced in prostate cancer. *Cancer Res* 65, 4218-4227.

Reviews:

Lodygin, D., and Hermeking, H. (2005). The role of epigenetic inactivation of 14-3-3sigma in human cancer. *Cell Res* 15, 237-246.

### **Parts of this work were presented at:**

12<sup>th</sup> International AEK Cancer Congress, March 25-28, 2003, Würzburg, Germany (poster)

1<sup>st</sup> Transregio 5 Symposium, Chromatin: Assembly and Inheritance of Functional States, October 9-11, 2003, Munich, Germany (poster)

88<sup>th</sup> Meeting of the German Society of Pathology, June 2-5 2004, Rostock, Germany (poster)

Cancer Genetics and Tumor Suppressor Genes Meeting, August 18-22, 2004, Cold Spring Harbor, NY, USA (poster)

3<sup>rd</sup> Petersberg Conference and 2<sup>nd</sup> Workshop of the German Prostate Cancer Consortium (DPKK e. V.) October 8-9, 2004 Bonn, Königswinter/Petersberg, Germany (oral presentation)

## Curriculum Vitae

### Dmitri Lodygin

**DATE OF BIRTH:** 20th May 1973

**PLACE OF BIRTH:** Nowgorod, Russia

#### EDUCATIONAL BACKGROUND:

- 1980–1990 Elementary and High School, Arkhangelsk
- 1990-1996 Arkhangelsk State Technical University, Faculty of Chemical Technology, *Northern Dvina Emb. 17, 163002 Arkhangelsk, Russia*  
Engineer's diploma in chemical technology (diploma with distinction)
- 1992-1996 Arkhangelsk State Medical Academy, *Troitzky Ave. 51, 163061 Arkhangelsk, Russia*
- 1996-1998 Moscow State University, Faculty of Basic Medicine, *Vorobjevy Gory, 119992 Moscow, Russia*  
Physician's diploma in general practice (diploma with distinction)

#### RESEARCH EXPERIENCE:

- 1997 -1998 Russian Cardiology Research Center, Institute of Experimental Cardiology, Laboratory of Experimental Pharmacology, *Cherepkovskaya St. 15, 121552 Moscow, Russia*  
Subject: The pathophysiology of circulation and CNS, mechanisms of hemodynamic effects of central hypotensive drugs.
- 1999-2001 Heinrich-Pette-Institut for Experimental Virology and Immunology, Department of Cellular Immunology, *Martinistrasse 52, D-20251, Hamburg, Germany*  
Subject: The role of DNA recombination and repair in diversification of Ig repertoire in chicken B-cells
- 2001-2005 Max-Planck Institute of Biochemistry, Molecular Oncology Junior Research Group, *Am Klopferspitz 18, D-82152 Martinsried/Munich, Germany*  
Subject: Cellular senescence, epigenetics and cancer